Durham University

Durham E-Theses

The preparation and properties of large single crystals of cadmium sulphide

Clark, L.

How to cite:

Clark, L. (1965) *The preparation and properties of large single crystals of cadmium sulphide*, Durham theses, Durham University. Available at Durham E-Theses Online: http://etheses.dur.ac.uk/8734/

Use policy

The full-text may be used and/or reproduced, and given to third parties in any format or medium, without prior permission or charge, for personal research or study, educational, or not-for-profit purposes provided that:

- a full bibliographic reference is made to the original source
- a link is made to the metadata record in Durham E-Theses
- the full-text is not changed in any way

The full-text must not be sold in any format or medium without the formal permission of the copyright holders.

Please consult the full Durham E-Theses policy for further details.

Academic Support Office, The Palatine Centre, Durham University, Stockton Road, Durham, DH1 3LE
e-mail: e-theses.admin@durham.ac.uk Tel: +44 0191 334 6107
http://etheses.dur.ac.uk

The Preparation and Properties of Large Single Crystals of Cadmium Sulphide

by

L. Clark, B.Sc.

Presented in candidature for the
degree of Doctor of Philosophy of
the University of Durham

15 FEB 1966
LIBRARY

ACKNOWLEDGEMENTS

The author wishes to thank the Science Research Council for financial support during the course of this research, and Professor D.A. Wright for permitting the use of his laboratory facilities. He is indebted to Dr. J. Woods for his excellent supervision and invaluable guidance. He would also like to thank the other members of the group, Mr. A. Rushby, Mr. T.A.T. Cowell, and Mr. J.R. Brailsford for their continued interest and assistance; the departmental workshop staff, headed by Mr. F. Spence and Mr. B. Blackburn, and electronics technician Mr. D. Ellis, in connection with the construction of much of the apparatus; and the photographer Mr. R. White and typists Miss Pat Stewart and Miss Anne Parnaby for assistance in the final preparation of the thesis.

CONTENTS

ABSTRACT

The photoconductive and luminescent properties of cadmium sulphide have long been of interest, and have only been studied extensively since 1947 when Frerichs reported a convenient method of preparing small single crystals. The properties of the material are summarised in Chapter Two of this thesis, following an outline of the essential theory of electrical conduction in semiconductors.

Conventional methods of single crystal preparation such as growth from the melt or from solution are not practicable with cadmium sulphide and most measurements have been made on small plates or rods grown by sublimation in a flow of carrier gas. However the preparation of large single crystal samples is desirable for certain measurements, e.g. Hall effect measurements, and essential if recent applications such as gamma-ray detectors or ultrasonic amplifiers are to be pursued. Various methods of growing large single crystals by sublimation have been reported, and these are reviewed in Chapter 4. However crystals produced by similar methods can show marked differences in their properties. The resistivities of crystals as grown can be as high as 10^{10} ohm-cm., or as low as 1 ohm-cm., with wide variations in the carrier mobility. Close control of the properties of the material produced is essential for any practical application or for any detailed study of the material itself.

The work which forms the basis of this thesis therefore consists of an investigation into the feasibility of growing large single crystals by several methods. The effect on the resultant properties is observed when parameters such as the growth temperature or the partial pressures of the components are altered. The suitability of various starting materials is

also discussed.

The conclusions from the present work are that departures from stoichiometry in the growth system are responsible for much of the difficulty in preparing large single crystals of good quality at low temperatures ($\sim$1050°C). Further, at the present time the properties of the ~~as-grown~~ material are controlled by departures from stoichiometry rather than by contamination from chemical impurities.

The final section of the thesis indicates which of the reported methods is most suitable for small-scale production of large single crystals of high resistivity cadmium sulphide. It also describes a growth method embodying the conclusions drawn from the present work as a basis for further study.

CHAPTER 1

THE THEORY OF CONDUCTION IN CRYSTALS

1.1 Bonding

1.1.1 Introduction

Crystals are regular three dimensional arrays of individual atoms bound together by inter-atomic forces. The binding force is usually electrostatic in nature, but the exact nature of forces acting can be of several forms. Only the principal types of bonding will be discussed.

1.1.2 Coulomb or Ionic Bonding

In ionic bonding the forces between atoms of the molecule arise from coulombic attraction. The atoms are ionised so that the electronic structure of each atom consists of closed shells. An example is sodium chloride, $Na^{+}Cl^{-}$. The 3s electron from the sodium atom is transferred to the lower energy 3p shell of the chlorine atom, leaving each ion with an overall charge. Coulombic attraction then draws the ions together; the equilibrium separation between the ions is that at which the attraction force is balanced by the strong repulsive forces as the electronic space clouds of the ions begin to overlap. The repulsive forces become large only at small separations so that the binding energy of an ionic crystal is large. Each ion tends to surround itself with as many ions of the opposite charge as possible, which leads to either the rocksalt or caesium chloride structure.

1.1.3 Metallic Bonding

In metallic bonding the electrostatic attractive forces are between

[illegible] FEB 1965

the fixed metal ions, which are positively charged, and a 'sea' of free electrons distributed throughout the crystal. The attractive force is again large and the strong binding usually results in the formation of a close packed structure, either hexagonal or cubic.

1.1.4 Covalent Bonding

Mutual sharing of electrons between two adjacent atoms leads to a reduction in energy and hence a bonding force. Where two atoms share an electron pair the bonds are particularly stable and are known as covalent bonds. Examples of such bonds are to be found in the group IV elements, which have four outer electrons. In germanium, silicon and diamond crystals each atom is linked by a covalent bond to each of its four nearest neighbours arranged tetrahedrally around it to form the face-centred cubic diamond lattice.

1.1.5 Mixed Bonding

It should be emphasised that in general the binding between the atoms in a solid can be a combination of several types of bond. Compounds such as lithium fluoride, LiF, can be regarded as dominantly ionic, and silicon, germanium, and possibly indium antimonide as covalent, but the nature of the bonding in intermediate compounds is not always obvious. This is particularly true in the case of the II-VI compounds (CdS,ZnS,etc.) where the bonding can only be regarded as a mixture of covalent and ionic. Determination of the degree of ionicity is difficult. A guide can be obtained from the electronegativity of the constituent atoms; the greater the difference between the electronegativities the more ionic the bond. The degree of ionicity is also indicated by the manner in which some

materials cleave. Perhaps the best information can be obtained from a study of the lattice optical absorption, by applying the Szigeti relations[1].

1.2 Band Theory

1.2.1 Introduction

To discover the effect on the allowed electronic energy levels when individual atoms are combined to form a solid, there are two important approaches within the framework of the one-electron approximation. In the first, the effect on the electronic levels of one atom when other atoms are brought near is discussed. This is called the Valence Bond Model or Tight Binding Approximation. In the second, the Band Theory or Zone Theory approach, the possible levels available to an electron moving in the periodic potential of the ions in the lattice of a solid are evaluated.

1.2.2 Tight Binding Approximation

The potential energy of an electron bound to an ion by coulombic forces is $\frac{Ze^2}{4\pi\epsilon_o r}$ where Z is the effective charge on the ion; e the electronic charge, ϵ_o the permittivity of free space and r the separation between the electron and the nucleus. Solution of the Schrodinger wave equation for an electron in such a potential field shows that the only allowed energies for the electron are a series of discrete energy levels. (For the hydrogen atom the levels are given by $E = -\frac{2\pi^2 e^4 m}{n^2 h^2}$).

In a second atom isolated from the first the energy levels would be identical with those of the first, or degenerate (indistinguishable). If the distance between the atoms were reduced, the electrons would be under the influence of attractive forces from both nuclei, and repulsive

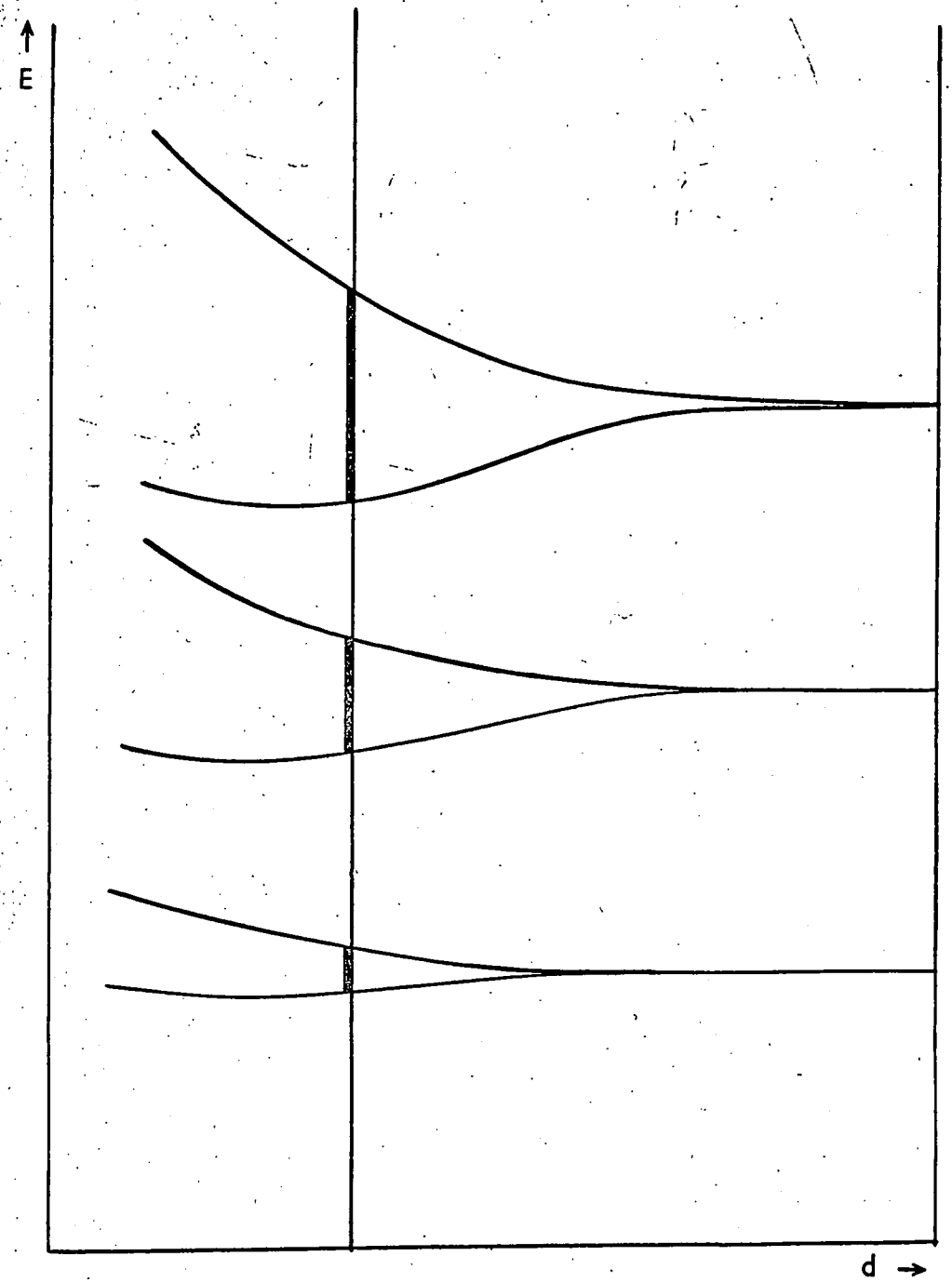

ENERGY LEVEL SPLITTING v. ATOMIC SPACING d

FIGURE 1.1

forces between the electron clouds. The outer electron energy levels would be split into two adjacent levels, analogous to the splitting of the resonant frequency when two identical resonant circuits are coupled. The degree of splitting depends on the degree of interaction of the electron clouds, or the atomic separation.

For a regular lattice of N atoms, each energy level will be split into N closely spaced levels, the separation between the levels increasing as the atoms are brought together. For the highest energy levels, occupied by the outer or valence electrons, the splitting is greatest, and the levels can be regarded as a permitted band of electron energies. The lower levels, corresponding to the more tightly bound electrons shielded by the outer electron shells, show little splitting. The effect is illustrated in Fig. 1.1.

The tight binding approximation illustrates the presence of permitted bands of energies for electrons in a solid, and can explain the differences between metals, semi-conductors and insulators. It provides a useful introduction to the electrical and optical properties of solids, but an approach incorporating more of the ideas and conditions of wave mechanics is necessary for a more detailed understanding of such properties.

1.2.3 Band Theory Approach

The band or zone theory of solids considers an electron moving in the potential field due to the crystal as a whole. It is assumed that the ions are effectively at rest.

The potential field for an electron moving in an array of positive ions in the lattice of a metal for example is a series of potential wells.

Electrons whose energies lie above the peaks between the wells are free to move through the solid, whereas electrons with lower energies are bound to their respective ions. The energies of electrons travelling through the crystal will be limited to certain permitted bands due to interaction with and scattering by the positive ions.

According to de Broglie an electron can be regarded as possessing an associated wavelength λ, where $\lambda = h/mv = h/p$; h is Planck's constant and p the momentum of the electron assumed to be in free space. The electron has associated with it a wave number vector K, with direction that of the electron's velocity, and magnitude $K = 2\pi/\lambda$. For a free electron the electron energy is

$$E = \frac{h^2K^2}{8\pi^2m} \qquad (1.1)$$

A plot of energy versus K for the free electron is the parabola described by equation (1.1) (Fig. 1.2(a)). Negative values of K represent motion in the opposite sense. The presence of a periodic potential field will introduce discontinuities in the E versus K curve as shown in Fig. 1.2(b).

F. Bloch[2] has shown how to take account of the periodic potential of the lattice. For a one-dimensional periodic potential with period d, the potential, V(x), is such that $V(x) = V(x + rd)$, where r is any integer. The solution of the Schrodinger equation can then be shown to be of the form

$$\psi_K(x) = U_K(x) \exp(iKx) \qquad (1.2)$$

where $U_K(x)$ is a periodic function of x of period d, and K is the wave

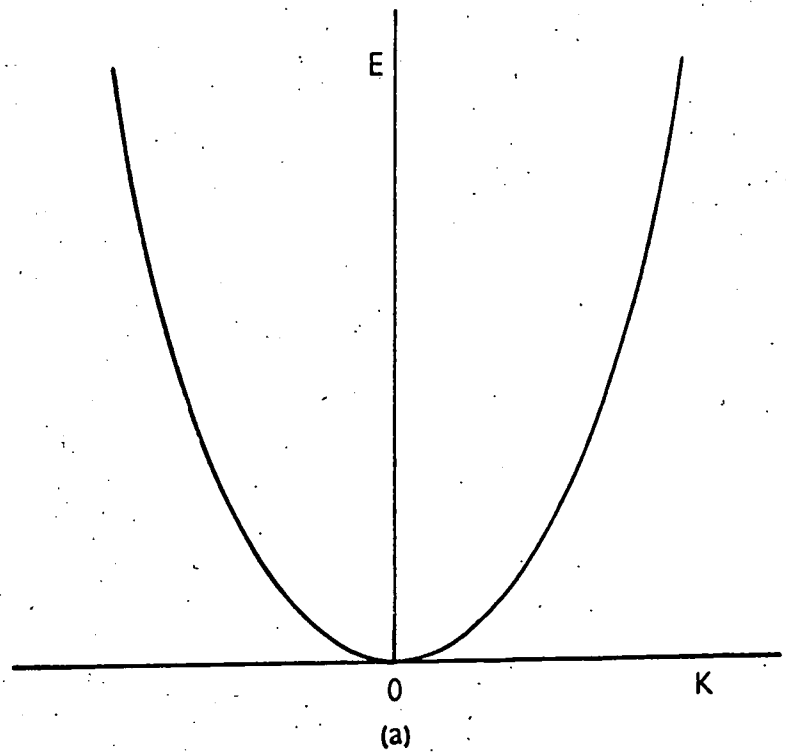

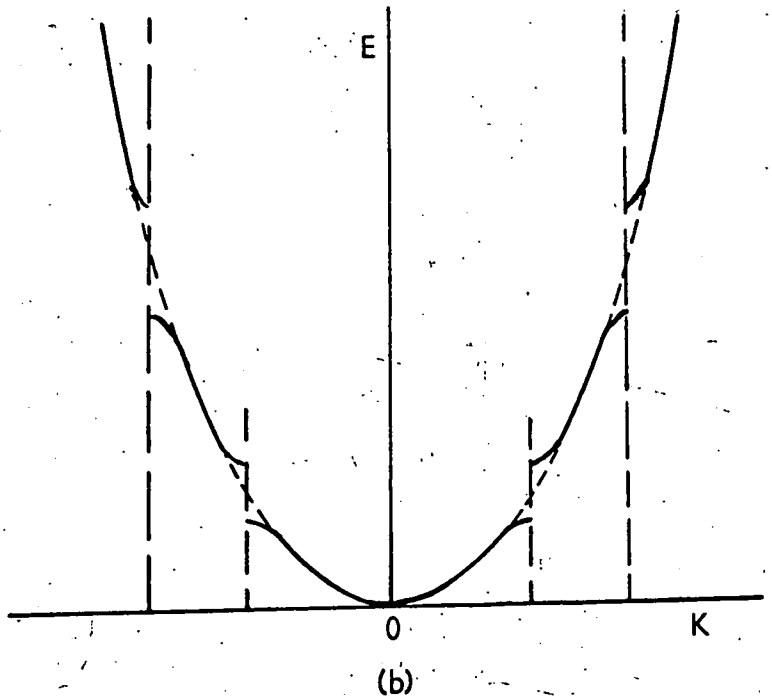

E versus K

(a) free electron: (b) in periodic potential.

FIGURE 1.2

number vector. A quantity P is defined as $P = Kh/2\pi$, and is known as the 'crystal momentum'. This has many properties of the electron momentum, but only reverts to the value of momentum of a free electron for V(x) constant.

Wave packets made up of functions like those given in equation (1.2) are required to describe the motion of localised electrons. The velocity of an electron is equal to the group velocity $d\omega/dK$, where ω is given in terms of energy by $\omega(K) = 2\pi\nu = 2\pi E_K/h$.

The velocity v is therefore $v = \frac{d\omega}{dK} = \frac{2\pi}{h} \cdot \frac{dE}{dK}$

However the energy E is no longer a simple function of K, but depends on the form of the periodic potential V(x). Kronig and Penney[3] discussed a model in which atoms formed square potential wells in a one-dimensional lattice. They showed that the distribution of possible electron energies

(i) consists of a series of allowed energy bands separated by forbidden regions

(ii) the width of the bands increases with increasing crystal binding energy.

(iii) the width of the bands decreases with increasing electron binding energy.

1.2.4 Brillouin Zones

The energies that are forbidden correspond to the wavelengths at which Bragg diffraction will occur for electrons, considered as waves, passing through the solid. The forbidden energies will be different for electrons travelling along different crystallographic directions, since the apparent atomic separation will alter. For example, in a cubic crystal

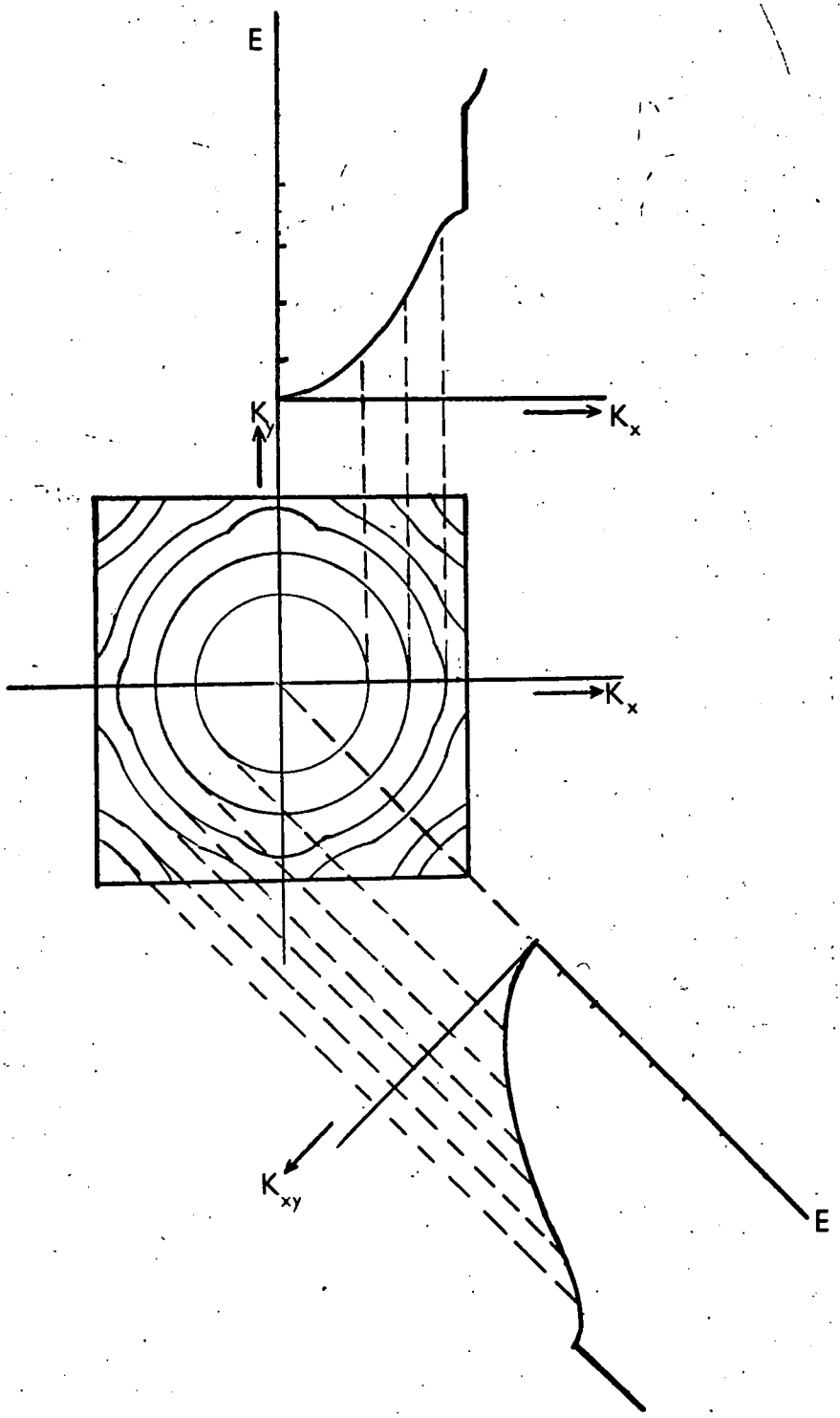

E vs. K for a cubic structure.

FIGURE 1.3

an electron travelling in the 100 direction with a velocity corresponding to a wavelength $\lambda = 2a$ will be diffracted. In terms of K, this happens at $K_x = \pi/a$. Similarly, diffraction occurs for K_y, $K_z = \pi/a$. For an electron travelling in the 110 directions, K_{xy}, K_{yz} or $K_{zx} = \frac{\pi\sqrt{2}}{a}$ for diffraction to occur. Similar limiting values apply for any direction of travel.

The limiting values can be plotted on a system of coordinates with axes K_x, K_y, K_z known as 'K-space', and the figure constructed from the limits of the first order diffraction is known as the first Brillouin zone. Wavelengths < 2a are of course possible for electrons with velocities in the 100 direction, and 2nd, 3rd and higher Brillouin zones can be constructed corresponding to the higher permitted energy ranges. These zone boundaries represent the maximum energies that electrons can have without a discontinuity in energy developing.

The zones are functions only of structure, and do not depend on chemical composition or number of atoms in the structure. The discontinuities for any particular crystal direction can be shown on an E versus K plot for that direction, and the energy gap between these permitted values is called a forbidden zone. However the possibility that an energy forbidden in one direction may be allowed in another must not be overlooked. This is illustrated in Fig. 1.3, which shows E versus K curves for the 100 and 110 directions, derived from an energy contour diagram for a cubic structure.

1.2.5 Effective Mass m^*

Near the maxima and minima of the allowed energy bands the relation

between the energy E and wave vector K changes, and is appreciably different from that for a free electron. Since K is proportional to momentum p there is therefore a change in the relation of electron energy to momentum. It can be shown that, in a solid, the normal laws of motion of particles can be applied to the electron provided that the free electron mass m is replaced by an effective mass m^*. This effective mass is not necessarily constant, and can vary for different crystallographic directions or electron energies. The effective mass is given by

$$\left(\frac{\delta^2 E}{\delta K^2}\right) = \frac{1}{m^*}\left(\frac{h}{2\pi}\right)^2 \qquad (1.3)$$

for a solid with spherical energy surfaces in K-space. For a free electron this gives m^* equal to m as expected, but in a solid m^* can be quite different from m, especially for an electron with an energy close to the band edge. However most of the results derived in the free electron model can be carried over to the solid provided that the equation (1.1), $E_K = \frac{h^2K^2}{8m\pi^2}$ is replaced by $E_K = \frac{h^2K^2}{8m^*\pi^2}$. m^* then replaces m in the expressions for the Fermi energy, conductivity, and similar cases.

The value of m^* is dependent on the position of the electron in the band and on the way in which E varies with K. However equation (1.3) together with a typical E versus K curve as in Fig. 1.2(b); enables a qualitative description of the expected variation of m^* through a band to be made. Electrons with an energy near the band minimum show behaviour associated with a positive, almost constant effective mass. As the electron passes to higher energies within the band, its effective mass increases and tends to infinity at the point of inflexion of the E versus K curve.

Electrons with still higher energies have an associated negative effective mass, increasing from $-\infty$ to a small negative value for electrons close to the top of the band.

1.2.6 Density of States

In the foregoing sections the factors governing the possible energy bands available to electrons in solids have been outlined; we now need to consider the density of the levels in these band and their degree of occupancy by electrons.

For an electron in a uniform potential well, we can apply the Pauli exclusion principle and the uncertainty principle to derive the density of levels $N(E)dE$ for electrons with energies between E and $E + dE$. We have

$$N(E)dE = \frac{2\pi}{h^3} (2m)^{3/2} . E^{\frac{1}{2}} . dE. \qquad (1.4)$$

An analogous treatment for the density of levels in a Brillouin zone can be performed, although generally elements of K-space rather than momentum space are considered. The distribution of levels follows that for the free electron initially; the number of possible elements of K-space for a given value of K increases as K^2, since for low E the surfaces of constant energy are spherical. A distortion of the spherical energy surfaces will become apparent near a Brillouin zone boundary, and as higher values of energy become forbidden in some directions in K-space, the density of levels will fall, becoming zero at the maximum energy of the band. Figure 1.4(a) compares the density of energy levels for the free electron and in the Brillouin zone.

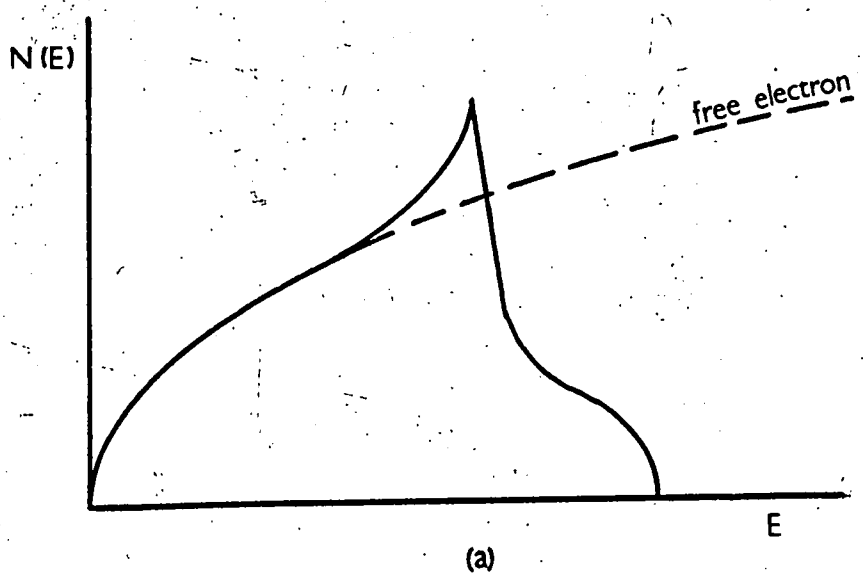

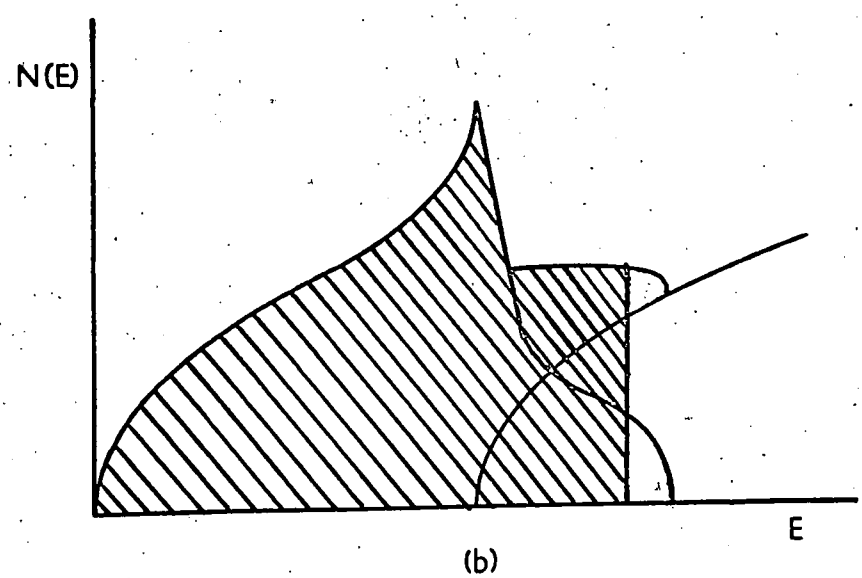

DENSITY OF STATES

(a) single zone (b) overlapping zones.

FIGURE 1.4

The Brillouin zones, i.e. the volumes in K-space between successive polyhedra denoting discontinuities of energy, are such that each Brillouin zone occupies the same volume. This volume contains levels sufficient to accommodate 2N electrons, where N is the total number of atoms in the crystal.

1.2.7 Metals, Semiconductors and Insulators

The presence of bands of permitted energies for the higher energy electrons in a solid, and the determination of the density of energy levels, allows the obvious differences in the conduction properties of metals, semiconductors and insulators to be explained. We saw in section 1.2.2 that in a solid of N atoms there will be N closely-spaced energy levels in an energy band, and each level can accommodate two electrons. For an atom with an odd number of valence electrons (e.g. Li; $2s_1$, $1s_2$) only half of the available energy levels in the highest occupied band will be filled. As a result, electrons in such a solid can be accelerated by an applied electric field and take part in conduction, since empty, higher energy levels are available. Such a material will be a good metallic conductor.

In a metal such as magnesium with an even number of valence electrons per atoms, empty energy levels are still available to the valence electrons since the top of the highest occupied band (3s) overlaps the bottom of the (3p) band above. The 2N electrons are therefore in a combined band of 2N levels, and empty levels are available to allow conduction to take place.

The density of permitted levels for overlapping bands is shown in Fig. 1.4(b). Note that the overlap in permitted energies does not occur for the same direction in K-space.

Where a material has an even number of valence electrons per atom, and the highest filled energy band is well below the next available band ($E_g >> kT$), no empty energy levels are available for conduction, and the material is therefore an insulator.

When, however, the energy gap separating a full band from an empty band is small (< lev), at temperatures above $0^{o}K$ a few electrons will be excited thermally across the gap, so that conduction can take place in both bands. Conduction in the previously full band via the empty energy levels is best thought of as being due to positively charged 'holes'; similar statistics can be applied to the holes as are used for electrons.

The temperature at which the electrical conduction becomes significant depends of course on the magnitude of the energy gap. A solid where the conduction takes place through thermally generated carriers is known as an intrinsic semiconductor. The lower, previously full band is termed the valence band, and the upper band the conduction band.

1.3 Semiconductors

Since this thesis is concerned with cadmium sulphide, a semiconductor or semi-insulator, only the properties of semiconductors will be discussed in any detail. The definition of semiconductors is not exact, but semiconducting materials are generally considered to have conductivities in the range 10^{2}-10^{-10} $(ohm\ cm)^{-1}$. The term semi-insulator is

sometimes used for semiconductors with conductivities lower than about 10^{-5} $(ohm\text{-}cm)^{-1}$.

1.3.1 Intrinsic Semiconductors

The term intrinsic semiconductor implies that the semiconducting property is a characteristic of the pure material. Extrinsic semiconductors, which are those where the semiconducting properties arise from chemical impurities or from departures from stoichiometry, will be discussed later.

In an intrinsic semiconductor the energy gap must be ~~only a few~~ less than 1 ev. ~~KT~~ in order to permit appreciably thermal excitation across the forbidden gap. The group IV elements illustrate the definition:-

Element	Gap	Type
C (Diamond)	7 ev	Insulator
Si	1.1 ev	Semiconductor
Ge	0.7 ev	"
Sn (Grey tin)	Very small, +ve	"
Pb	-	Metal

Grey tin is a semiconductor at room temperature; Ge and Si in a pure state are insulators at room temperature and become 'intrinsic' above $100^{\circ}C$. On this scale, pure stoichiometric cadmium sulphide with an energy gap of ~ 2.4 ev could be regarded as intermediate between a semiconductor and an insulator, i.e. a semi-insulator.

1.3.2 Fermi Level and Free Carrier Density in Intrinsic Semiconductors

The density of energy levels available to electrons in a band was evaluated in section 1.2.6. Since the electrons in the levels are subject to the Pauli exclusion principle, the probability of a level being occupied is given by the Fermi-Dirac distribution function

$$P(E) = \frac{1}{\exp\left(\frac{E-E_f}{kT}\right) + 1} \qquad (1.5)$$

E_f is a parameter which is determined so as to normalise the distribution for the total number of electrons present. It is equal to the energy at which the probability of a level being occupied is 0.5, and is called the 'Fermi Energy Level.'

Equation (1.5) can be written as $P(E) = f((E-E_f)/kT)$, (1.6)

where $f(x) = \frac{1}{e^x+1}$ is the Fermi-Dirace function. (1.7)

Note that $f(x)$ varies from zero through 0.5 to one as E goes from $E-E_f >> kT$ through $E = E_f$ to $E-E_f << kT$.

For an intrinsic semiconductor with an energy gap ΔE, we take as $E = 0$ the bottom of the conduction band. If $N_{cb}(E)dE$ is the density of allowed levels in the conduction band between E and $E + dE$, then the carrier density in this energy range is $n(E)dE = 2N_{cb}(E).P(E)dE$, and the total density in the band from $E = 0$ to $E = E_t$ is

$$n_i = 2\int_0^{E_t} N_{cb}(E).P(E).dE \qquad (1.8)$$

Now providing only a few levels are occupied and we can assume spherically symmetric energy bands, $N_{cb}(E)dE$ is given by (1.4). Hence

for the non-degenerate case, i.e. $(E-E_f) > 2kT$, using (1.4), (1.5) and (1.8), and letting $E_t \to \infty$,

$$n_i = \frac{4\pi(2m_e^*)^{3/2}}{h^3} \int_0^\infty \frac{E^{1/2}\,dE}{\exp\left[(E-E_f)/kT\right]+1} \qquad (1.9)$$

Now using $E-E_f >> kT$, and substituting for $x = E/kT$,

$$n_i = \frac{4\pi(2m_e^*)^{3/2}}{h^3} \exp\frac{E_f}{kT} \int_0^\infty \frac{(kT)^{3/2}x^{1/2}dx}{\exp x}$$

$$= \frac{2(2\pi m_e^* kT)^{3/2}}{h^3} \exp(E_f/kT) \qquad (1.10)$$

$$\text{or} \quad n_i = N_c \exp(E_f/kT) \qquad (1.11)$$

where $N_c = \frac{2(2\pi m_e^* kT)^{3/2}}{h^3}$ is called the effective density of states in the conduction band.

Similar statistics apply for the number of vacant levels, or holes, in the valence band due to the excitation of electrons to the conduction band. As mentioned in 1.2.7, conduction by electrons in the valence band involving these vacant levels can best be interpreted as movement of positive holes.

The equivalent of (1.4), or the density of levels, for holes is

$$N_{vb}(E)\,dE = \frac{2\pi(2m_h^*)^{3/2}}{h^3}(-\Delta E - E)^{1/2}\,dE \qquad (1.12)$$

Again for the non-degenerate case

$$p_i = \frac{4\pi(2m_h^*)^{3/2}}{h^3}\int_{-\infty}^{-\Delta E}\frac{(-\Delta E - E)^{1/2}\,dE}{\exp[(E_f - E)/kT]+1} \qquad (1.13)$$

and

$$p_i = N_v \exp(-(E_f + \Delta E)/kT) \qquad (1.14)$$

where $N_v = \frac{2(2\pi m_h^* kT)}{h^3}$, the effective density of states in the valence band. In intrinsic conduction, the density of electrons in the conduction band must equal the density of holes in the valence band. Equating p_i and n_i gives from (1.11) and (1.14)

$$m_e^{*3/2}\exp(E_f/kT) = m_h^{*3/2}\exp[-(E_f - \Delta E)/kT]$$

$$\text{or} \qquad E_f = \frac{-\Delta E}{2} + \frac{3kT}{4}\ln(m_h^*/m_e^*) \qquad (1.15)$$

Substituting for (1.15) in (1.11) we have

$$n_i = \frac{2(2\pi m_e^* kT)^{3/2}}{h^3}\exp\left[\frac{-\Delta E}{2kT} + \frac{3}{4}\ln\left(\frac{m_h^*}{m_e^*}\right)\right]$$

$$n_i = p_i = \frac{2(2\pi kT)^{3/2}(m_e^* m_h^*)^{3/4}}{h^3}\exp(-\Delta E/2kT). \qquad (1.16)$$

1.3.3 Impurity or Extrinsic Semiconductors

Impurity semiconductors are formed by the addition of small quantities of an element into a solid so that the atomic energy levels of the impurity atom lie in the energy gap between the valence and conduction bands of the solid. If this energy gap is very large few

intrinsic carriers will be generated. If however the highest normally filled electron level of the impurity atom has an energy only a few KT below the bottom of the conduction band, electrons from this 'donor' level can readily be thermally excited into the band. A semiconductor in which the carriers are predominantly electrons is aalled 'n'-type.

An analogous situation occurs when a normally empty energy level due to an impurity atom lies a few kT above the top of the filled valence band in a normally insulating material. Electrons can be excited to these 'acceptor' levels to form holes in the valence band. Where conduction by holes is dominant, the material is termed 'p'-type. Donor and acceptor levels can also be caused by departure from stoichiometry as well as chemical impurities.

The impurity states can be regarded as localised levels and not energy bands since the concentration of the impurity is low and interaction between the impurity atoms is therefore small. When the impurity concentration is very high, the interaction may not be neglegible, and a delocalised band of permitted energies may be formed, allowing movement of electrons and conduction within the so-called impurity band.

The most familiar impurity semiconductors are Ge and Si doped with group III or group V impurities to provide p and n-type conduction respectively. A group V atom such as phosphorus incorporated substitutionally into a germanium lattice has five valence electrons, only four of which are required for bonding to the four nearest neighbours. The fifth valence electron is only loosely bound to the phosphorus atom,

and can easily be excited thermally and removed into the conduction band of the crystal. The energy needed to release an electron from a donor can be calculated by treating the atom and its outer electron as a hydrogen atom in a region of the appropriate dielectric constant.(4) Such a calculation for a group V donor in Ge indicates a value of 0.01 ev. as the depth of a donor level below the conduction band. This value is found in practice to be a good estimate, although variations from it do occur.

In the case of a group III atom, such as indium, only three valence electrons are available for bonding. The resulting hole is only loosely bound to the indium atom, and can easily be freed thermally to give a hole in the valence band. The group III impurities therefore act as acceptors in group IV materials.

One of the main difference between the elemental semiconductors of group IV and the compound semiconductors is that the latter contain more than one type of atom and departures from stoichiometry can occur. Such departures can often have much more effect on the properties of the semiconductors than chemical impurities, since departures from stoichiometry of 1 in 10^4 are common, and can lead to carrier densities greater than $10^{18}/cm^3$. Overall electrical neutrality in the lattice must still be observed, and departures from stoichiometry are accommodated in the lattice by a change in the ratios of Frenkel defects (interstitials) and Schottky defects (vacancies) of either element.

An anion vacancy will act as a donor, since the valence electron normally shared by the anion will only be loosely bound to the neigh-

bouring cations, and can easily be excited from the defect to move through the conduction band. Thus a sulphur vacancy in CdS acts as a donor. Similarly a cation vacancy caused by an excess of anions can give rise to free positive holes at ordinary temperatures. This occurs with an excess of S in PbS. In CdS however, excess S does not give rise to free holes at room temperatures - the acceptor levels corresponding to the cation vacancy are too far removed from the valence band to be ionised, and are compensated by donors.

Ions of a different valency from those of the host lattice can also give rise to donor and acceptor levels in compound semiconductors as well as in the elemental case. A common example is chlorine, which can enter a II-VI compound as Cl^-, substituting for an anion, and release an electron to the conduction band.

1.3.4 Free carrier density in impurity semiconductors

For a non-degenerate situation, $(E - E_f > kT)$, the number of electrons in the conduction band is still given by (1.11),

$$\text{i.e. } n = N_c \exp(E_f/kT)$$

but E_f will now be modified by the extra levels present. Again p is given by (1.14), and

$$np = N_c N_v \exp(-\Delta E/kT) = n_i^2$$

Consider first an n-type semiconductor with N_D donors per unit volume at an energy depth E_D below the conduction band; $E_D << \Delta E$. At a temperature high enough for the donor levels to be considered as ionised, but not too high so that the concentration of intrinsic electrons n_i

is still much less than N_D, we have $n \doteqdot N_D$. The fermi level is given in this situation by $n = N_D = N_c \exp(E_f/kT)$, or

$$E_f = kT \ln (N_D/N_c) \qquad (1.17)$$

Note that for the assumption of non-degeneracy to hold, we must have $N_D \ll N_c$, and lower limit to N_D is given by the condition $N_D \gg n_i$, or $N_D \gg N_c \, (m_H^*/m_e^*)^{\frac{3}{4}} . \exp(-\Delta E/2kT)$. In these circumstances the semiconductor is said to be saturated.

Where both shallow donors and acceptors are present, under the same temperature conditions as above, so that intrinsic carriers are negligible, with $N_D \gg N_A$ the fermi level will be well above the middle of the forbidden gap. The acceptor levels will have a high probability of being occupied by an electron, since they are well below the fermi level, and the electrons will come from the donor levels. The effective number of donors is therefore $N_D - N_A$, and the fermi level is given by $N_D - N_A = N_c \exp(E_f/kT)$. (1.18)

As $N_A \to N_D$, the donors are neutralised by the acceptors and the fermi level approaches its intrinsic value. For $N_A \gg N_D$ the fermi level approaches the valence band.

Consider now the low temperature case where full ionisation has not taken place. (E_D, E_A not small cf. kT). We neglect any degeneracy of the impurity levels and consider only the case where a level can contain only one electron, of either spin. The probability of an electron of either spin occupying the level is

$$P(E) = \frac{1}{1/2 \exp\left[(E-E_f)/kT\right] + 1} \qquad (1.19)$$

Therefore with N_D donors, the number of unionised donors is N_d, where

$$N_d = \frac{N_D}{1+1/2\ \exp[(E-E_f)/kT]} \qquad \& E=-E_D$$

Similarly the number of 'unionised' acceptors is N_a;

$$N_a = \frac{N_A}{1+1/2\ \exp[(E_f-E)/kT]} \qquad E=-\Delta E+E_A$$

To calculate the electron and hole concentrations we utilise the condition that for electrical neutrality in the crystal, we have

$$n + N_d + N_A = p + N_a + N_D$$

Under the conditions assumed, we can neglect p, the number of free holes, and N_a will be small.

Hence $$n = N_D - N_A - \frac{N_D}{1+1/2\ \exp[(E-E_f)/kT]} \qquad (1.20)$$

Writing $n = N_c \exp(E_f/kT)$ we obtain a quadratic for $\exp(E_f/kT)$ or for n,

$$n^2 + n(N_A + N_c') - N_c'\ (N_D - N_A) = 0$$

$$\text{where } N_c' = \tfrac{1}{2}N_c \exp(-E_D/kT)$$

The appropriate solution is

$$n = \tfrac{1}{2}\ (N_A + N_c') + \tfrac{1}{2}\ ((N_A + N_c')^2 + 4N_c'\ (N_D - N_A))^{\frac{1}{2}} \qquad (1.21)$$

When $E_D/kT >> 1$, N_c' will be small and we may approximate. For partially compensated semiconductors, we can assume $N_c' << N_A$, and can expand $(N_A + N_c')^2$.

Then $$n \doteq \frac{N_c'\ (N_D - N_A)}{N_A} = \frac{N_D - N_A}{2N_A}\ N_c \exp(-E_D/kT) \qquad (1.22)$$

Where N_A is so small that $N_A << N_c' << N_D$,

$$n \doteq (N_c'N_D)^{\frac{1}{2}} = \tfrac{1}{2}(N_DN_c)^{\frac{1}{2}} \exp\ (-E_D/2kT) \qquad (1.23)$$

Thus a measurement of the free electron density n as a function of temperature can lead to a value of E_D provided the temperature range

is such that the appropriate limitations mentioned are satisfied. In this case a plot of $\ln.(\frac{n}{T^{3/2}})$ against $\frac{1}{T}$ would be a straight line of slope - E_D/k, or - $E_D/2k$ in the non-compensated case.

1.3.5 Electrical conduction

First consider the effect of an electric field ϵ on a classical gas of free electrons. The electrons in the absence of an electric field move in a random way, with a velocity distribution appropriate to their temperature T. The net drift velocity v_d of the electrons in any direction is zero. Under the influence of an applied force the electrons acquire an average drift velocity in the direction of the force given by $v_d = \frac{1}{N}\sum_{i=1}^{N} v_i$ where N is the electron concentration.

We introduce a constant relaxation time τ, related to the mean free time between electron collisions, and therefore also related to their mean free path and velocity. The relaxation time is the characteristic time which determined the establishment of equilibrium by collisions from an initial situation where $v_d \neq 0$.

For an external force F acting on an electron, we can write the equation of motion

$$F = m(\frac{dv_d}{dt} - \frac{1}{\tau} \cdot v_d)$$

Where no external force acts, the variation of v_d with time is given by $v_d(t) = v_d(0)\exp(-t/\tau)$, so an initial disturbance dies away with a characteristic time τ.

In an electric field ϵ the force on each electron is $\epsilon.e$,

$$\therefore \quad \epsilon.e = m(\frac{dv_d}{dt} - \frac{v_d}{\tau})$$

The assumption of a finite relaxation time gives a steady state solution in keeping with Ohm's law, and the solution when $\frac{dv_d}{dt} = 0$ is

$$v_d = \frac{e.\tau.\epsilon}{m}$$

The drift mobility μ is defined as the drift velocity per unit electric field, and is given from the above equation by

$$\mu = \frac{e\tau}{m} \qquad (1.24)$$

The electric current density j is defined as the electric charge transported through unit area in unit time; hence

$$j = n\ e\ v_d$$

where n is the carrier concentration and e the electronic charge. Substituting for v_d we have the result

$$j = \frac{n\ e^2\ \tau.\epsilon}{m} \qquad \text{(Ohm's law)}$$

Current density $j = \sigma\epsilon$, where σ is the electrical conductivity, so that

$$\sigma = \frac{n\ e^2\tau}{m}\ , \text{ or } \sigma = n\ e\mu. \qquad (1.25)$$

1.3.6 Conduction electrons in solids

Within certain limits the band theory approach gives similar results for electrons in solids. The free electron mass m must be replaced by the appropriate effective mass m^*. Since only those electrons with energies near the Fermi level effectively take part in conduction in a degenerate semiconductor, the relaxation time is that appropriate to electrons near the Fermi level, and $\mu = \frac{e\tau_{(E_f)}}{m^*}$.

For non-degenerate semiconductors, where the energy distribution of the electrons in the conduction band is Maxwellian, the assumption that τ can be considered as a constant for all electrons is no longer valid. Consider a simple n-type semiconductor with isotropic effective mass, i.e. spherical energy surfaces. In an applied field ϵ_x the current density J_x is given by the Boltzmann transport equation,

$$J_x = \frac{-e^2\epsilon_x}{3}\int_0^\infty \frac{\partial F_0}{\partial E} v^2\tau(E).\frac{8\pi}{h^3}.p^2.dp \qquad (1.26)$$

Nowdifferentiating the Fermi-Dirac function F_0, $\frac{\partial F_0}{\partial E} = \frac{F_0(1-F_0)}{kT}$

and since we assume non-degeneracy $F_0 << 1$, and $\frac{\partial F_0}{\partial E} \doteq \frac{F_0}{kT}$

Hence

$$J_x = \frac{e^2\epsilon_x}{3kT}\int_0^\infty F_0 v^2\tau(E)\frac{8\pi}{h^3}.p^2.dp \qquad (1.27)$$

However $\frac{8\pi}{h^3}.F_0.p^2.dp$ is the concentration of electrons with momentum lying between p and p + dp, so on integration we obtain

$$J_x = \frac{e^2\epsilon_x}{3kT}.n.\langle v^2\tau(E)\rangle$$

where n is the electron concentration in the conduction band, and $\langle v^2\tau\rangle$ is the mean value of $v^2\tau$ averaged over the Maxwellian velocity distribution. According to kinetic theory $3/2kT = m^*\langle v^2\rangle/2$ so we can write

$$J_x = \frac{n e^2\epsilon_x\langle v^2\tau\rangle}{m^*\langle v^2\rangle} \qquad (1.28)$$

and the mobility μ becomes

$$\mu = \frac{\langle v^2\tau\rangle e}{\langle v^2\rangle m^*} \qquad (1.29)$$

(This reduces to $\frac{e\tau}{m^*}$ where τ is no longer a function of E and therefore independent of v^2.)

The mobility so defined is called the conductivity mobility.

The way in which τ depends on the electron energy E is determined by the dominant scattering mechanism in the sample. The dependence for the major forms of scattering will be summarised later in table 1.1.

1.3.7 Conduction due to both electrons and holes

We have seen (Eqn. 1.25) that the conductivity for an n-type semiconductor is given by $\sigma = ne\mu$. Similar results apply for p-type semiconductors, and in general the conductivity σ due to both sets of carriers is given by

$$\sigma = ne\mu_e + pe\mu_p \qquad (1.30)$$

where μ_e and μ_p are the mobilities for electrons and holes respectively.

1.4 Hall Effect

1.4.1 Simple treatment

Measurements of the Hall voltage and electrical conductivity provide a means of determining the values both of the carrier density and of the mobility, and indicate whether electrons or holes are the dominant carriers in the conduction process.

We shall consider first a simple treatment in which the relaxation time τ is regarded as independent of energy, so that we can regard the carriers in a solid as having an average drift velocity and need take no account of the velocity distribution. The treatment is in general applicable to metals and degenerate semi-conductors.

Consider an electric field ϵ_x applied to a long narrow rectangular conductor as shown in Fig. 1.5., with the resulting current density J_x. A magnetic field B_z in the z-direction will give rise to an electric field in the y-direction, mutually perpendicular to the applied electric

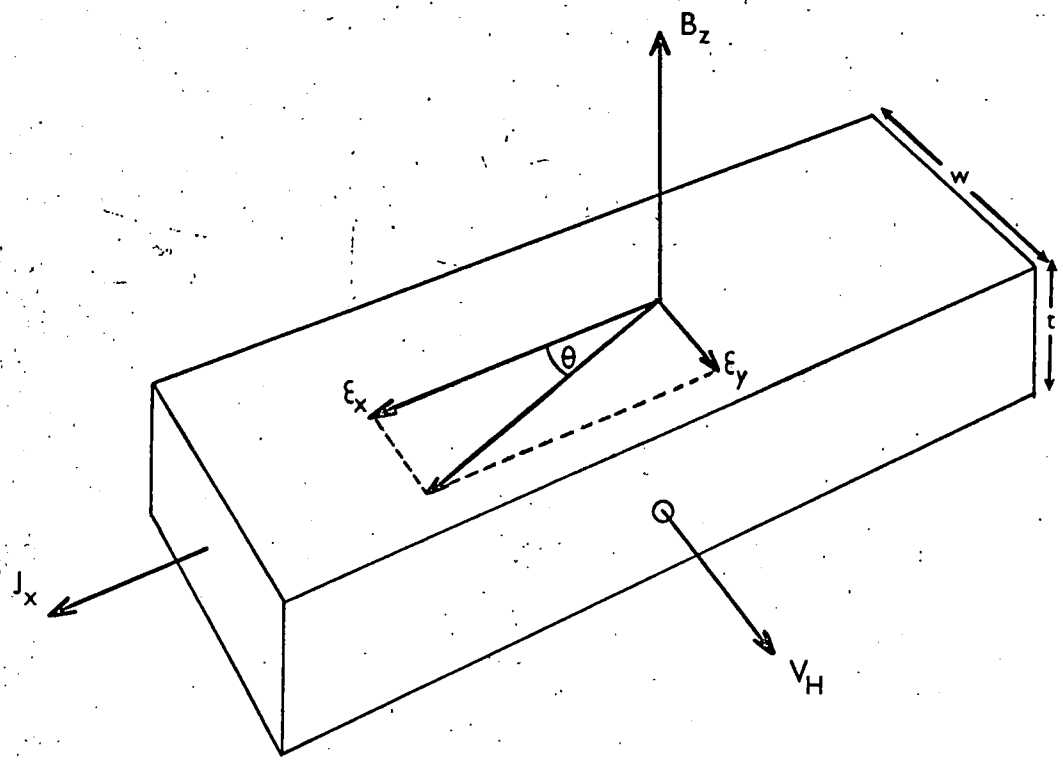

THE HALL EFFECT.

FIGURE 1.5

and magnetic fields, which owes its origin to the deflection of the charged carriers by the magnetic field. Carriers will be deflected and will build up a space charge at one side of the sample until the electric field set up, ϵ_y, is sufficient to balance the Lorentz forces. ϵ_y is called the Hall field and $\epsilon_y = R_H J_x . B_z$ where R_H is called the Hall constant.

With an n-type semi-conductor, in equilibrium,

$$e.\epsilon_y = -e.B_z.\bar{v}_x \qquad (1.31)$$

where $\bar{v}_x$ is the mean drift velocity.

Now the current $i = n.e.\bar{v}_x$, so the Hall constant

$$R_H = \frac{\epsilon_y}{B_z J_x} = \frac{-1}{ne} \qquad (1.32)$$

The resultant electric field due to ϵ_x and ϵ_y deviates from the X-direction by the Hall angle θ, where $\tan\theta = \epsilon_y/\epsilon_x = R_H \sigma . B_z$.

If the sample is of thickness 't' in the z-direction, the measured Hall voltage will be

$$V_H = \frac{-B_z I_x}{n.e.t.} \qquad (1.33)$$

and the carrier density can be obtained from the experimentally obtained parameters since

$$\frac{-1}{ne} = R_H = \frac{-V_H . t}{I_x B_z} \qquad (1.34)$$

A simultaneous measurement of the conductivity σ of the sample enables the Hall mobility μ_H to be found, since $\sigma = ne\mu$, and the Hall mobility $\mu_H = \sigma . R_H$.

For a p-type semi-conductor, the carriers would be deflected to the same side of the sample. As a result V_H and R_H would be reversed in sign, indicating that hole conduction was dominant.

1.4.2 Two-carrier Conduction

The Hall coefficient is more complex if the solid contains appreciable numbers of both types of carriers. It can be shown that in this case

$$R_H = \frac{1}{e} \cdot \frac{p-b^2n}{(nb+p)^2} \qquad (1.35)$$

where $b = \mu_e/\mu_h$.

It is obvious from this that $R_H \to 0$ as $p \to b^2n$, so that the change in sign of the Hall coefficient is dependent both on the carrier density and the mobility of each carrier.

1.4.3 Hall Effect - τ a function of energy

The Hall effect will now be considered for an n-type semiconductor under conditions where τ, although still isotropic, is a function of the carrier energy E.

We use again the situation depicted in Fig. 1.5., and suppose that the Hall contacts are short-circuited, allowing a Hall current I_y to flow. An electron moving in the x-direction with velocity v_x will experience an acceleration in the y-direction of $\frac{B_z e v_x}{m^*}$.

$$\therefore \quad \left(\frac{\partial v_y}{\partial t}\right)_{B_z} = \frac{e v_x B_z}{m^*} = \omega v_x \qquad (1.36)$$

where $\omega = \frac{eB}{m^*}$ is the Larmor frequency.

This acceleration will be opposed by forces due to collisions with the lattice, so that $\left(\frac{\partial v_y}{\partial t}\right)_{coll.} = \frac{-v_y}{\tau(E)}$,

and in equilibrium we have $v_y = \omega \tau v_x$. (1.37)

Now from eqn. (1.27),

$$J_x = \frac{e^2 \epsilon_x}{3kT} \int_0^\infty F_0 v^2 \tau(E) \frac{8\pi}{h^3} p^2 dp = \frac{n e^2 \epsilon_x}{3kT} \langle v^2 \tau(E) \rangle$$

Since I_y can be related to I_x through the relation of the velocities, (Eqns. 1.27, 1.31), multiplication under the integral by $\omega\tau$, followed by evaluation as in 1.3.6., gives

$$I_y = \frac{ne^2\epsilon_x\omega}{3kT} \langle v^2\tau^2 \rangle \qquad (1.38)$$

where $\langle v^2\tau^2 \rangle$ is the mean value of $v^2\tau^2$ over the Maxwellian distribution of electron velocities.

When the Hall contacts are not short-circuited, an electric field $\epsilon_y = I_y/\sigma$ is set up which reduces the current in the y-direction to zero. The Hall coefficient R_H then becomes

$$R_H = \frac{\epsilon_y}{I_x B_z} = \frac{I_y}{\sigma . I_x B_z} \qquad (1.39)$$

Using equations (1.28) and (1.29) we can therefore evaluate the Hall mobility μ_H as

$$\mu_H = R_H\sigma = \frac{e\langle v^2\tau^2 \rangle}{m^* \langle v^2\tau \rangle} \qquad (1.40)$$

Comparing this with the conductivity mobility we find that in general $\mu_H \neq \mu$, unless τ is independent of energy as in the case of a metal or degenerate semi-conductor. The Hall coefficient

$$R_H = \frac{1}{ne} \frac{\langle v^2\tau^2 \rangle \langle v^2 \rangle}{\langle v^2\tau \rangle^2} \qquad (1.41)$$

and in general is written as $R_H = r/ne$, where $r = \frac{\langle v^2\tau^2 \rangle \langle v^2 \rangle}{\langle v^2\tau \rangle^2}$. The value of the factor r depends on the form of the variation of τ with energy E. The nature of this variation is determined by the nature of the electron scattering in the solid. The major types of electron scattering will now be discussed.

1.5 Electron Scattering in Crystals

1.5.1 Types of scattering

We have seen already that the conductivity of a material is determined by (a) the number of carriers, and (b) their mobility or mean free path, which is determined by the various carrier scattering mechanisms present. In a perfect crystal (at $0^{\circ}K$) there would be no electron scattering; only perturbations caused by departures from perfection can deflect the electron.

The most important sources of electron or hole scattering are:-

1. Lattice scattering, by thermal vibrations of the lattice.
2. Impurity scattering, by charged or neutral impurities.
3. Scattering by imperfections, e.g. dislocations, bubbles.
4. Scattering of carriers by each other.

1.5.2 Lattice scattering

The scattering produced by thermal vibrations in the lattice can be considered in several ways. In the 'deformation potential' method, the lattice vibration, which is an acoustic wave of definite velocity and wavelength, is considered as superimposing a new periodicity on the lattice potential. In a semiconductor this is seen as a 'ripple' in the bottom of the conduction band. A detailed discussion of the method was given by Bardeen and Shockley,[5] with a simplified account by Shockley[6]. In his discussion, he treats the semiconductor as a group of independent blocks, each representing a potential barrier which can scatter electrons.

The average energy of thermal vibration, 3/2 kT, is shown to be equivalent to an energy change in the conduction band E_c, where

$$E_c = kTE_{ln}^2/v_oB$$

and B is the bulk modulus of the material, E_{ln} the change in the bottom of the conduction band per unit deformation and v_o the specific volume.

The energy barrier E_c is then considered as a barrier which can reflect electrons according to quantum mechanical principles, even if the electron energy is much greater than the height of the barrier. A mean free path 'l' is calculated from the reflection coefficient, since the probability of a scattering collision in a distance L is $e^{-L/l}$, where L is the width of the scattering 'block'.

The expression for l is

$$l = \frac{\pi h^4 c_{ll}}{(2\pi)^4 m^{*2} E_{ln}^2 kT}$$

where c_{ll} is the longitudinal elastic constant. The resulting mobility μ_L is

$$\mu_L = \frac{2\sqrt{2}\,.\,\pi}{3}\,\frac{c_{ll}}{E_{ln}^2}\left(\frac{k}{m^*}\right)^{5/2} T^{-3/2} \qquad (1.42)$$

We note here that the mobility varies as $T^{-3/2}$, and also that mobility depends on the effective mass to the power $-5/2$. A consequence of this treatment is that the collision time associated with barrier scattering is spherically symmetric, with no preferential direction for scattering, although in many materials this is known not to be the case. Shockley points out that the discussion is highly oversimplified, since the blocks were considered as independent, not tightly coupled as in a real material.

Scattering by optical vibrations was invoked to explain deviations from the $T^{-3/2}$ dependence of mobility in the covalent semiconductors Ge

and Si; the resultant mobility is given by

$$\frac{1}{\mu} = \frac{1}{\mu_{ac}} + \frac{1}{\mu_{op}} \qquad (1.43)$$

where

$$\mu_{ac} \propto T^{-3/2}$$

$$\mu_{op} \propto T^{-\frac{1}{2}} (e^{\theta/T} - 1), \qquad (1.44)$$

and θ is the equivalent temperature of the optical phonons involved[7]. Optical scattering can be the dominant lattice scattering mechanism in ionic materials.

In a piezo-electric material, scattering of conduction electrons by the longitudinal electric fields accompanying acoustic lattice vibrations results in departures from the mobility predicted by the deformation-potential scattering method of Bardeen and Shockley. The modifications necessary to take account of piezo-electric scattering in CdS have been considered by Hutson[8], who found that

$$\mu \doteqdot 400(m/m^{*})^{3/2}(300/T)^{\frac{1}{2}} \qquad (1.45)$$

1.5.3 Charged impurity scattering

Conwell and Weisskopf[9] have considered the scattering of carriers by charged impurities, using the Rutherford scattering formula to show that the scattering cross-section is

$$\sigma(\theta) = \frac{e^4}{(2Km^{*}v^2)^2} \operatorname{cosec}^4 \frac{\theta}{2} \qquad (1.46)$$

where θ is the angle of scattering.

Averaging the cross-section over the velocities found in a semiconductor gives the time between collisions as

$$\tau \equiv \frac{2d}{v} = \frac{(2E/E_1)^2}{\ln[1+(2E/E_1)^2]}$$

where E is $mv^2/2$, $E_1 = 2e^2/\kappa d$, and d is the distance between impurity centres, assumed to be uniform.

Averaging over the Boltzmann distribution gives the mobility due to impurity scattering

$$\mu_I = \frac{8}{\pi}\sqrt{\frac{2}{\pi}} \frac{\left(\frac{\kappa^2 (kT)^{3/2}}{N e^2 m^{*1/2}}\right)}{\ln\left[\left(1+\frac{3\kappa kT}{e^2 N_I^{1/3}}\right)^2\right]} \qquad (1.47)$$

Thus $\mu_I \propto T^{+3/2}$, and imperfection scattering can be particularly important at low temperatures, when lattice scattering decreases.

Later calculations by Blatt[10] indicate that this temperature dependence is only an approximation, being most accurate at higher temperatures; at lower temperatures μ is strictly not proportional to T^n. Sclar[10] has shown that considerable deviations from $T^{+3/2}$ can occur, especially at low temperatures or for large impurity densities.

When both lattice and impurity scattering are important, it is generally assumed that resistivities due to different scattering mechanisms are additive, and

$$\frac{1}{\mu} = \frac{1}{\mu_L} + \frac{1}{\mu_I} \qquad (1.48)$$

Conwell[12] has shown that this is not accurate, since the lattice scattering collision time and impurity collision time depend in different ways upon the energy. Fig. 1.6 shows the ratio of total to lattice mobility, plotted against the lattice to impurity mobility ratio. These results assume the validity of a spherical Fermi surface model.

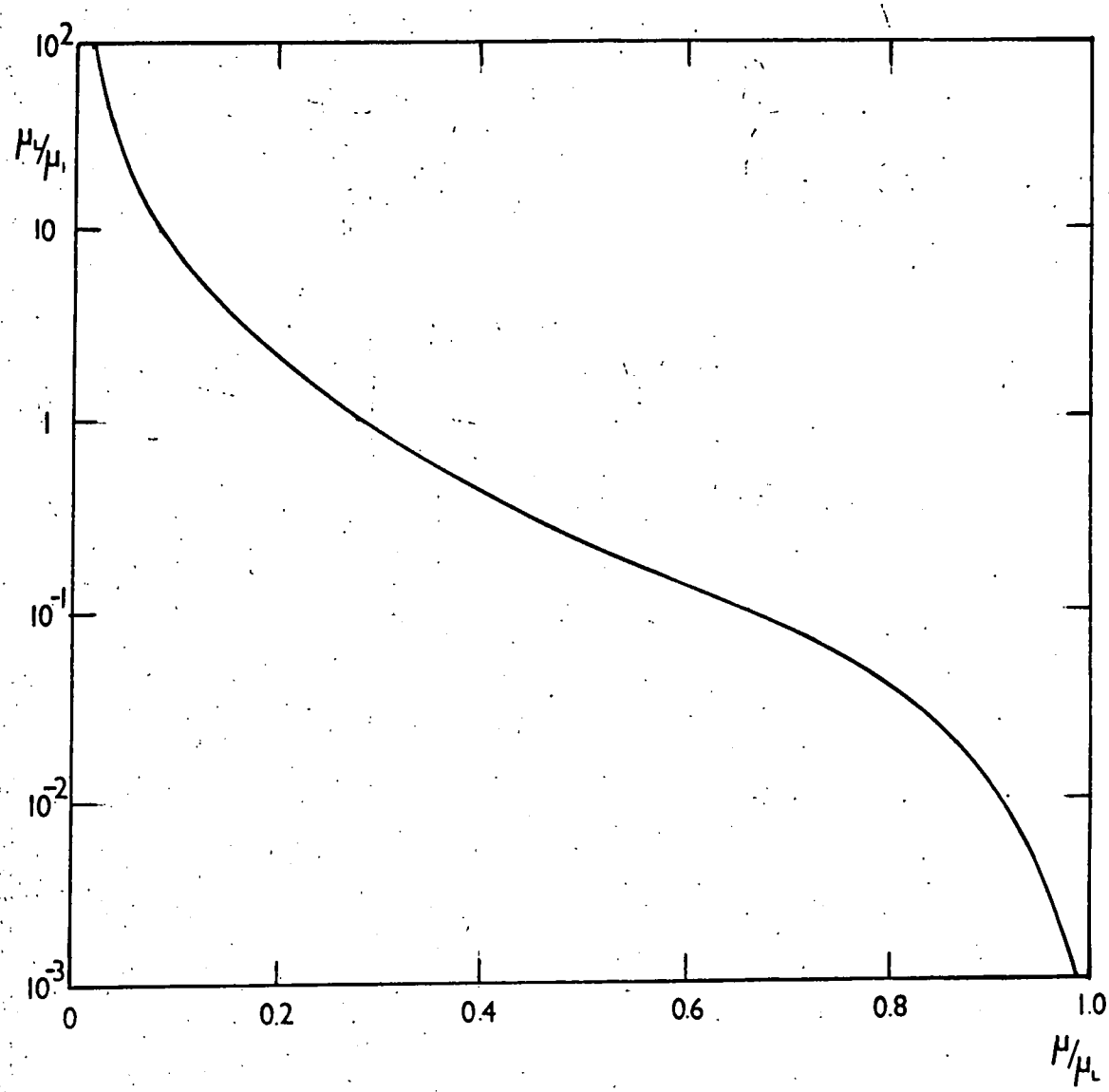

Total to lattice mobility ratio versus lattice to impurity mobility ratio.

FIGURE 1.6

1.5.4 Neutral impurity scattering

Neutral impurities can give rise to large scattering effects in crystals, but the theory is very uncertain.

Pearson and Bardeen[13] estimated that

$$\frac{1}{\mu_I} = 7.6 \times 10^{-22} N_n T^{\frac{1}{2}} \qquad (1.49)$$

Erginsoy[14] treated the neutral impurity as a hydrogen atom in a material of the appropriate dielectric constant, and found

$$\rho_n = 20\pi N_n h^3 / 8\pi^3 n\, m^{*} e^4 \qquad (1.50)$$

so that mobility should be inversely proportional to impurity density with no temperature dependence.

Sclar[15] has performed further calculations which indicate a slight temperature dependence.

1.5.5 Dislocation scattering

Dislocations are one form of crystal imperfection which can have an effect on carrier mobility. Because of their irregularity, their influence is difficult to calculate with an accuracy, but Dexter and Seitz[16] have applied a method similar to the deformation potentials for lattice scattering. They conclude that, if the dislocation density were as high as $10^8/cm^2$, the effect on mobility should become apparent, and with a density of $10^{11}/cm^2$ the dislocation scattering has about the same magnitude as vibration scattering, at room temperature. At a temperature T, dislocation scattering is comparable to vibrational scattering for a dislocation density $N_{dis} = 6 \times 10^4 . T^{5/2}\ cm^{-2}$.

Table 1.1 Summary of Scattering Mechanisms (From[18])

Mechanism	$\mu \propto (m^*)^x T^y$		$\tau \propto E^z$	$R_H = -r/ne$,
	x	y	z	r
Acoustic	-5/2	-3/2	-1/2	$3\pi/8$
Polar	-3/2	Exponential	Independent	1.00-1.14
Ionised Impurity	-1/2	3/2	3/2	$315\pi/512$
Neutral Impurity	1	Indep.	Independent	1
Electron-Hole	-1/2	3/2	3/2	$315\pi/512$

Read[17] has considered the effect of charged dislocations, and finds that $1/\mu$ varies as T^{-1}.

1.5.6 Carrier-carrier scattering

When the effective mass of holes is larger than that of electrons, electron-hole collisions can reduce the electron mobility. The analysis of the effect and resultant temperature dependence is similar to that for ionised impurities. Electron-electron collisions are more complex; but can generally be neglected.

1.6 PhotoHall effect in semiconductors

1.6.1 Introduction

Conventional Hall effect measurements may not be possible on high resistivity samples due to the measurement problems posed by the high impedance. In these circumstances a PhotoHall measurement can be made; i.e. the Hall effect is measured on a sample in which extra carriers are being generated by illumination. However the measured Hall mobility μ_H may vary with intensity of illumination. This variation could be due to (i) change in the mobility for single carrier conduction, or (ii) initiation of two-carrier conductivity. Initial experiments showing this mobility variation were confined to germanium and silicon[19-22]. Bube and MacDonald give a detailed account of the evaluation of properties of CdS and CdSe using photoHall data[23]. Mobility changes by a factor of 6 at room temperatures have been observed in CdS. As will be seen later, where these can be attributed to changes in the number or charge of scattering centres, a value of the scattering cross-section of the centre can be determined. In addition, the sign of the mobility change indicates the

effective charge of the centre. The variations in mobility can also lead to an estimate of the energy depth of the centre relative to the conduction band.

1.6.2 Scattering cross-sections

Imperfection centres play a large part in determining the mobility of free carriers in semiconducting materials, especially when these centres are charged and thus have an appreciable associated coulomb field. (See section 1.5.3) Any variation in the state of charge of such centres, e.g. by capture or loss of an electron or hole, will have a resulting effect on the mobility.

If we equate the coulomb attraction of a centre, $\frac{Ze^2}{\epsilon r}$, to the thermal energy of an electron, kT, we can obtain an approximate value for its capture cross-section.

$$\frac{Ze^2}{\epsilon r} = kT$$

where Z is the electronic charge on the centre, r its radius and ϵ the dielectric constant of the material. Hence the scattering cross-section S_o is

$$S_o \doteq \pi r^2 = \frac{Z^2 \pi e^4}{\epsilon^2 k^2 T^2} \qquad (1.51)$$

More detailed calculations for the scattering cross-section can be performed. The Conwell-Weisskopf[18] equation for the mobility due to coulomb scattering gives a cross-section $S_{cw} = K_{cw} S_o$, for singly charged centres, and K_{cw} varies between 1.4 and 0.4 as the density of singly charged carriers varies from 10^{12} to 10^{18} cm^{-3}. (This assumes a value of $\epsilon = 10$ at 300°K). The mobility equation due to Brooks and Herring[24] gives a

similar result. Hence we can safely use the approximate expression for S_o given in (1.51) and have values of the correct order. At room temperature we have $S \sim 10^{-12} cm^2$ for a singly charged centre, or more generally $S \sim 10^{-12}.Z^2 cm^2$.

1.6.3 Hall mobility

In the situation where carriers of one type dominate, we can write the conductivity $\sigma = ne\mu$, (n is the free carrier density, μ the conductivity mobility). The Hall constant $R_H = r/ne$, and the Hall mobility $\mu_H = \sigma R_H = r\mu$, where r is a constant between 1 and 2 which depends on the scattering mechanism and the band structure. (See section 1.5). Hence the variation of Hall mobility with light intensity L is given by

$$\frac{d\mu_H}{dL} = \mu . \frac{dr}{dL} + r. \frac{d\mu}{dL} \qquad (1.52)$$

The term $\mu.\frac{dr}{dL}$ represents the change in Hall mobility due to any change in the scattering mechanism with increased photoexcitation, and can in general be neglected. Since r can only take values between 1 and 2, any variation from this cause will be less than a factor of 2, even when going from completely impurity-dominated to phonon-dominated scattering.[26] Moreover it can be shown that r decreases with L in this case.[23]

In the case of two-carrier conduction, the Hall constant R_H is given by

$$R_H = \frac{\sigma_n^2 . R_n + \sigma_p^2 . Rp}{(\sigma_n + \sigma_p)^2} \qquad (1.53)$$

where R_n, R_p, σ_n, σ_p are the Hall constants and conductivities due to electrons and holes respectively, and the Hall mobility, $\mu_H = \sigma R_H$ is therefore given by

$$\mu_H = \frac{p.\mu_p^2 - n.\mu_n^2}{p.\mu_p + n.\mu_n} \qquad (1.54)$$

neglecting r as before.

We can see from (1.54) that the measured Hall mobility μ_H is almost independent of p and μ_p if n >> p, especially as in CdS $\mu_n > \mu_p$. However should the excitation by incident light be capable of producing comparable numbers of electrons and holes, the onset of two-carrier conductivity will give a variation in Hall mobility if the photoexcitation intensity is varied. This is one of the two possible causes of the PhotoHall effect. With a typical ratio of $\mu_n:\mu_p$ of 10:1, the Hall mobility is reduced by 10% for p ~ n, and by 50% for p ~ 10n. Bube[23] has found mobility variations indicating a hole concentration some 30 to 60 times the concentration of free electrons under conditions of infra-red quenching. Onuki and Hase[26] were able to measure a hole mobility in CdS of 38 $cm^2/v.sec.$, rising to 48 $cm^2/v.sec.$ under more intense illumination.

1.6.4 Effect of impurity centres on mobility

The second possible cause of the PhotoHall effect; i.e. the variation of Hall mobility under conditions of single carrier conduction, arises from variations in effective charge, and hence the scattering cross-section of impurity of the centres. As we have seen from (1.52), we can neglect variation in μ_H from other causes in comparison with changes due to variations in the drift mobility, i.e. $\frac{d\mu_H}{dL} \doteqdot \frac{d\mu}{dL}$. To find the variation of μ with L we consider a simple case. Normally ionised donor levels lying above the Fermi level in the dark are filled with electrons as the Fermi level rises under increasing illumination. Thus their charge is removed, and their scattering decreases markedly. This case is illustrated in Fig. 1.7 (a). The mobility μ is given by

$$1/\mu = \beta/\tau_0 + vS_+\beta(N_+ - n_+) \qquad (1.55)$$

where $\beta = m^*/e$ is the proportionality factor between mobility and time between scatterings. β/τ_o allows for all scattering processes e.g. lattice scattering, not dependent on the number of charged centres; v is the electron thermal velocity, and S_+ is the scattering cross-section of the positive centre, where the density of centres is N_+ and the density of electrons in these centres n_+. The number of impurity centres ionised, $(N_+ - n_+)$, is given by

$$N_+ - n_+ = \frac{N_+}{1 + 2\exp\left[(E_f - E_+)/kT\right]} \qquad (1.56)$$

Here E_+ and E_f are the energy levels of the impurity centres and the electron Fermi level, measured below the conduction band, E being positive upwards. If we consider E_f varying from $E_f << E_+$ to $E_f >> E_+$, i.e. as more and more centres are filled by electrons, we have $(N_+ - n_+)$ going from N_+, through $N_+/3$ for $E_f = E_+$, to $(N_+ - n_+) \Rightarrow 0$. Thus for this change in E_f, $1/\mu$ passes through a single step, $1/\mu$ decreasing as E_f increases, due to the reduced scattering from the now neutral centres.

Let the change in $1/\mu$ be $\Delta(1/\mu)$

Then $\Delta(1/\mu) = \beta v S_+ N_+$ (1.57)

Since $\beta = m^*_e/e$, and $v = \left(\frac{2kT}{m^*_e}\right)^{\frac{1}{2}}$ the change $\Delta(1/\mu)$ gives a value of $S_+ N_+$, and for S_+ if N_+ is known from an alternative measurement e.g. thermally stimulated currents. (see Section 2.2). The diagram (Fig.1.7(b)) shows the expected variation of $1/\mu$ with E_f.

Bube and MacDonald have also considered the variation in $1/\mu$ for other types of centres; the detailed analysis can be found in the original reference.

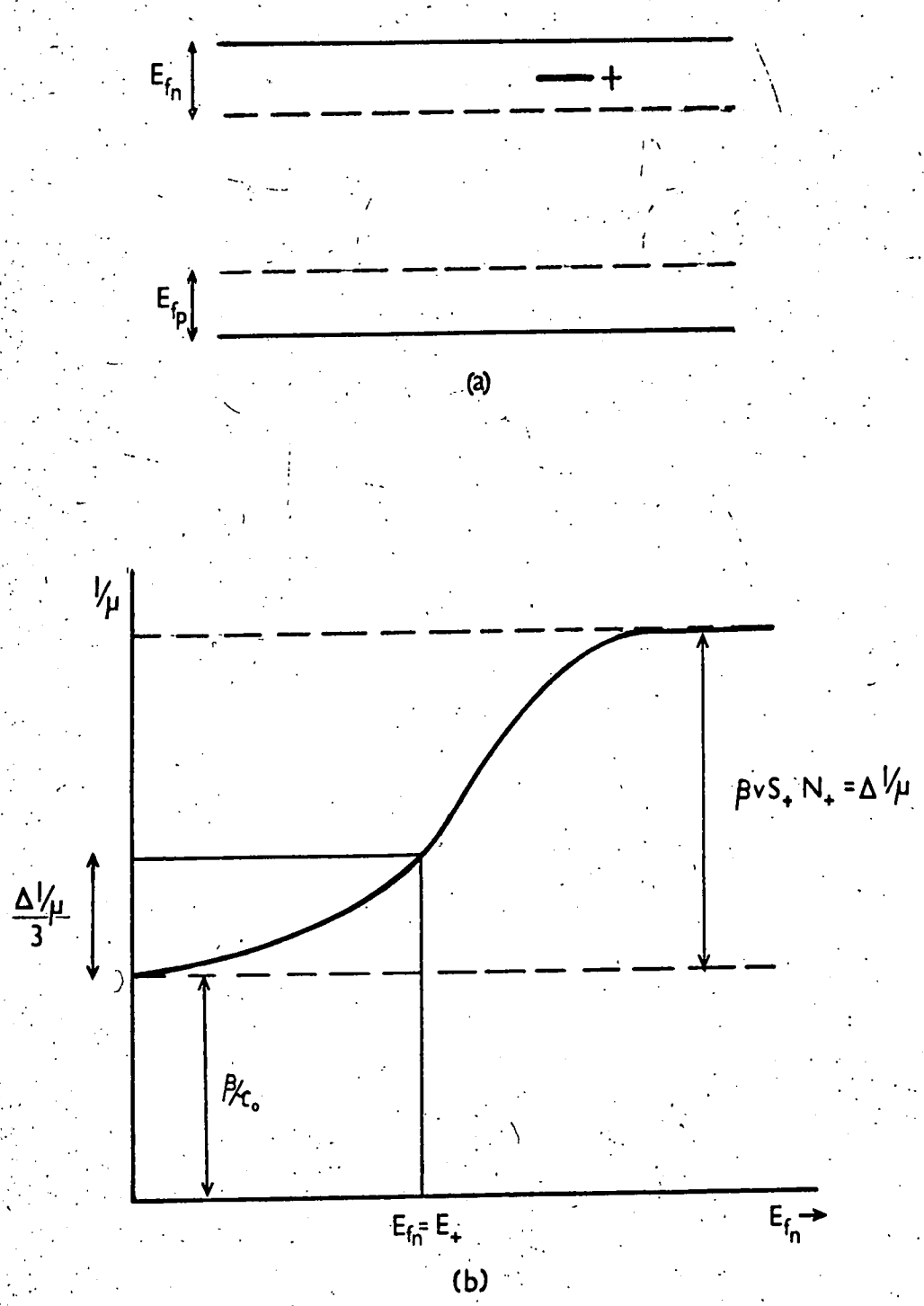

PHOTOHALL EFFECT: level system (a) gives mobility change (b).

FIGURE 1.7

CHAPTER 2.

PROPERTIES OF CADMIUM SULPHIDE

2.1 Introduction

Cadmium sulphide is a II-VI compound which normally crystallises in the hexagonal (wurtzite) structure. The inter-atomic distance between the cadmium atom and its four sulphur nearest neighbours is 2.52Å, with the lattice parameters a = 4.13Å and c = 6.69Å.[27] A cubic phase can also exist, but is not common (e.g. 28).

In common with zinc sulphide and the selenides and tellurides of zinc and cadmium, cadmium sulphide is a wide band gap semiconductor, or semi-insulator. The energy gap of cadmium sulphide is usually quoted as 2.43 ev. at room temperature[29] and 2.52 ev. at liquid nitrogen temperature, although the value found may depend on the method of measurement. For instance Sommers[30] obtained a value of 2.48 ev. from the photoelectromagnetic effect (PEM) measured at room temperature.

The pure stoichiometric high resistivity ($>10^{10}$ cm) n-type CdS can readily be converted to a low resistivity n-type semiconductor by the introduction of group I (halide) impurities which substitute for the sulphur atoms and act as shallow donor levels 0.03 ev. below the conduction band. Aluminium, gallium or indium will substitute for cadmium and produce similar levels.[31] Incorporation of a non-stoichiometric excess of cadmium will also produce shallow donor levels, which are due to the formation of sulphur vacancies.

P-type cadmium sulphide cannot yet be produced, probably because of the high activation energy of acceptors, which lie ~1.0 ev. above the valence band,[32,33] / and of the problems of compensation. Copper and silver impurities, or cadmium vacancies, will

produce such levels. A very high level of copper doping produces samples which show p-type conduction, but this is most probably due to conduction in an impurity band.(34)

The defect or impurity levels which lie between the bands can dominate the electrical and optical properties of the material. This has resulted in widespread studies of defect levels in cadmium sulphide, in attempts to obtain information about the exact nature of the centres themselves, with a view to improving and extending the use of the material in practical devices.

2.2 Photoconductivity

The absorption of light by a photoconductor frees charge carriers which contribute to the electrical conductivity of the material until they are trapped or recombine. The important parameters of photoconductors, i.e. speed of response, sensitivity, dark conductivity, etc., are strongly affected by the nature and density of crystal imperfections present. In an intrinsic photoconductor, incident radiation of energy $h\nu$ greater than the band gap generates equal numbers of electrons and holes in the conduction and valence bands respectively. The probability of direct recombination between a free electron and a free hole is extremely low, and free carriers are usually captured by imperfection centres. These centres can be of two types; 'trapping centres', where there is a high probability that the electron (hole) will be thermally freed to the nearest band; and 'recombination centres' where the probability for thermal release is lower than the probability of recombination with a free carrier of opposite charge.

In CdS, impurities such as copper, or cadmium vacancies, produce levels $\sim$1 ev above the valence band which have a large capture cross-section for

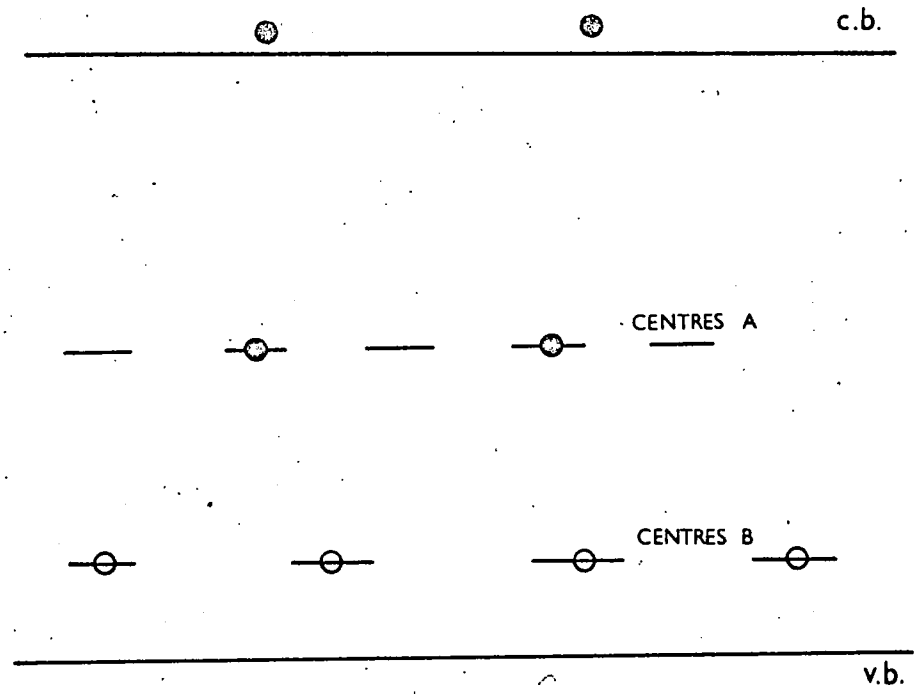

SENSITISING CENTRES

FIGURE 2.1

holes. Such centres are known as sensitizing centres, because their subsequent cross-section for the capture of a free electron is very low, perhaps less than 10^{-4} times the capture cross-section for holes.(35) Consequently the photo-excited electrons have a long effective lifetime, since the probability of recombination with a hole is low. The transit time for an electron to pass through the crystal under the influence of an applied field can therefore be small compared with the electron lifetime; this leads to a high value of the photoconductive gain G, defined as

$$G = \frac{\text{Number of electrons flowing between electrodes}}{\text{Number of photons absorbed}}$$

$$= \frac{\text{Lifetime of a free electron}}{\text{Transit time between electrodes}}$$

$$= \frac{\tau \mu V}{d^2}$$

τ free electron lifetime
μ free electron mobility
V applied voltage
d electrode spacing

Other centres which act as recombination centres are also present: These would dominate in the absence of sensitizing centres and reduce the free electron lifetime and the photoconductive gain. The two types of centres are illustrated in Fig. 2.1, for an n-type photoconductor such as CdS. Centres A have a large probability of capturing a free electron after capturing a hole, and are always present in the CdS so far produced. Centres B can be incorporated deliberately to produce a sensitive photoconductor since they reduce the probability of a type A centre being occupied by a hole. The electron lifetime in a material with deliberately incorporated recombination centres can be as low as 10^{-10} seconds; this rises to 10^{-6} seconds for pure material, and to 10^{-2} seconds if impurities such as copper

are added to give sensitizing centres.

The study of the energy depths of levels in the forbidden gap due to defect centres, and their capture cross-section, is therefore of the greatest importance in the study of photosensitive material. Investigations of the nature and properties of the deep-lying recombination centres are difficult, especially as the presence of defects in concentrations as low as 1 in 10^{12} can have a marked effect on crystal properties. Bube has used measurements of photoconductivity against temperature and against light intensity to evaluate some of the parameters of these levels.(36)

Measurements on shallow trapping levels are easier in comparison. One widely-used method is to measure the 'thermally stimulated current'. For thermally stimulated current measurements the crystal is cooled to liquid nitrogen temperature, and then exposed to illumination which will homogeneously excite the crystal. The radiation is removed, and the crystal heated at a linear heating rate in the dark. The current through the sample under constant applied field is monitored, and current peaks higher than the normal dark current result from carriers which are thermally excited from trapping levels as the temperature rises. Correlation exists between the maxima of the current versus temperature curve and the energy depth of the trap; the number of trapping centres can also be calculated from the area under the curve. In a recent investigation, Nicholas(37) found that at least six major trapping levels are common in cadmium sulphide single crystals, although each level does not occur in each sample. The levels, together with tentative identification, are as follows:

(i) 0.05 ev. Double negatively charged sulphur vacancy.

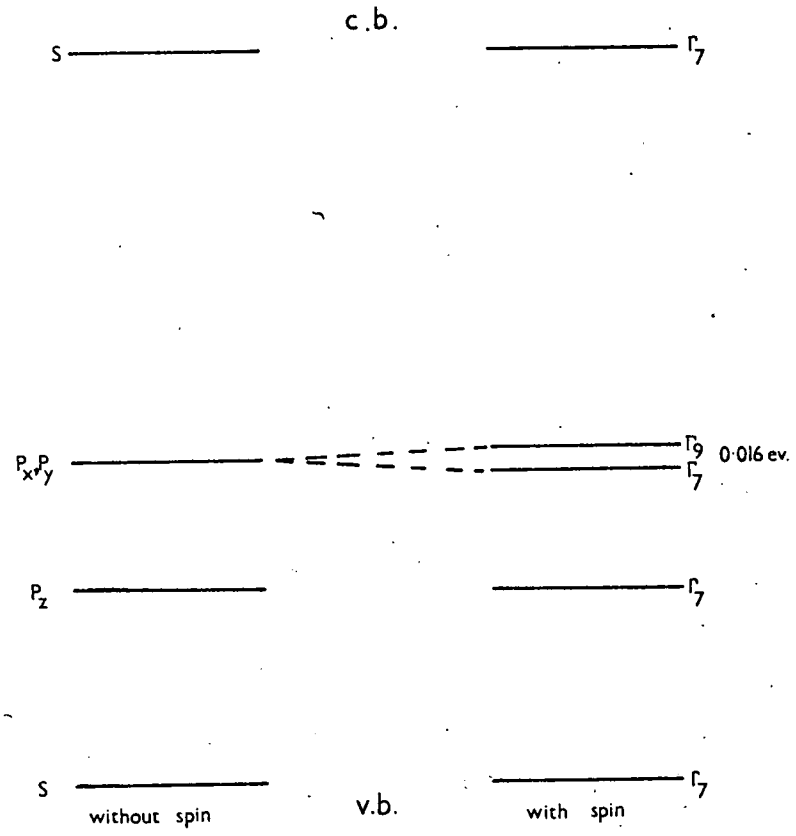

CdS BAND STRUCTURE [38]

FIGURE 2.2

(ii) 0.14 ev. Also associated with sulphur vacancies.

(iii) 0.25 ev. Singly charged sulphur vacancy.

(iv) 0.41 ev. An unidentified neutral level.

(v) 0.63 ev. A single positively charged cadmium vacancy.

(vi) 0.83 ev. is the activation energy for the destruction of a trap complex.

2.3 Band Structure

Calculations by Balkanski and des Cloiseaux[38] on the band structure of cadmium sulphide indicate that the valence band is split into three sub-bands. The lowest band arises from the s-orbitals of the sulphur ions. Crystal field splitting of the p-orbitals gives rise to the other two bands, the higher of which is further split into two closely spaced bands, 0.016 ev. apart, by spin-orbit coupling. The band structure is depicted in Fig. 2.2. The work of Thomas and Hopfield[39,40] on the reflectance and luminescence of cadmium sulphide, provides strong support for these ideas.

The selection rules for electronic transitions forbid excitation from the highest valence band to the conduction band ($\Gamma_9 \rightarrow \Gamma_7$) by light polarised parallel to the crystal c-axis.[41] This gives rise to anisotropies in the optical and luminescent properties. In measurements of the optical absorption Dutton[42] found a shift in the absorption edge comparing light polarised parallel with light polarised perpendicular to the c-axis. The shift of 0.016 ev. was equivalent to the splitting of the upper two valence bands. A similar effect is found in the photoconductive spectral response to polarised light.[43]

Estimates of the electron effective mass have been made by many workers.

Kröger, Vink and Volger[31] evaluated the effective mass from measurements of the Hall effect, resistivity, and thermo-electric power, and concluded that $0.20m_e \leqslant m^* \leqslant 0.27m_e$. Piper and Halstead,[44] using the temperature dependence of the Hall constant, found $m^* = 0.19m_e$. Cyclotron resonance experiments have been performed by Dexter,[45] who found an average value of $m^* = 0.25m_e$; and by Sawamoto.[46] The latter found both an effective mass of 0.17 m_e, and a heavier mass of 0.81 m_e which he attributed to holes. The temperature dependence of the mobility and magneto-resistance as measured by Zook and Dexter[47] could be explained by an essentially isotropic effective mass of $0.19m_e$, with the conduction band minimum occurring at k = 0.

The effective mass of holes varies for the different valence bands. Values of 0.7 m_e and 3.0 m_e have been measured for the upper and lower levels of the highest band by Thomas and Hopfield.[40]

The Hall mobility of electrons in CdS in the temperature range 20 - 700°K was measured by Kröger et al.,[31] and found to be ~210 $cm.^2/v.sec.$ at room temperature. The temperature variation of the mobility above 75°K could be accounted for by a combination of acoustical mode scattering $\propto T^{-3/2}$ and scattering by longitudinal optical vibrations with a characteristic temperature of between 250 and 300°K. (See section 1.5.2.). The appropriate elastic constants for a calculation of the effect of piezo-electric scattering were not then available.

In a recent study of the temperature dependence of electron mobility in large single crystal CdS, Zook and Dexter[47] found that the temperature dependence above 200°K could best be explained on the basis of combined optical mode and piezo-electric scattering, assuming an effective mass of

$0.19m_e$. Charged impurity scattering became dominant below 200°K.

Few measurements of the mobility of free holes in CdS have been reported. Spear and Mort[48] measured the drift mobility of holes in bombardment-induced conductivity experiments. The mobilities were between 10 and 18 $cm.^2/v.sec.$ Recently Onuki and Hase[26] reported a hole mobility of 38 - 48 $cm.^2/v.sec.$ under illumination in PhotoHall measurements.

2.4 Luminescence.

The principal luminescence bands in CdS can conveniently be divided into two; the 'edge emission' and the infra-red luminescence bands.

The edge emission fluorescence lies just to the long wavelength side of the fundamental absorption edge, and is characterised at low temperature by a series of equally-spaced peaks, the separation of which is about 296 $cm.^{-1}$. It has been suggested that the emission is due to recombination via an impurity centre with the emission of an integral number of longitudinal optical phonons. By measuring the reflectivity in the infra-red Collins[49] showed that the wave number of the optical vibrations is 305 $cm.^{-1}$. The separation of the zero phonon peak from the absorption edge is 0.15 ev., but there is speculation as to whether the recombination centre is near the conduction band or the valence band. The centre is probably due to a native defect, and not a chemical impurity.[50]

Due to the ionic and non-cubic nature of the material, the upper valence bands have different symmetries, as mentioned in 2,3, and Dutton[51] found a preferential polarization of the edge emission with respect to the c-axis of the crystal.

Other luminescence bands can occur in the region of the absorption edge

which are connected with the presence of impurities in the material, and are the subject of current study.[52] A further band at 5800Å is present in crystals prepared under reducing conditions, and may be associated with a loss of sulphur.

The infra-red luminescence bands occur in the range 0.8 - 2.3 μm, and consist of two broad bands centred at 1.6 and 1.8 μm, together with two bands centred at 0.82 and 1.02 μm. The latter are sometimes referred to as the 'blue' and 'green' bands by analogy to their counterparts in zinc sulphide.

Previous models proposed (e.g.53) to account for the corresponding excitation spectra involve (in absorption) transitions from the top of the valence band to different ionisation states of a luminescent centre. It is known that copper enhances the emission, but the nature of the luminescent centre has not yet been resolved. It could be a sustitutional copper impurity, a cation vacancy, or a more complex imperfection.

In a recent study of the excitation spectra of the infra-red luminescence in pure and copper-doped cadmium sulphide, Bryant and Cox[54] found two excitation bands centred on 0.89 and 1.49 μm, corresponding to 1.39 and 0.83 ev. Either band was found to excite the full infra-red emission spectrum. Now Browne[53] had predicted that the two-level centre model would be supported by a change in emission spectrum on long-wavelength excitation only; this change did not in fact occur. Bryant and Cox therefore proposed a new luminescent model based on the band structure of CdS as suggested by Balkanski and des Cloiseaux[38]. The low energy excitation bands were attributed to excitation from the p-orbitals to a level in the forbidden gap,

while the high energy band was due to excitation to the same level from the s-bands. Recombination of electrons from the conduction band to the level in the forbidden gap is responsible for the 'blue' emission. To explain the 'green' emission it is necessary to postulate that conduction electrons are first trapped in an excited state before recombining to the same ground state.

2.5 Acousto-electric effect in CdS

Attention has recently been drawn to acousto-electric effects in piezo-electric photoconductors by the observation of light-sensitive ultrasonic attenuation.[55-57] The attenuation was attributed to the interaction of mobile charge carriers with the strong longitudinal electric fields accompanying the acoustic waves in piezo-electric crystals.[59] White[60] indicated the possibility of achieving acoustic gain by applying a d.c. electric field in the direction of the ultrasonic wave. With a carrier drift velocity slightly higher than the wave velocity, interaction between the drifting electrons and the acoustic wave would amplify the latter by drawing energy from the electric field.

Successful amplification of ultrasonic waves in CdS was reported by Hutson, McFee and White.[61] A quartz transducer was mounted on one side of a block of high resistivity cadmium sulphide, and a second transducer mounted on the opposite face detected the output. Indium contacts between the transducers and the sample allowed a drift field to be applied. The sample was illuminated to increase the carrier density. Attenuation of the ultrasonic waves was severe for a drift field of ~300 volts/cm., but above a crossover at 700 volts/cm. ultrasonic gain of more than 38 db. at 45 Mc/s was obtained. As predicted by White, the crossover point corresponded to a drift velocity equal to the appropriate shear wave velocity ($v = 2 \times 10^5$ cm./sec.)

for negative carriers with mobility $\mu = 285$ cm.^{2}/v.sec. This drift mobility is in good agreement with Hall mobility values of 300 cm.^{2}/v.sec. reported for high resistivity CdS (see chapter 8). Amplification has also been observed in CdSe.(62)

The interaction of the electrons with acoustic lattice waves also leads to departures from Ohmic behaviour at fields above ~1000 v/cm. The current is reduced below the expected value, and current oscillations at frequencies of ~100 kc/s build up.(63) In addition to the onset of current oscillations there is a build-up of ultrasonic flux in the sample with no ultrasonic input applied.(64) The effect is being pursued with a view to the construction of ultrasonic amplifiers and generators, and possibly a high frequency current source. (see also 65-67).

2.6 Practical Applications

The most widespread practical application of cadmium sulphide has long been its use as a photoconductor. The material is sensitive to visible radiation, and can be prepared with photoconductive gains as high as $10^4 - 10^5$ by the incorporation of appropriate sensitizing centres (see 2.2). However the preparation of suitable material is often performed in a very empirical manner. Small single crystal detectors are used, but thin evaporated film and sintered powder devices are also common.

Cadmium sulphide can also be used as a γ-ray detector, and offers the possibility of making very small detectors for personal radiation dose monitoring. Large single crystals are desirable for this application, to increase the stopping power of the detector. However the properties of the large crystals must be very closely controlled, since for a suitable

detector a combination of high sensitivity and fast speed of response is required. In addition, long term stability of the detector under irradiation is required. At the present time, sensitivity can usually be obtained only at the expense of a very long response time due to the presence of a high density of electron trapping levels. Further study of the native defects in large high resistivity samples is needed to obtain better control of the material.

Acousto-electric ultrasonic amplifiers are another possible application for high resistivity single crystals of cadmium sulphide, as discussed in 2.5. However the field is a very new one and many practical problems must be solved before devices are readily available. Here again the quality of the material used in the experiments is critical, and the effects of trapping levels in the crystals are only beginning to be investigated.(68) A similar interest is being shown in the development of electro-optical devices, where the piezo-electric distortion of the lattice due to an applied electrical signal will affect optical waves travelling through the sample.

Apart from the interest in single crystal CdS, the application of thin films to device work is of great importance. Heterojunctions between CdS and CdSe are being studied as photovoltaic elements.(69) The development of the thin film transistor may lead to an active device for use in evaporated film circuits.(70) Another recent development is the combination of a piezo-electric transducer and MOS transistor to produce a transducer with built-in gain.(71) The device is basically a metal-oxide-semiconductor structure, the semiconductor layer is cadmium sulphide deposited as a thin film on a glass substrate. Current through the semiconducting layer flows

between source and sink electrodes, and mechanical strain applied via the glass substrate modulates the surface charge on the layer, and hence its conductivity.

The most important feature in any discussion of possible applications of cadmium sulphide is the requirement to control the electrical and optical properties of the material. These properties are strongly dependent on the type and numbers of defect levels present, and hence depend on the mode of sample preparation and its purity. The work described in this thesis is an investigation into the effect of different growth methods on the electrical parameters of single crystals, with a view to achieving the necessary control over material preparation.

CHAPTER 3.

FLOW METHOD PREPARATION OF CADMIUM SULPHIDE

3.1 Introduction

The luminescent and photoconductive properties of cadmium sulphide and zinc sulphide have been of interest for many years, and early investigators, e.g. Gudden and Pohl[72] used natural greenockite (CdS) or zinc blende (ZnS) for their studies. Such natural materials contained so many impurities that the intrinsic properties of the material were often masked. Many studies of the photoconducting or luminescent properties of CdS powders have been undertaken, but these are hindered by the effects of grain boundaries. This resulted in the investigation of methods to produce, in the laboratory, crystals of useful size and purity. Large single crystals with centimetre dimensions are desirable for measurement of bulk properties as in the Hall effect, and have become essential for recent applications utilising the interaction of ultrasonic waves and electrons in the crystal.[66]

Since cadmium sulphide sublimes readily at temperatures $\sim 1000^{\circ}C$, vapour phase crystal growth techniques have received most attention. Other accepted methods of producing single crystals such as growth from the melt or from solution have also been investigated, but usually present considerable practical difficulty. Such methods will be discussed further in relation to the growth of large crystals, in Chapter 4.

Sublimation methods can be divided into two main categories; (i) dynamic and (ii) static. In (i) the cadmium sulphide vapourises in a hot region and the vapour is carried to a cooler growth region by a flow of a suitable carrier gas; in (ii) the transport of vapour is by diffusion down a temperature gradient, with no external gas flow.

3.2 Dynamic (or flow) Sublimation Growth.

The basis of flow growth is the 'Frerich's Technique',[73] which is a modification of an earlier method reported by Lorenz.[74] Hydrogen sulphide is led to the hot zone of a tubular furnace. Here it is mixed with a stream of carrier gas (H_2) containing cadmium vapour from a boat held at 800 - 1000°C. The CdS produced by reaction between the H_2S and cadmium is deposited in a cooler region of the system, generally in the form of rods or thin plates.

Many variations of this method have since been reported. Stanley[75] used an inert carrier gas flowing at a rate of 175 c.c./min. over a cadmium sulphide powder charge held at a temperature of ~1000°C. Vapour from the charge was carried to the growth region where crystals grew as before, at a temperature of about 900°C. Fochs[76] refined this technique by steadily cooling the growth zone of the furnace while the run was in progress, so that the point at which supersaturation resulted in growth moved slowly along the tube towards the centre. This allowed crystals to grow without congestion, and enabled the purity and properties of crystals grown at different times during the run to be examined and compared.

Bishop and Liebson[77] modified the Frerich's technique by replacing the H_2S flow with argon passing over molten sulphur. This argon flow met a second stream of argon, which had passed over the boat of molten cadmium, the reaction taking place at 1000°C. Fahrig[78] has reported a similar method of preparing high-purity cadmium sulphide crystals using the purified elements as starting material. Separate external furnaces or 'boilers' are used to hold the sulphur at 500°C and the cadmium at 825°C. An inert carrier gas stream flowing through each boiler brings the vapours together in the

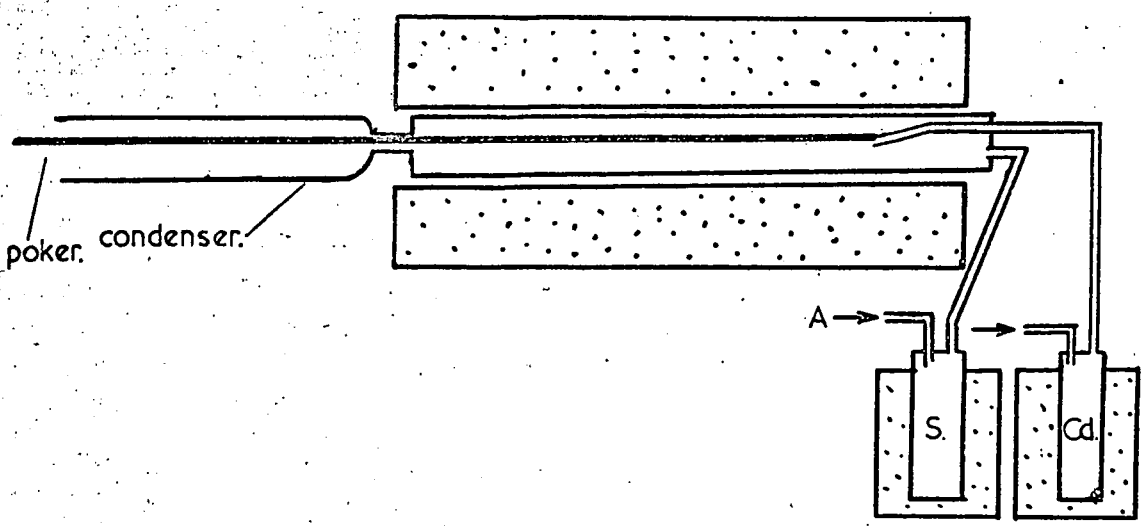

a.

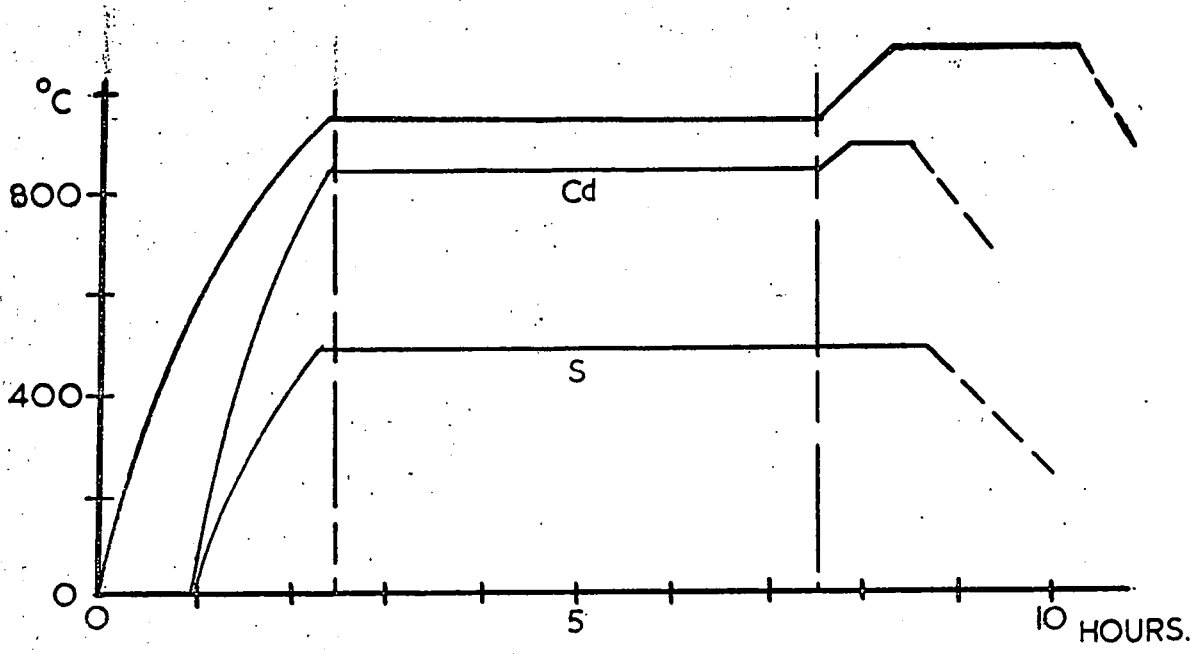

TIME - TEMPERATURE CURVES.

b.

FAHRIG'S METHOD.

FIGURE 3.1

TABLE 3.1

Composition of Vapour above CdS at 1014°K (After[78]).

Ion	Intensity
S^-	1,270
S_2^-	15,840
S_3^-	8.75
S_4^-	0.36
Cd^-	14,000
CdS^-	0.1

main growth tube at a temperature of 975°C. Sufficient sulphur is present to provide an excess over the stoichiometric amount required. When the cadmium supply is exhausted, the main tube is heated to 1050°C to ensure complete reaction and to remove any unreacted elements that may still be present. The apparatus is outlined in Fig. 3.1(a), with idealised time-temperature curves in (b).

3.3 Conditions in the Vapour.

There has been considerable discussion as to whether the vapour above cadmium sulphide at temperatures in the region of 1000°C is composed principally of CdS molecules, or is almost completely dissociated. For instance Ibuki[79] has assumed that the degree of dissociation is small. Recently Marquart and Berkowitz[80] have reported a detailed study of the composition of sulphur vapour, and the vapours above some metal sulphides, including CdS, in this temperature range. The information was derived from mass spectrometry measurements.

The authors found that at a temperature of 1014°K, the cadmium sulphide vapour could be regarded as completely dissociated; the concentration of undissociated molecules being less than 10 p.p.m. Most of the sulphur occurs as S_2, with approximately 10% monatomic sulphur; traces of S_3 and S_4 are found, but no larger molecules.

The results of this investigation are given in Table 3.1.

3.4. Differences between the methods.

It is evident from section 3.3 that at the growth temperature involved in flow methods, any cadmium sulphide vapour can be regarded as completely dissociated. Differences in growth conditions have their origin in variations

in the partial pressures, or concentrations, of the elements in the reaction zone.

In Stanley's method the ratio of cadmium to sulphur in the vapour is controlled by dissociation of the CdS powder according to the reaction $2CdS \rightleftharpoons 2Cd + S_2$, (assuming we can regard the sulphur as S_2). Equal atomic concentrations are produced therefore. (Small departures from stoichiometry are possible, depending on the previous history of the powder). The inert carrier gas does not affect the reaction.

When elemental cadmium and sulphur are used (Bishop and Liebsen, Fahrig) adjustment of the temperature of one of the elements, or alteration of the flow rates, can lead to an excess of cadmium or sulphur in the vapour; stoichiometric growth conditions are difficult to achieve and maintain. This is also true of the Frerich's method, with the additional complication that, since hydrogen is present, growth is occurring in a reducing atmosphere.

3.5 Purity.

Commercial cadmium sulphide powder used as starting material for crystal growth usually contains common metallic impurities (e.g. Pb, Cu, Mn, Fe,) in concentrations of a few parts per million, and can contain much higher concentrations of non-metals or traces of solvents, depending on the method of its preparation. Volatile impurities can be removed and an improvement in purity obtained by fractional distillation,[81] but care must be taken to prevent preferential loss of one of the elements (generally sulphur) from the powder. Distillation is usually performed at temperatures of the order of 900°C for a few days, treatments both in vacuum and in H_2S being used. The distillation can be repeated as often as desired, depending on the initial purity of the powder. In this way final concentrations below 1 ppm. can be obtained.

Vecht, Ely and Apling[82] have shown that further purification takes place

during crystal growth. Volatile impurities are driven past the growth region, whilst less volatile materials concentrate in the charge. For maximum purity not all of the charge is sublimed, and the substrate of cadmium sulphide in contact with the quartz tube is not removed as this is contaminated by diffusion of silicon or other impurities from the tube walls.

Jackson[83] has recently described a method of producing cadmium sulphide powder with a total metallic impurity of less than 1 ppm. A cadmium chloride solution is purified by ion-exchange, then converted to cadmium sulphide using ultra-high purity organo-sulphur compounds. These hydrolyse in the cadmium chloride solution to give hydrogen sulphide and thence cadmium sulphide. The final precipitation is performed at room temperature, and because of this departures from stoichiometry are minimised.

For growth of CdS from the elements a very high degree of purity of the starting material can be attained. Fahrig[78] used multiple distillations to remove zinc and lead from the cadmium metal together with subsequent zone refining to reduce the concentrations of metallic impurities to below 0.5 p.p.m. The principal impurities in the sulphur were organic materials, with traces of silicon, magnesium, and copper. Washing in acids, then water, followed by drying in nitrogen and distillation in a partial vacuum removed the organic matter. The remaining impurities were typically Si 5 ppm., Cu 1 ppm., Mg 0.5 ppm.

With Frerich's method the cadmium metal can be purified as described above; but special care must be taken to remove impurities from the H_2S. The common Kipp's apparatus is usually unsuitable since it is a source of iron impurity, but methods of producing high purity hydrogen sulphide have

been described.[84] The generator is chosen so that any likely impurities in the H_2S can be easily removed in wash bottles or cold traps.

Several problems of purity are common to all methods. The growth (and often the initial purification) is performed in silica vessels at elevated temperatures, and contamination of the final crystals by silicon must be prevented as far as possible. In general this is done by minimising the time taken for the growth runs, and by selecting material which has grown on a CdS substrate, and not in direct contact with the silica.

The carrier gas must also be free from impurities. Particularly troublesome in this respect are oxygen and water vapour, which are both difficult to exclude, and can have a marked effect on the properties of the crystals produced. (See, for example, [85-87]).

3.6 Properties of Flow crystals.

The properties of crystals grown by flow methods have been reported in detail by many authors, and will not be discussed here. Ibuki[79] has investigated the growth conditions necessary for formation of the various possible crystal habits, and considers the associated vapour pressure conditions. Sturner and Bleil[88] have given a comprehensive study of defect structures by optical and electron microscopy. Other details can be found in the original papers.

CHAPTER 4.

GROWTH OF LARGE SINGLE CRYSTALS OF CADMIUM SULPHIDE

4.1 In recent years many methods of growing large single crystals of cadmium sulphide have been reported in the literature, in varying detail. The conventional techniques of growing large single crystals such as pulling from the melt, or directional freezing, are not convenient for CdS because it sublimes. Growth from solution has only been successful in the production of very thin layers[89]. The ease with which sublimation occurs provides the basis of the majority of crystal growing methods. However successful growth from the melt has been achieved under conditions of high temperature and pressure.

4.2 Melt Growth.

The melting point of cadmium sulphide was reported by Addamiano[90] to be 1475°C ± 15°C, and Metcalf and Fahrig[91] obtained large single crystals by cooling from a temperature of 1500°C under an argon pressure of 1500 p.s.i. A charge of 150 gms. was held in a high purity graphite crucible heated by a current flowing through a multiply split graphite cylinder from a 20 kw. supply. The furnace was contained in a forged steel pressure shell, which was lined with fused stabalised zirconia brick enclosing a porous carbon cylinder. After flushing and filling with argon to a pressure of 1000 p.s.i., the furnace was brought to temperature and the pressure adjusted to 1500 p.s.i. The temperature was reduced over a period of six hours to promote the progressive freezing of the melt from bottom to top of the crucible. A boron graphite-graphite thermocouple was used to monitor the temperature.

Some of the ingots produced contained crystals weighing more than 100 gms.

The growth direction lay within 15° of the c-axis. The crystals had a dark colouration, and low resistivity ($\rho \sim 1\,\Omega$cm, $\mu \sim 100$-200 cm.^{2}/v.sec.). Crystallographic imperfections such as bubbles or inclusions were also present. Problems of purity are obviously inherent with this method, and although there was evidence that segregation of Si, Ca, Cu and Pb occurred on freezing, Zn, In, and Mn were distributed homogeneously.

The Czochralski technique of pulling from the melt cannot be used because excessive vapourisation of the charge would occur from the open-topped crucible. Metcalf and Fahrig's technique has been improved however by lowering the melt from the hot zone to promote freezing.(78) Seeding was introduced by using a two cavity crucible. The small lower cavity was connected to the main cavity by a narrow neck; so that freezing occurred first in the lower cavity and generally only one crystal grew through the constriction to the upper chamber.

A similar growth method has been reported by Takahashi et.al.,(92), using temperatures of 1400°C and pressures in the range 350-1300 p.s.i. In this arrangement the crucible could be fixed, or lowered through the hot zone; larger crystals (several cm.^{3}) were found in the latter case.

4.3 Sublimation Growth.

4.3.1. If a closed system containing a charge of CdS is maintained at a high temperature, then vapourisation of the charge will occur to create in the system the vapour pressures of cadmium, sulphur, and CdS appropriate to the charge temperature, and a dynamic equilibrium will be reached between the solid and the vapour. The relevant vapour pressures above cadmium sulphide are shown in figure 4.1.

If however the system is such that there is a region of lower temperature

FIGURE 4.1

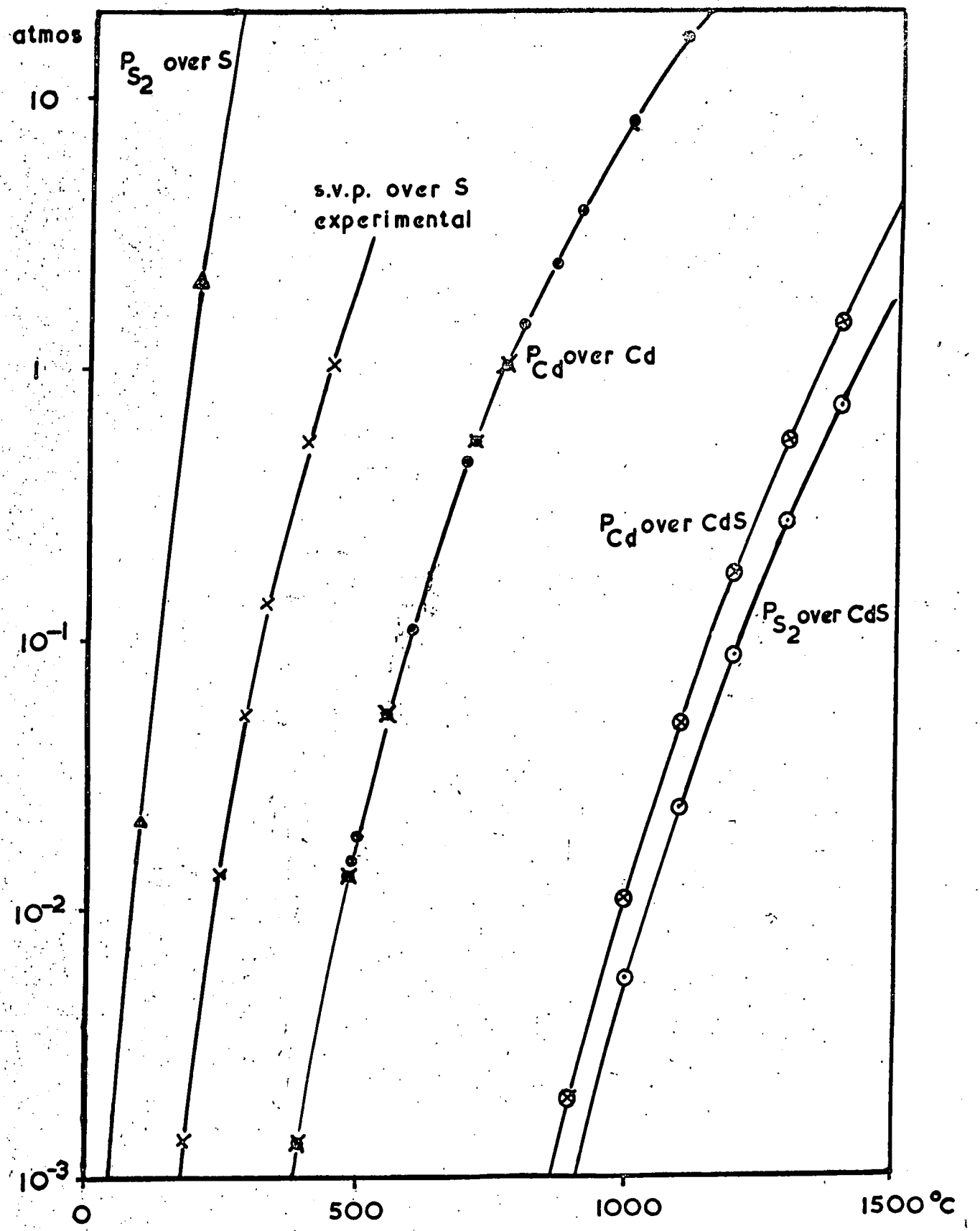

SATURATED VAPOUR PRESSURES OVER Cd, S, & CdS.

than that of the charge, the partial vapour pressures above the cadmium sulphide will be higher than those needed to maintain a solid-vapour equilibrium at the lower temperature. Material will sublime from the charge and diffuse to the cooler region where it deposits. To utilise this non-equilibrium situation for growth of crystals, the temperatures and pressure of the system must be chosen to give a suitable rate of material transport. In general also the region into which material can be deposited is constrained in some way, so that large crystals are formed by continued deposition in the same volume.

4. 3.2. Growth on the charge.

The simplest case of sublimation growth relies on the interchange of material between the charge and the vapour to produce growth of crystals on the charge itself. No transport of material to other parts of the system is involved. The method has been used by Reynolds and Czyzack,[93] for zinc sulphide, but conditions for the growth of cadmium sulphide are similar. The applicability of various techniques to both compounds will be found in many references. The growth temperature for CdS is usually some 100°C lower than for ZnS. Reynolds and Czyzack spread a powder charge inside a quartz tube, which was then evacuated and filled to a pressure of 6 p.s.i. with H_2S. The tube was heated in a furnace for two to four days at 1150°C, when crystals of a few mm. dimensions were formed. Some of the resulting crystals showed blue fluorescence under u.v. excitation, this was attributed to a non-stoichiometric excess of zinc.

When evacuated tubes were used, no crystal growth occurred. The introduction of H_2S to the system is a feature of many crystal growing methods

and must be discussed later.

4. 3.3. Sublimation down a temperature gradient.

The main disadvantage with the method described in 4. 3.2. is that there is a strong possibility of the crystals being contaminated with impurities from the charge. Absorbed gas and volatile impurities can be driven off during a suitable heat-treatment of the starting material, but less volatile impurities will remain. Contamination of the final crystals can be reduced if they are grown by sublimation from the charge to a cooler region; the less volatile impurities concentrate in the charge, not all of which is allowed to sublime.

A charge of outgassed cadmium sulphide is contained in a quartz tube in one end of a two-zone electric furnace. The charge temperature is maintained at 1150°C, with the other end of the quartz tube some 50° cooler. The tube can be evacuated, or contain H_2S or an inert gas. Material is transported from the charge to the cool end of the tube over several days, and crystals of mm. dimensions are formed. Growth on the charge also occurs. (See 4. 3.2.)

This method can conveniently be combined with that of chemical transport, (94) where a volatile intermediary carries a compound by diffusion and convection to a region of different temperature, where decomposition occurs with the production of the original compound. In the case of cadmium sulphide, incorporation of a small concentration of iodine into the tube (~ 1 mg/cc.) results in equilibrium between the CdS charge and the iodine vapour according to the reaction $CdI_2 + S \rightleftharpoons CdS + I_2$, (neglecting any association of the S). This reaction is exothermic, so that if the charge of CdS is held at a higher temperature than some other portion of the tube, material will be deposited

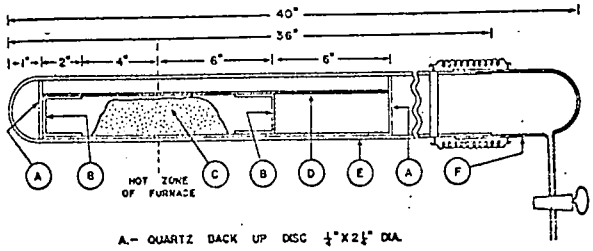

A.– QUARTZ BACK UP DISC $\frac{1}{4}$"X2$\frac{1}{2}$" DIA.

B.– QUARTZ CUP 2"X1$\frac{1}{2}$" DIA.

C.– CdS OR ZnS POWDER

D.– QUARTZ LINER 18"X 2" DIA.

E.– MULLITE TUBE 36"X 2$\frac{1}{2}$" DIA., WITH ONE END GROUND TO FIT (F.)

F.– GROUND GLASS VACUUM CAP

Cross section of mullite tube and contents.

Crystals	Center zone	Growing zone	Pressure
ZnS	1550–1600°C	1475–1500°C	760–900 mm
CdS	1250–1300°C	1135–1175°C	760–900 mm

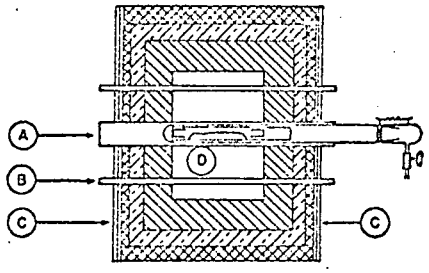

2400°–3000°F LIGHT WEIGHT REFRACTORY

2300°F INSULATING BRICK

1800°F INSULATING BRICK

A– ALUNDUM TUBE – 3$\frac{3}{4}$" DIA. x 36" LG.

B– GLOBAR – $\frac{3}{4}$"DIA. x 36" LG. – 6 REQUIRED – EQUALLY SPACED ON 14$\frac{1}{2}$" DIA. CIRCLE CONCENTRIC WITH "A"

C– $\frac{1}{4}$" TRANSITE HEAT RESISTANT INSULATING SHIELD

D– WORK CHAMBER – 19$\frac{3}{4}$"DIA. x 14"LG. EQUIDISTANT FROM BOTH ENDS AND CONCENTRIC WITH "A"

FIGURE 4.2

in the cooler region, the iodine thus freed diffusing back and combining with more CdS. Since CdI_2 and S are both more volatile than CdS, the temperatures involved in this method are lower than for direct sublimation, the charge being held at about 650°C. The temperature gradient is adjusted to give a suitable rate of transport for appreciable growth to occur. Crystals can be grown at temperatures as low as 500°C. However the transport agent is necessarily an impurity in the resulting material.

4.4. Growth on a Substrate.

4.4.1. Introduction.

More recently work on growth of large crystals of cadmium sulphide has been concentrated on sublimation from a heated charge to a silica substrate at a lower temperature. A large outer jacket which contains either an inert gas or H_2S, surrounds both charge and substrate. Since the jacket extends from the furnace the gas atmosphere can readily be controlled during the run, but the vapour pressures which determine the growth conditions will be those appropriate to a tube with one end at room temperature. As much of the recent data on CdS has been obtained from crystals grown by variations of this method, the individual techniques will be considered in some detail.

4.4.2. The Method of Greene, Reynolds, Czyzack and Baker[81].

Commercial powder was first dried and purified by baking in one atmosphere of H_2S at 930 - 950°C for 2 - 3 days, followed by a similar heat treatment in vacuum. The powder charge was then placed in a quartz liner at the centre of a 'globar' furnace (Fig. 4.2). Quartz cups were placed at either side of the charge and at a little distance from it to act as substrates for the crystal growth. The exact position depended on the furnace profile and desired growth

TABLE 4.1

Greene, Reynolds, Czyzack and Baker's Method.[81]

Summary of Crystal Properties and Effects of Heat Treatment

Purification	Resistivity (as grown)	Heat Treatment	Resistivity
In H_2S only	10^3 ohm-cm.	800 - 900°C, in H_2S,	10^5 - 10^6 ohm-cm.
		in A,	10^8 - 10^{10} ohm-cm.
		in vac.	10^8 - 10^{10} ohm-cm.
H_2S and vacuum	10^5 - 10^7 ohm-cm.	800 - 900°C, any of above	10^8 - 10^{10} ohm-cm.

temperature, which was usually $\sim 100^{\circ}C$ below the charge temperature. The mullite outer tube which contained the liner was then flushed and filled with the desired atmosphere gas (A, H_2S, H_2 or N). The pressure was adjusted to be 760 - 900 mm. Hg. at the growth temperature, which for CdS was with the centre zone at $1250^{\circ}C$ - $1300^{\circ}C$, and the substrates at 1135 - $1175^{\circ}C$. A polycrystalline mass of some 400 gm. was formed in each cup, from which single crystals of 5 to 115 gm. weight could be cleaved.

The electrical properties of these crystals were found to be dependent on the method of outgassing and purifying the charge. Crystals grown after purification in H_2S only had a resistivity considerably less than the normal high resistance flow crystals; their resistance was $\leq 10^3$ ohm.cm. compared with 10^9 - 10^{10} ohm. cm. However if the purification in H_2S was followed by a vacuum bake, then the resistivities of crystals as grown rose to 10^5 - 10^7 ohm.cm. The resistivity of the more conducting crystals could be increased to 10^5 - 10^6 ohm.cm. by baking in H_2S at 800 - $900^{\circ}C$, for up to twelve hours, and to 10^8 - 10^{10} ohm.cm. on baking in an inert gas, or in vacuum. The effects of various heat treatments are summarised in Table 4.1.

4. 4.3. Method of Boyd and Sihvonen.

Boyd and Sihvonen[95] used a similar apparatus to grow single crystals of CdS, and investigated the properties of crystals grown under various conditions. As before, a large mullite (or silica) outer tube was used to contain the ambient gas. The mullite tube was mounted in a three zone electric furnace, each zone equipped with independent temperature control.

The charge consisted of CdS powder which had been heated in vacuum at $150^{\circ}C$ for 1 hour, before being fired for 24 hours at $900^{\circ}C$ in H_2S at 380 mm.Hg.

The powder was placed inside a silica growth tube in the centre of the furnace, and the growth chamber evacuated and heated at 150°C for 24 hours. Then, as the furnace temperature was raised, the tube was purged with H_2S. At the growth temperature the pressure was adjusted to its optimum initial value of 350 mm. Hg. During a run lasting seven days diffusion of hydrogen through the walls of the tube reduced the pressure to a value of ~200 mm.

Three types of crystals were produced by the method. Type 1 crystals grew radially inward from the walls of the liner in a region where the temperature was ~825°C. The charge was at 950°C. The crystals were similar to those produced by flow methods, being clear yellow thin plates or rods, with sizes up to 5 x 4 x 0.1 mm. and 25 x 1 x 1 mm. respectively.

Crystals also grew out of the powder charge (see section 4.3.2); they appeared most readily at constant gas pressure, and were transparent prisms ranging in colour from light to dark amber. These crystals, designated 'type 2', grew up to 20 mm. long, with cross-sections of the order of 5 $mm.^2$ The largest sizes and most rapid growth of type 2 crystals occurred with higher charge temperatures; the optimum pressure of H_2S increased also as the charge temperature was increased (e.g. rising to 400 mm. at 955°C). Helium and argon atmospheres promoted little growth compared with H_2S at temperatures below 1000°C.

Argon at a pressure near 760 mm. was used in preference to H_2S at the higher temperatures, since it provided a more stable atmosphere. High temperature type 2 crystals were transparent, and varied in colour from a very light amber when grown at 1050°C or less, to a very dark amber when grown at temperatures above 1100°C.

Since appreciable sublimation of material from the charge occurred at these temperatures, closing the silica liner with end cups gave rise to polycrystalline growth on the silica substrate as described in the previous section. Growth was observed at temperatures from 975°C to 1125°C, the largest and most perfect crystals grew at the higher temperatures. The colour of these (type 3) crystals ranged from light to very dark amber with a temperature dependence as for type 2 crystals.

No electrical properties were quoted by the authors, but a subsequent paper by Dreeben and Bube[96] describes the electrical properties of crystals grown by this method. Starting material was prepared by precipitation from aqueous solution followed by firing in H_2S at 900°C, or by a vapour-phase reaction of the elements.

Crystals grown at about 1200°C in 1 atmosphere of argon, away from the charge, had centimetre dimensions and very high dark resistivities of $\geq 10^{12}$ Ω cm. The density of deep trapping levels in these crystals was of the order of $10^{15}/cm^3$. Other crystals were grown in argon at a lower temperature, 950°C, but grew directly out of the powder charge. Analysis showed that these were less pure, particularly with respect to Cu and Zn, and had higher trap densities of $10^{16} - 10^{17}/cm^3$., but they were highly photosensitive. Needle, rod, and plate-shaped crystals were obtained at temperatures as low as 800°C, but in an H_2S atmosphere. These grew at some distance from the charge. The pressure of H_2S used lay in the range 200 - 700 torr. Variation of pressure of the atmosphere gas did not appear to affect the size of the crystals, in contrast with the previous report.[95] However the photosensitivity of the crystals did vary with pressure; those grown in pressures greater than 300

torr were the more sensitive. Some crystals also showed a good speed of response as well as good sensitivity; these were grown in the pressure range 300 - 500 torr. Thermally stimulated current measurements revealed that these latter crystals had a total trap density of 5.10^{15} cm.$^{-3}$, but the deep trap density was only 3.10^{13} cm.$^{-3}$. In contrast, crystals grown at 700 torr have deep trap densities of the order of 10^{15} cm.$^{-3}$, with a total trap density of 10^{16} cm.$^{-3}$.

Copper-doped crystals have also been grown by this method; the sensitivity of the crystals decreased strongly with increasing copper concentration. There is evidence that the copper impurity segregates strongly as a function of temperature.

4. 4.4 Fahrig's Method.(78)

This method is very similar to that of Reynolds et. al. (Section 4. 4.2). The charge material was CdS powder produced from vapour phase reaction of the elements (see section 3.2). The powder was baked for over four hours in vacuum at 900°C to produce a hard bar of dense CdS. Further binding of the charge was achieved by heating with 2.5 to 5% of sulphur at 300°C. This charge could then be easily handled, and could be accurately positioned in the furnace tube without fouling the silica substrates.

The charge was maintained at 1250 - 1300°C for 100 hours to allow crystallites to grow on the silica substrates at either side of the charge, at a temperature of 1175°C. Individual crystals generally weighed 10 - 50 gms., and occasionally crystals of up to 400 gms. were obtained. No quantitative assessment of the properties of the crystals was given, but the crystals showed high resistivity, and were photosensitive. Incorporation of 0.003% indium chloride in the charge before sintering gave optimum results with regard to improved photovoltaic properties of the materials.

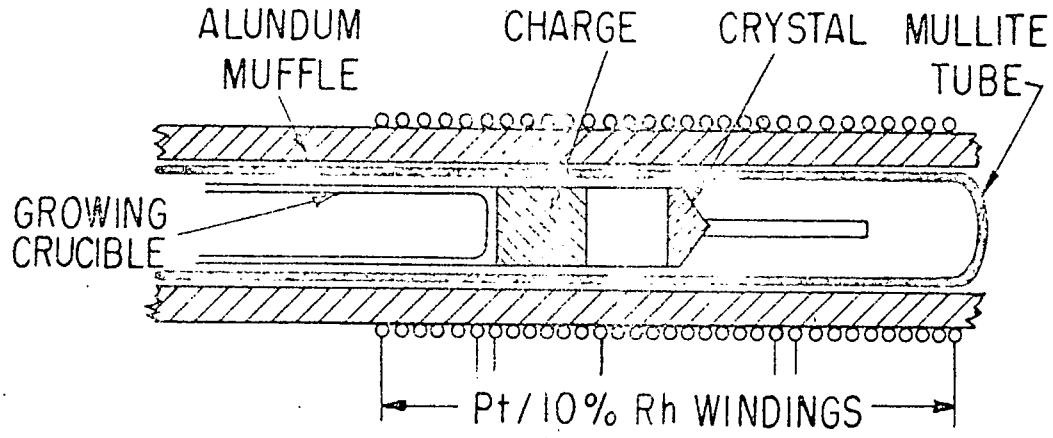
ALUNDUM
MUFFLE
CHARGE
CRYSTAL
MULLITE
TUBE
GROWING
CRUCIBLE
Pt/10% Rh WINDINGS

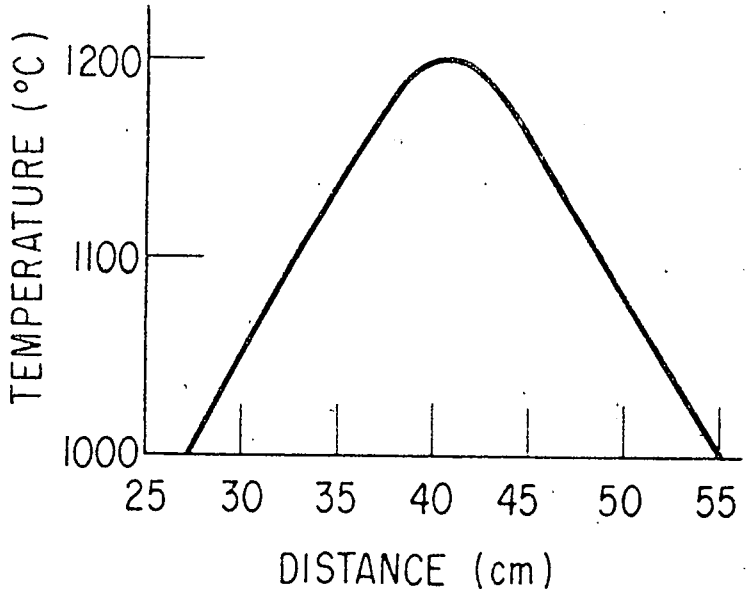
TEMPERATURE (°C)
1200
1100
1000
25
30
35
40
45
50
55
DISTANCE (cm)

FIGURE 4.3

4. 4.5. Konezenko and Yctyanov[97]

The method is similar to those reported above except that the inert gas (N_2) flows through the furnace during the run. The flow is directed on to the substrate to cool the latter relative to the charge. A mosaic of crystals grew from the substrate as before. Apart from their structural properties, the authors investigated dark conductivity versus temperature; sensitivity to light, x-rays, and γ-rays; and the thermally stimulated conductivity. The resistivity of the crystals was high, of the order 10^9 - 10^{13} ohm.cm., at room temperature.

4. 5.1. Growth using a moving temperature gradient.

The next refinement introduced was the movement of the growth tube relative to the furnace, and was first described by Piper and Polich[98].

The charge is a block of CdS powder which has been sintered until its density is some 60 - 80% of the value for crystalline CdS, and is a sliding fit inside a short silica tube closed at one end in the form of a wide-angled cone. A 'back-up tube' is slid in the other end to contain the charge without forming a gas-tight seal (see Fig. 4.3), and the whole is positioned in an outer mullite tube which contains the inert gas atmosphere. At the commencement of a run the conical end of the silica tube is at the centre of the furnace, where the temperature is brought up to 1200°C. Sublimation of material from the charge then seals the tube; the pressure inside the growth tube is therefore that of the atmosphere gas plus the vapour pressures of cadmium and sulphur above cadmium sulphide, which are ~0.1 atmospheres (Fig. 4.1). The mullite tube is drawn through the furnace at a rate of 0.2 - 1.0 mm. per hour, so that the apex of the cone gradually becomes cooler than the front face of the charge, and supersaturation results in nucleation and growth.

Usually one seed crowds out any others which may have been formed, and a single crystal grows from the tip at approximately the rate of movement of the tube; the temperature of the growth face being some 30°C below the charge temperature. A silica rod attached to the apex of the tube assists in removing heat from the boule.

The resulting crystals were 13 mm. diameter, and about 3 cm. long, although the authors comment that in principle one should not be limited in the length that can be grown. Crystals of other II-VI compounds have also been grown by this method (see also Aven and Piper[99]). Since the crucible is in thermal equilibrium, any impurities incorporated in the charge will be transferred to the crystal without segregation. Incorporation of Ga in the charge in the concentration range 10 - 10^4 ppm. produced a crystal containing the same Ga concentration to within 30%. Virtually no segregation occurs in the growth of mixed crystals of $Zn_xCd_{1-x}S$, and $ZnSe_xTe_{1-x}$.

Several important features of this method should be emphasised. The sintered charge is necessary to ensure that the distance from the front face of the charge to the growth face of the crystal does not alter appreciably during growth, otherwise the temperature gradients and rate of transport would vary. Sintering is accomplished by baking in vacuum at 500 - 700°C for 1 hour, followed by firing in a stream of H_2S at 900 - 1000°C for 10 hours.

Although during sublimation the method is essentially a short sealed tube technique, any volatile impurities are driven off before sealing, and the partial pressures inside the tube should be completely reproducible.

The method relies on controlled nucleation at one point and growth of a single crystal from a small charge rather than growth of many crystals

together in a large system.

No electrical or optical measurements on the crystals produced were described in the reference.

4. 5.2. Borisov and Vasilev's Method

A further 'moving gradient' method was very recently described by Borisov and Vasilev[100]. In this case however the furnace was moved at between 1 and 5 mm/hour, while the growth tube remained stationary. This tube was 2cm. in diameter, and 50 cm. long, closed at one end by means of a flat base, which acted as the substrate. The charge was commercial CdS, (or alternatively material formed by precipitation from cadmium sulphate by H_2S or sodium thiosulphate), which was pressed and sintered into tablets by baking in H_2S at 1000°C. The tablets were positioned in the tube at the appropriate distance from the closed end, so as to be at the centre of the furnace. The other open end of the tube was 'teed' into an H_2S flow, so that the system was effectively open to the atmosphere while shielded from it, and any high vapour pressure materials were free to escape. This open tube system was found to reduce the incorporation of a non-stoichiometric excess of cadmium into the crystals.

During growth the charge temperature was held at 1200 - 1250°C, whilst the substrate was at the desired growth temperature, typically 1100°C. The rate of movement of the furnace was adjusted to keep the growing face of the crystal at an approximately constant temperature. Initially, a large number of crystals grew on the substrate, but generally a few dominated and produced large single crystals. Material was also transported down the furnace in the opposite direction, but this was minimised by choosing a suitable temperature profile. The type of crystals produced were influenced by the temperature

at which they were grown, and by their rate of growth. As the growth temperature was decreased, the crystal colour became lighter; at the same time the resistivity of the material increased sharply. Crystals prepared at a temperature of 1100°C had a resistivity of 10^{10} Ωcm., and were very photosensitive, but the production of large crystals at lower temperatures became increasingly difficult.

CHAPTER 5.

PREPARATION OF CHARGE MATERIAL FOR LARGE CRYSTAL GROWTH

5.1 Starting Material.

Throughout this research, commercial cadmium sulphide in powder form was used as starting material. This was supplied by L. Light & Co., (high purity grade) or Derby Luminescents Ltd., (electronic grade). These powders do not contain any deliberately incorporated impurities. However various metals; particularly B, Si, Mg, Pb, Cu, Fe; were present in concentrations of less than 100 ppm together with much larger concentrations of compounds such as ammonium chloride, (5 - 10%), formed during the precipitation of the powder. Moisture and a little free sulphur may also have been present, but little or no K, Na, or SO_4. Thorough drying, outgassing, and purifying was therefore necessary before using the material for crystal growth.

5.2 Powder Purification.

The powder could be outgassed and volatile impurities removed by heating in an evacuated vessel. Cadmium sulphide powder was spread loosely inside a 1 inch bore silica tube, which was connected to a vacuum system comprising a conventional oil rotary pump and mercury diffusion pump with a liquid nitrogen cold trap. The system was capable of attaining a pressure of 10^{-5} mm. Hg. A tubular electric furnace was used to heat the powder to a temperature of 900°C for 48 hours. Material prepared by this treatment will be referred to as 'outgassed powder'.

It appeared from later studies of crystals grown from this material that the outgassed powder contained a non-stoichiometric excess of cadmium, due to preferential loss of sulphur during the heat treatment. Reynolds et. al.[81] recommend outgassing in an H_2S atmosphere as well as in vacuum

to obtain reproducible high resistance crystals, but hydrogen sulphide was not readily available in this laboratory in a suitable form. Outgassing in sealed evacuated tubes, and in argon filled tubes, was tried but did not produce any significant improvement.

5.3 Purification by a Flow Run.

5. 3.1. Introduction.

Purification of the powder by simple outgassing was replaced by purification in an argon flow, using a modified form of Stanley's method[75] for growth of CdS crystals. The aims were thoroughly to dry and outgas the powder, to purify it by sublimation down a temperature gradient, and to obtain a material of increased density. (This latter point will be seen to be of importance in large crystal growth). The process should be easily reproducible to give a consistent product. Cadmium sulphide powder was retained as the starting material instead of using the purified elements because the apparatus required is simpler and consequently conditions should be more reproducible; the vapour will also be more stoichiometric (see Sec. 3.4). Moreover the cost is lower. Growth from the elements should permit an improvement in purity to be made, but the properties of the final crystals seem at this stage to be controlled more by departures from stoichiometry than by foreign impurities.

5. 3.2. Apparatus.

The experimental arrangement is shown in Fig. 5.1. The tubular electric furnace is resistance heated through a Kanthal wire element wound on a 5.5 cm. bore mullite tube. The resistance of the winding is chosen so that it can be run directly from mains voltage, passing 5 amps. With 250 volts

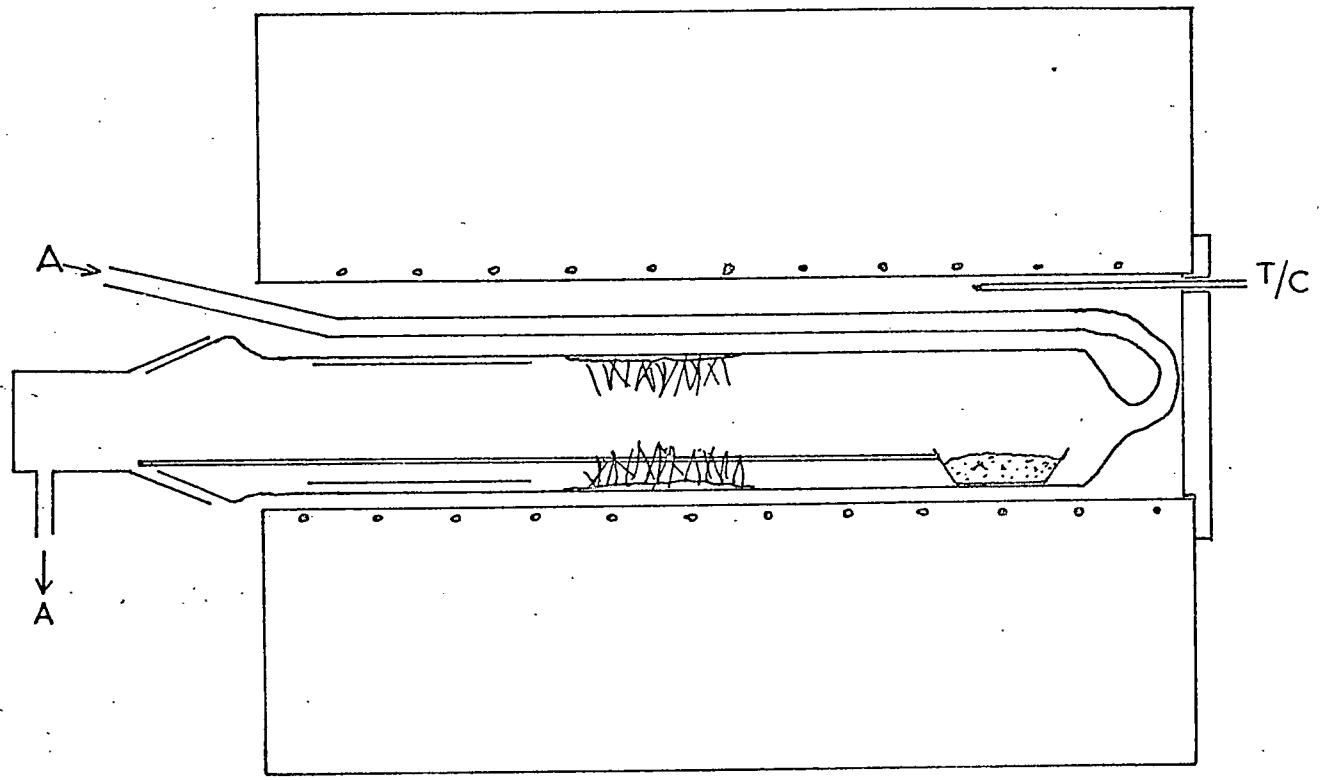

FIGURE 5.1

applied, a temperature of 1250°C can be attained. An Ether anticipatory controller switches the input to the furnace so as to maintain a desired temperature at the position of the charge; the temperature is measured using a platinum/platinum - 13% rhodium thermocouple. The furnace winding is centre-tapped, and a 'regavolt' transformer is connected in parallel with it as shown in Fig. 5.2(b). Adjustment of the regavolt alters the proportion of the applied voltage dropped across each half of the furnace, and hence their relative temperatures. Note that since the current flowing in the regavolt is equal to ~~only~~ the difference in currents flowing in either half of the furnace, a low power (2 amp) type can be used.

A 32 mm. bore transparent silica tube forms the main part of the apparatus, and is terminated at the outlet in a B 45 cone to permit easy insertion of the charge and removal of the product. This end is closed during growth with a Pyrex end cap and gas outlet tube. Argon enters the system through a 10 mm. bore silica tube alongside the main tube, ensuring thorough heating of the gas. The charge is contained in a silica boat attached to a silica rod which enables it to be accurately positioned in the furnace. Near the outlet is a silica liner which is a loose fit in the growth tube.

The carrier gas, B.O.C.99.995% pure argon, is passed through a needle valve to reduce the pressure, then through a molecular seive of aluminium calcium silicate pellets and over heated copper turnings to remove water vapour and oxygen respectively (Fig.5.2). The gas flow to the furnace of 350 cc/min is controlled by a further needle valve and measured on a Rotameter flow meter. The flow rate is constant over 24 hours to within

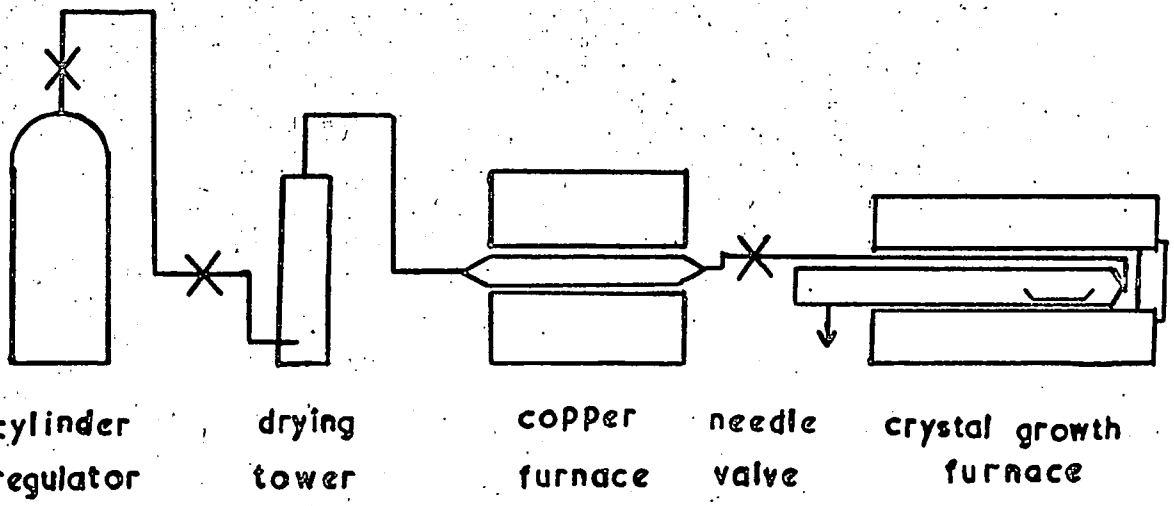

ARGON SYSTEM

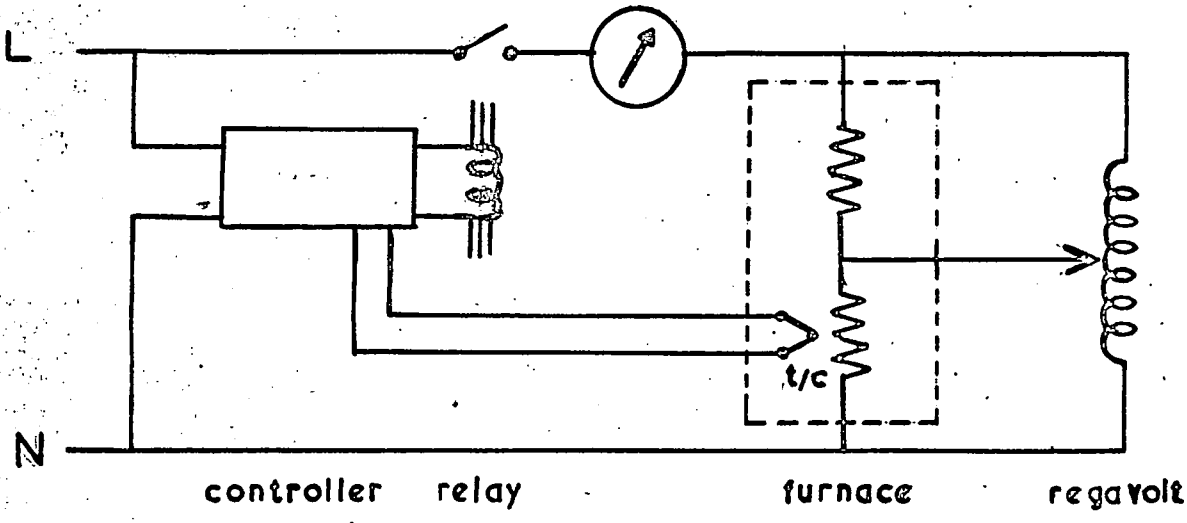

FURNACE CONTROL

FIGURE 5.2

(a) FLOW RUN DEPOSIT

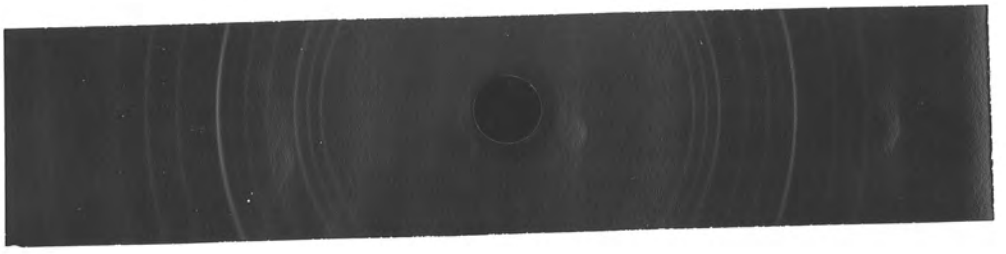

(b) CdS + 5% Cd

X-RAY POWDER PHOTOGRAPHS

FIGURE 5.3

5 cc/min; (pressure variations were much more marked if the first needle valve was omitted and pressure reduced by the cylinder regulator alone).

5. 3.3 Flow Run Sequence.

The silica boat is loosely filled with cadmium sulphide powder (35 gms) and positioned in the tube. After argon has been flowing for 2 hours, the charge is heated to 600°C, and held at this temperature for 5 hours. This ensures that any volatile impurities, including water vapour and solvents, are driven off. After this period the furnace is further heated so that the charge is at 1130°C; at this temperature approximately two thirds of the charge will sublime in three hours. Further along the tube, in a region at about 950 - 900°C, rods and plates grow radially from a cadmium sulphide substrate on the silica wall. Near the end of the furnace, on the silica liner, a grey-black deposit forms at a temperature of 200°C or less. This has been shown by X-ray powder photographs to be a mixture of cadmium sulphide and cadmium. Fig. 5.3(a) shows a powder photograph of the deposit; (b) shows CdS with 5% Cd for comparison. Sulphur is deposited in the gas exit tube as a pale yellow dust. After three hours at the growth temperature, the furnace is switched off and the tube slowly cools. The argon flow is maintained until the furnace is cold ($\leq 50°C$).

The silica liner and cadmium-rich deposits are removed, to prevent them contaminating the crystals, after which the crystals growing out of the substrate are dislodged and collected, avoiding any unnecessary disturbance of the substrate. The remains of the charge are then withdrawn. The cadmium sulphide residue is now a pale yellow sintered solid, as opposed to the original bright orange powder; the colour change is due to the change in physical form(101)

rather than to an alteration in purity. The substrate is not disturbed since the use of acids necessary for its complete removal would lead to possible contamination of the apparatus, and would also reduce the life of the silicaware. Further, Vecht, Ely and Apling[82] have shown that the cadmium sulphide substrate can become heavily doped with silicon and/or other impurities by diffusion from the walls of the tube, whereas crystals grown on the substrate are much less affected.

After many runs the substrate is removed and the tube cleaned. At the same time the molecular seive is dried by gently heating in vacuum, and the copper turnings regenerated with hydrogen. The first run after cleaning is performed as for a normal run, but is used solely to deposit a new substrate and any crystals formed during this run are discarded.

5. 3.4. Properties of the flow crystals.

The crystals produced are pale yellow rods or thick striated plates; a few thin, clear plates are usually found in each run and are removed for use by other members of the group. The resistivity of the crystals is high, and under ultra-violet excitation ($\lambda = 3650$Å) at 77°K green luminescence is observed, turning orange before extinction on warming.

The purity of the crystals should be much improved compared with the original starting powder since volatile impurities are swept away, and impurities less volatile than CdS will tend to remain in the boat. No analytical techniques capable of detecting impurities in quantities of less than 20 ppm. are available in these laboratories, but X-ray fluorescence analysis showed that zinc is present at about this concentration.

The paper by Vecht, Ely and Apling was concerned with crystal

purification in a very similar apparatus, and appeared during the course of this research. It confirmed that considerable improvements in purity could be obtained by this method. The authors note, however, that small quantities of oxygen in the product cannot be assessed, and that no satisfactory chemical means is available for detecting small departures from stoichiometry.

5.4. Sulphur-rich flow crystals

Since there appears to be a tendency to lose sulphur in preference to cadmium in open tube growth of the type described in section 5.3, some runs were performed using a charge of cadmium sulphide powder mixed with 1% sulphur (purity 6N), other conditions remaining unchanged. This method of incorporating the sulphur was chosen for simplicity, although more uniform conditions throughout the run would have been obtained using an external sulphur boiler and separate gas flow. There was an increase in the amount of sulphur deposited in the gas exit tube during the run, and the amount of free cadmium on the liner was reduced, but the appearance of the crystals grown was unchanged. Crystals produced by this method as charge material for the growth of large crystals will be referred to as 'sulphur-rich' flow crystals.

5.5. Control equipment

To ensure that flow runs were performed under similar conditions each time, and to cut down the time needed in supervision of the equipment, a set of motor driven cams was arranged to supply power to the furnaces and controller at appropriate times.

The type 991 Ether controller was first modified by the insertion of a second control arm and relay to break the power supply to the furnace when it had reached 600°C. Removal of the voltage from this second control arm restored the furnace power until the normal control point at 1130°C.

A synchronous motor and reduction box were used to drive a shaft at a speed of one revolution per 25 hours. On this shaft four cams were mounted. The lobes of the cams operated S.P.C.O. microswitches, connected to the appropriate equipment. To permit easy alteration of the duration of various stages of the growth, double cams were used; e.g. for the outgassing period of approximately five hours, two adjacent cams with lobes corresponding to times of three and a half hours each are used in preference to a single cam. This allows the period of outgassing to be set to between three and a half and seven hours. The equipment is illustrated in Fig. 5.4. The apparatus controlled and sequence of operations are listed in Table 5.1.

TABLE 5.1 - DETAILS OF SEQUENCE TIMING

APPARATUS CONTROLLED

Cam No. 1	Cam drive motor
Cam No. 2	Copper turnings furnace
Cam No. 3	Ether controller mains supply
Cam No. 4	Ether controller second control arm (600°C)

CONTROL SEQUENCE

Time elapsed (hours)	Switching operation	Effect
0	Microswitch 1 makes	Cam drive motor on
$\frac{1}{2}$	Microswitch 2 makes	Copper furnace on
2	Microswitch 3 & 4 make	Furnace on, heats to 600°C
5	Microswitch 4 breaks	600° control off, furnace heats to 1130°
$8\frac{1}{2}$	Microswitch 3 breaks	Ether controller off, furnace cools
23	Microswitch 2 breaks	Copper furnace cools
24	Microswitch 1 breaks	Cam drive motor stopped

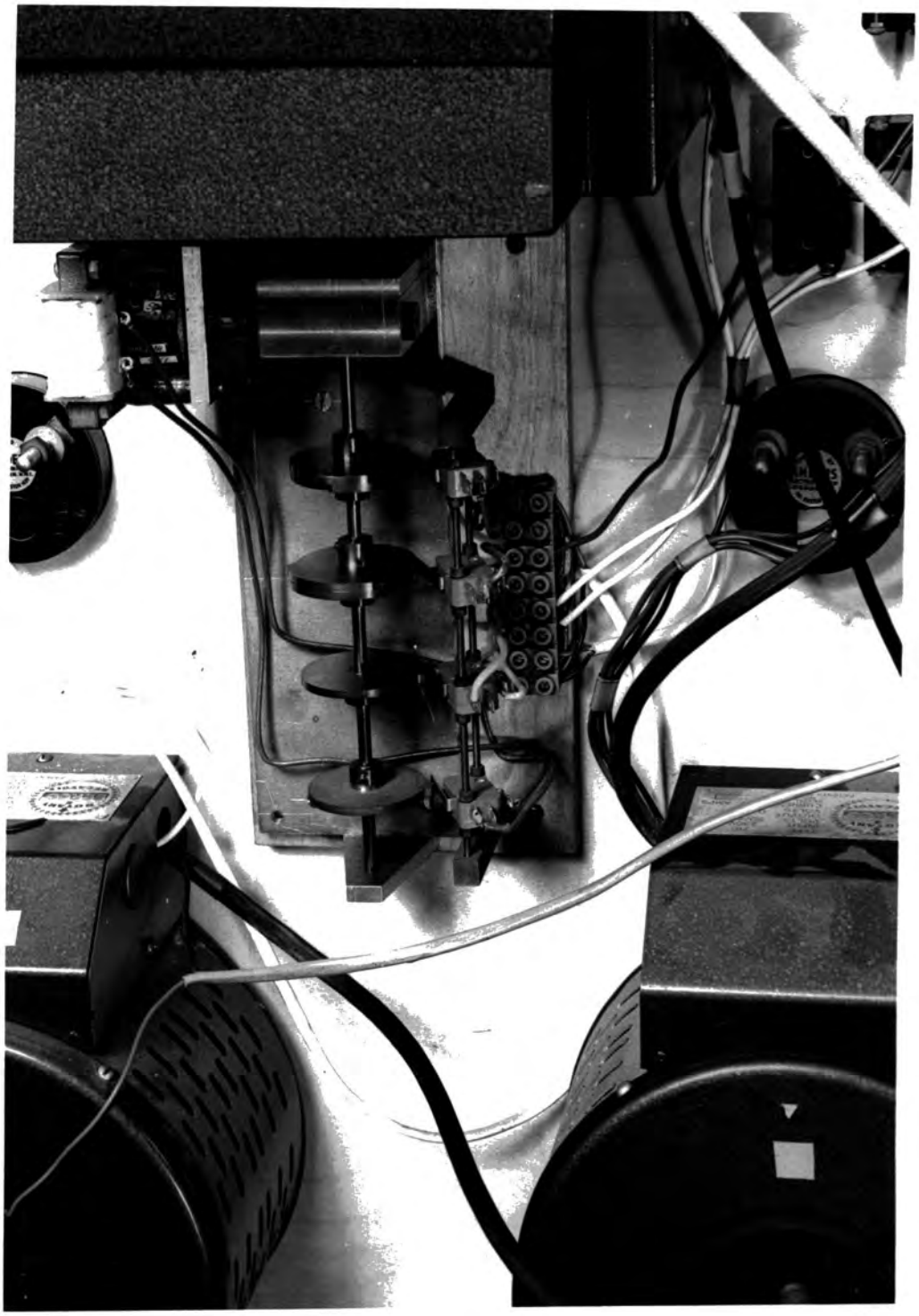

FIGURE 5.4

CHAPTER 6

LARGE CRYSTAL GROWTH IN THIS RESEARCH

6.1 Introduction

Sublimation of cadmium sulphide from one end of a sealed evacuated quartz tube to the other was chosen as a starting point for large crystal growth, since the experimental arrangements are relatively simple. The even simpler method of growth directly on to a cadmium sulphide charge[93] was avoided since the many nucleation sites present would lead to the growth of many small crystals rather than one large one, and the crystals would be contaminated with non-volatile impurities from the charge. It was hoped to avoid both of these disadvantages with the sublimation method.

6.2 Sublimation in sealed evacuated tubes

In the first experiments cadmium sulphide powder, dried and outgassed as described in section 5.2, was used. For each run, 10 grams of the powder was inserted into a 10mm. bore, 6" long silica tube. The tube was then connected to a vacuum system via a silica to Pyrex graded seal. After pumping for six hours at a pressure of 10^{-5} mm.Hg. the tube was sealed under vacuum and positioned in a tubular electric furnace. Each end of the furnace was provided with a separate power supply and temperature controller, so that the temperature at either end of the sealed tube could be set as required. The cadmium sulphide charge was held at 1100°C, with the other end of the tube at 1050°C, for a period of 72 hours, to sublime material from the charge to the cooler end of the tube. The furnace was then slowly cooled.

Little of the powder was transported. Instead the charge sintered and small crystals with well pronounced crystallographic faces grew from its surface. Both the charge residues and the crystals were very dark brown, almost black in colour. Two-probe resistance measurements using indium contacts on small crystals showed that the material had a resistivity of less than 10^{-1} ohm-cm. The use of a thermo-electric probe technique showed that the conduction was n-type.

Further runs were tried using slightly higher temperatures, and a larger temperature gradient (1150°-1050°C) for longer periods, but there was little increase in the amount of material transported along the tube. The higher temperatures did however promote the growth of larger crystals on the charge, and some as large as 8 x 3 x 2 mm. were obtained. (Figure 6.1). The increased size permitted Hall effect samples to be obtained; the room temperature resistivity was 10^{-1} ohm-cm., with $n = 10^{17} cm^{-3}$, and $\mu = 270$ $cm^2/v.sec.$ The mobility rose to ~ 750 $cm^2/v.sec.$ at 100°K. The Hall results and the dark appearance of the crystals show a marked similarity to the properties of CdS crystals prepared in a large excess of cadmium.(32)

In a final attempt to promote sublimation the short tubes were replaced with longer evacuated tubes so that the cool end was now at 400°C. This resulted in sublimation of material from the charge at 1100°C to the region of the tube at about 900°C. The crystals grew in the form of rods; those which grew nearest the charge were brown, whereas those grown in a slightly cooler region were yellow. Since the growth was distributed over several inches, the individual crystals were very small. Two probe

FIGURE 6.1

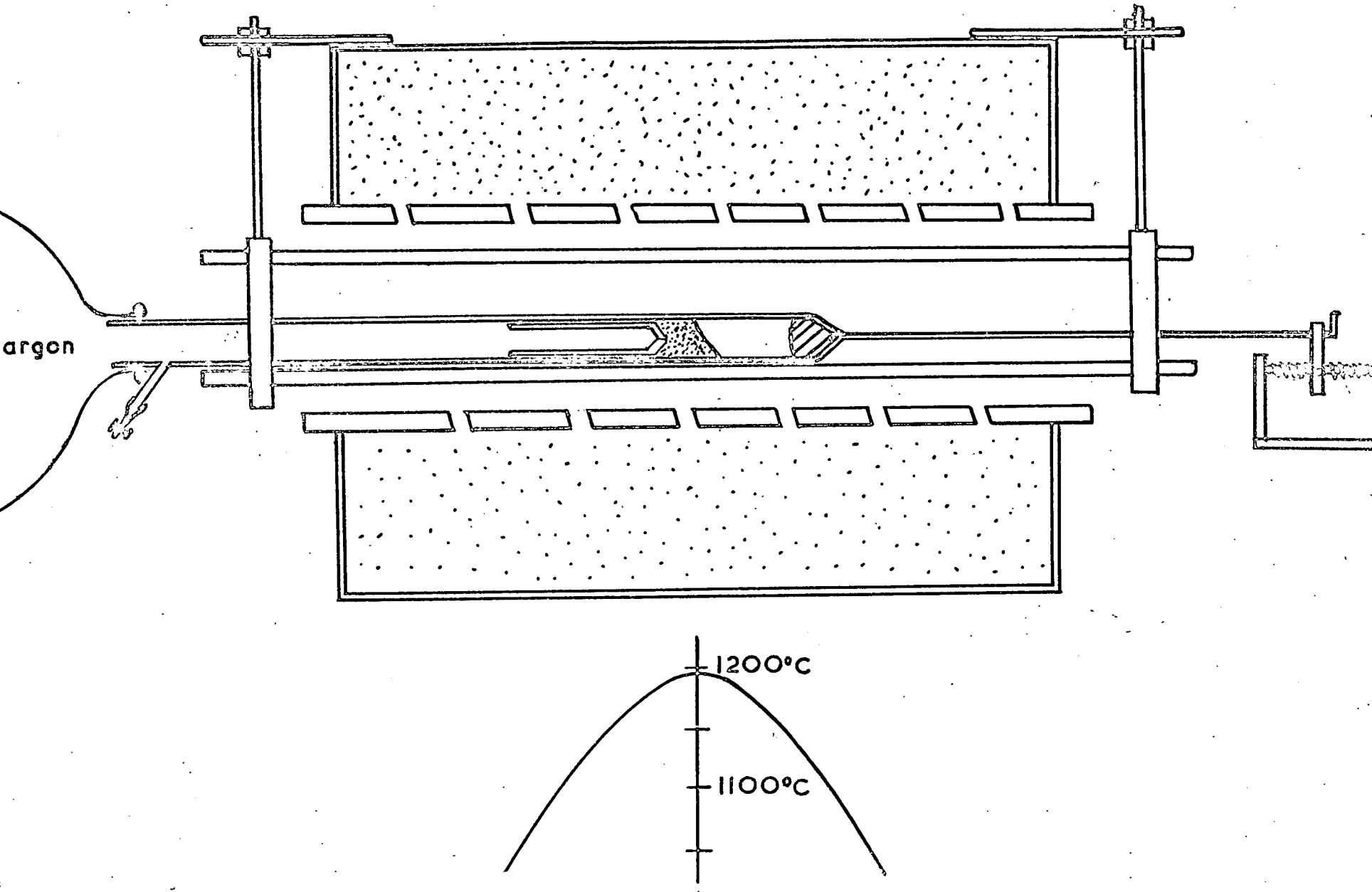

EXPERIMENTAL ARRANGEMENT AND TEMPERATURE PROFILE — PULLING METHOD

FIGURE 6.2

resistivity measurements on several rods showed a dark resistivity of 10^5 ohm-cm., which decreased on illumination.

6.3 Use of argon filled tubes

The experiments with evacuated tubes suggested that the factor reducing the rate of sublimation in sealed tubes could be a high partial pressure of one of the elements, (probably cadmium) as a result of large departures from stoichiometry in the powder charge. To overcome this, long argon filled tubes were used instead of short evacuated ones. 1 cm. bore tubing was used again, sealed at one end in a conical point, but the other end projected from the furnace. The charge was contained near the closed end by a piece of capilliary tubing which was a sliding fit in the main tube. At the outer end, the tube could be evacuated, then connected to an argon-filled balloon to maintain a slight positive pressure of inert gas throughout the run. The apparatus is similar to that shown in Fig. 6.2.

The two-zone electric furnace was used as before, so that the temperature could be controlled both at the charge and at the closed end of the tube. The furnace was slowly brought to temperature, with the charge at 1100°C and the point at 1200°C, to clear the latter of any contaminating material. Any constituent in the charge with a high vapour pressure would be driven off at this stage, before sublimation of the cadmium sulphide sealed off the capilliary tubing. This method of self-sealing of the tube at the final temperature is similar to that of Piper and Polich[98]. After 24 hours the temperature of the charge was raised to 1200°C, and that of the closed end reduced to 1100°C, and maintained for

72 hours to allow sublimation from the charge to the point.

A boule of clear, orange-yellow CdS was formed, composed of several crystals with a cross-section of 2 or 3 mm. square, growing parallel to each other. The boundaries on the growth face between the crystals were of the hexagonal chicken-wire pattern noted by Grillot[102] and individual crystals could readily be cleaved from the block.

Increasing the bore of the tube to increase the amount of material in the system resulted in the growth of more crystals of a similar size rather than larger crystals. Part of such a boule is shown in Fig. 6.3.

The crystals had a low resistivity of $\sim 10^{-1}$ ohm-cm., with $\mu \sim 260$ $cm^2/v.sec.$, and $n \sim 10^{17}$ cm^{-3}. The resistance could be increased by heat-treatment; this will be discussed later in chapter 8.

6.4 Pulling method Fig. 6.2.

To promote the formation of one or a few large crystals as opposed to the many small ones, it was desirable to exercise better control over the nucleation of the boules. The apparatus was modified to allow the growth tube to be pulled slowly though the maximum temperature region of the furnace, as suggested by Piper and Polich[98]. The tubes used were prepared as before, with the addition that a silica rod was attached to the apex of the tube and extended from the furnace. This was drawn along by a synchronous motor and screwed thread drive, with a gearbox to provide pulling speeds in the range 0.5 - 3 mm./hour. The tube was positioned so that the apex was initially at the hottest point (1200°C) of a silicon carbide element furnace, and when the tube had moved so that the point became colder than the charge, supersaturation

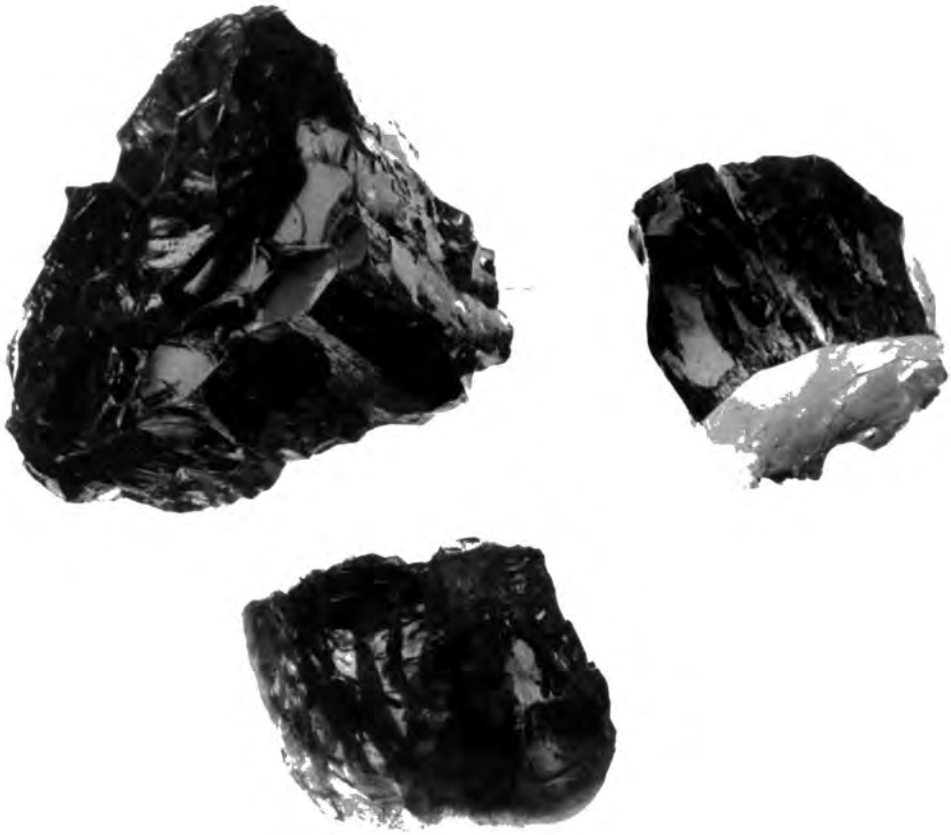

1 CM.

FIGURE 6.3

resulted in growth from the tip. As the run continued the boule grew on the seed so formed, either as one single crystal or as a few sizeable crystallites, over a period of several days.

The material produced was a clear yellow in colour, (Fig. 6.5(a) appendix) in the form of boules 1 cm. diameter and up to 2 cm. long. Occasionally the boule grew as one single crystal but multi-crystalline growth often occurred, especially if the apex of the tube had a very large or a very small semi-angle. Experiments showed that using a tube with large semi-angle encouraged nucleation at several points, since there was little temperature variation between points on the cone. The use of a very sharp, tapering point resulted in nucleation only at the extreme end of the tube, but the growth direction was across rather than along the tube, and broken growth again resulted. An angle of between 45° and 60° seemed the most suitable. A possible increase in the size of the crystals by using larger diameter tubes was investigated, but a diameter of 15 mm. proved the practical limit as multicrystalline boules formed more readily in the larger bore tubes. Crystals from these runs still showed the low resistivities ($\sim 10^{-1}$ ohm-cm.) found in earlier methods.

A change to the use of flow crystals, prepared as described in section 5.3, instead of outgassed powder as starting material was made for some of these pulling runs. The product had a clear yellow colour and sublimation occurred readily. Some crystals were obtained which had a high resistivity of 10^{5} ohm-cm., but the resistivity was non-uniform along

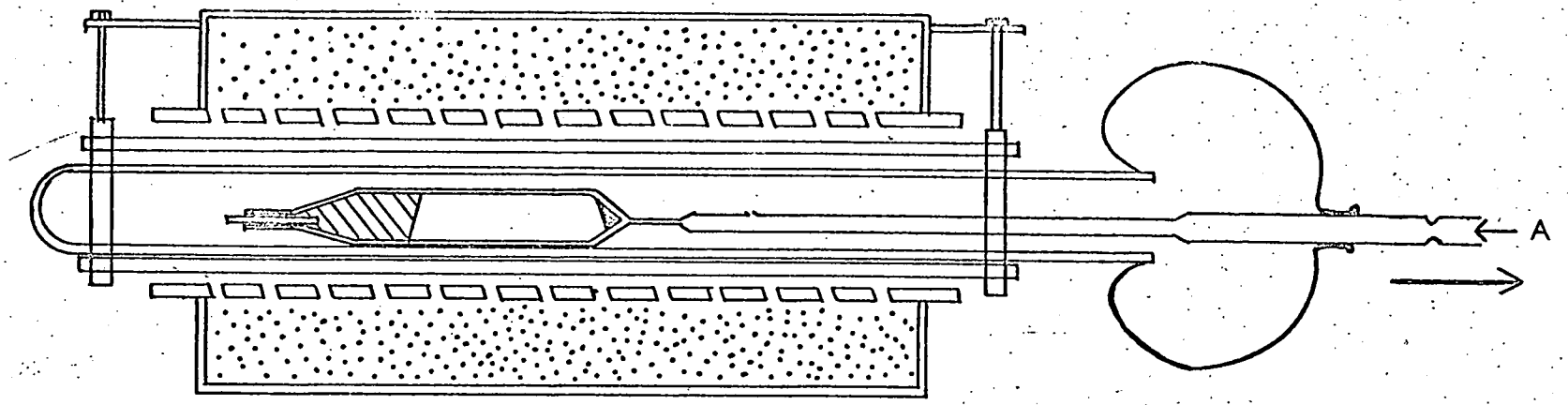

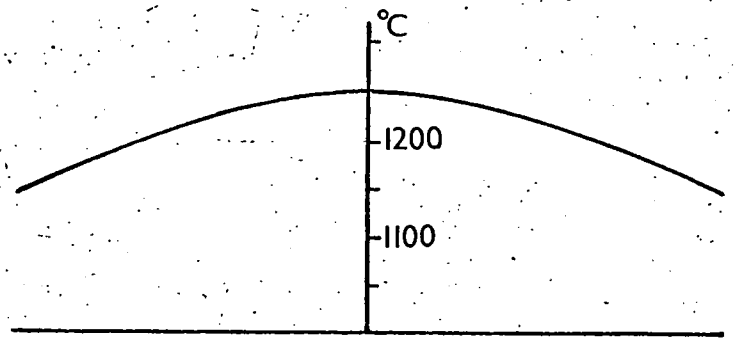

FIGURE 6.4

the length of the boule. Single crystals with a dark resistivity of $> 10^6$ ohm-cm. could be obtained however by using the product of one run as the charge for the next. The amount of material transported in a given time during the second run was higher, and several large crystals were grown in this way. (Fig. 6.5b).

6.5 Piper and Polich's Method

A series of runs using the Piper and Polich method,[98] as described in 4.5.1, were made for comparison with other techniques. This also allowed the properties of crystals grown in this way to be studied, since the properties were not reported in the original reference.

Most of the features of the method were already in use; the principal difference required compared with our previous runs was in the use of short tubes surrounded by a mullite argon jacket, instead of long tubes terminating in a balloon. The mullite outer is provided with an argon inlet and outlet, and a continuous stream of gas is passed through the apparatus.

Some departures were made from the Piper and Polich arrangement to simplify the apparatus. (See Fig. 6.4) Instead of the whole mullite gas jacket being pulled through the furnace, it was fixed in position. The rod attached to the apex of the charge tube (which assists in cooling the condensing material) was extended with a silica tube to the pulling motor. This tube also served as the inlet for the argon flow, which therefore enhanced the removal of heat down the silica rod. Efficient purging of the system was also ensured since the argon was introduced well into the system instead of near to the outlet. To permit longitudinal movement of

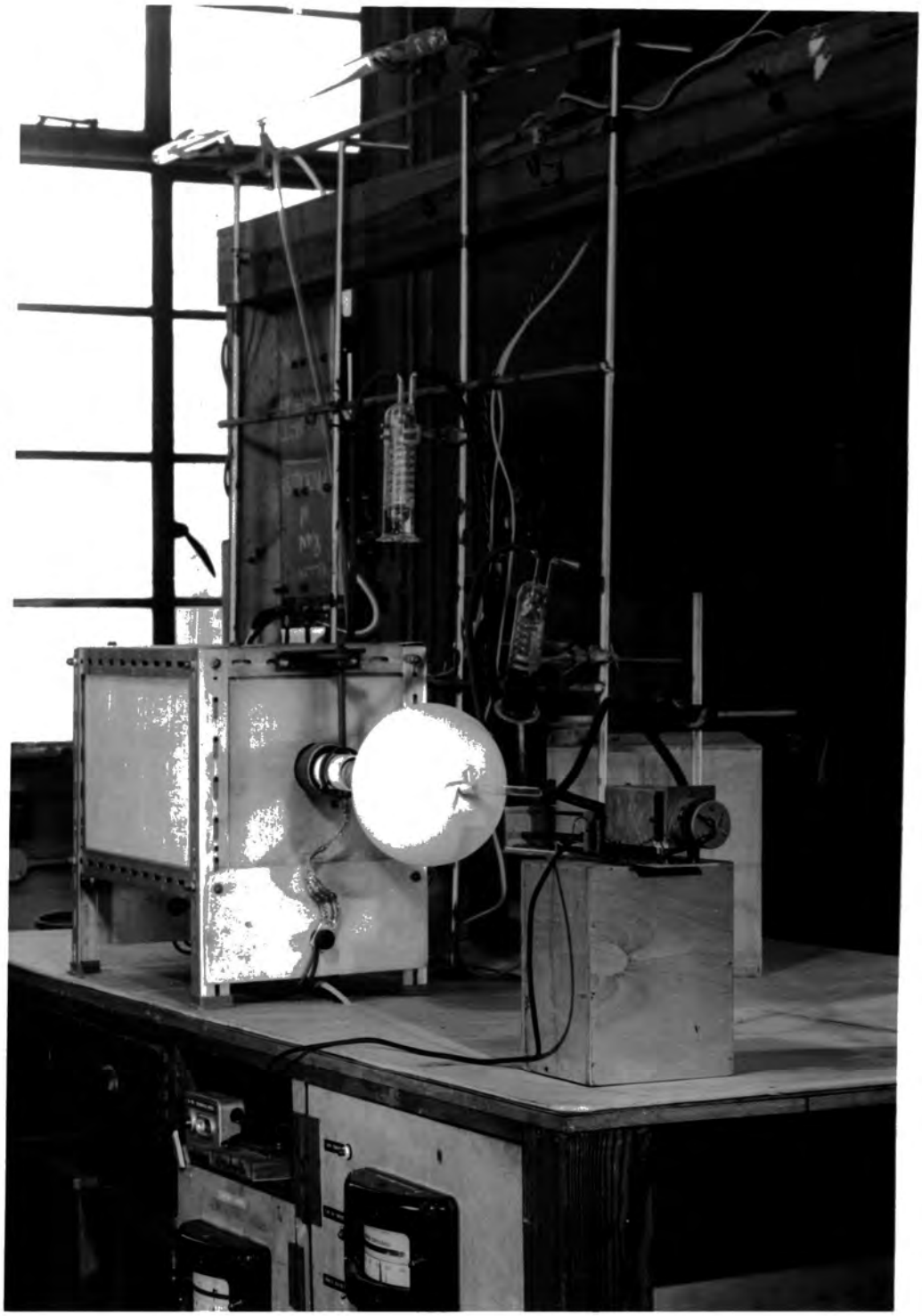

FIGURE 6.4b.

the pulling tube while maintaining a positive gas pressure inside the system, a flexible seal was made by closing the outer end of the mullite jacket with a balloon (of the type used in meteorological work). The pulling rod was a tight fit in the neck of the balloon. The argon gas inlet and outlet were both provided with heavy white oil bubblers to maintain the positive pressure. The temperature at the point of the tube could be monitored by a platinum/platinum-13% rhodium thermocouple attached to the pulling rod; a similar thermocouple outside the mullite at the centre of the furnace was connected to the temperature controller.

Flow crystals produced as described in 5.3 were used as starting material. Approximately 15 gms. was required to fill the 10 mm. bore, 5" long silica tube when loosely packed. After the quartz rod 'seal' had been inserted, the tube was evacuated, and then filled with high purity argon, several times. The tube was positioned in the argon-filled mullite outer, and the system purged for several hours. During this time the furnace was slowly warmed to ~ 150°C to drive out any moisture which may have condensed in the system. After purging, the argon flow was reduced to 50 c.c./min., and the furnace brought up to 1300°C at the control point. The apex of the tube, at the centre of the furnace but inside the mullite, was at 1250°C, with the charge at about 1175°C. This was maintained for 24 hours, so that the flow crystals sublimed back from the point to form a dense charge, and sealed the constriction. The centre temperature was reduced to the desired value for the run, (runs were performed with temperature in the range 1050 - 1300°C) and the pulling motor started.

The run was terminated when the constriction reached the centre of the furnace, before the last of the charge had sublimed. The furnace could be cooled gradually, by feeding the silicon carbide furnace element via its associated Voltmobile transformer from a motor-driven regavolt, so that the current through the element was slowly reduced over two days. Alternatively fast cooling or quenching was obtained by switching off the current, giving an initial cooling rate of > 20°C/min.

The properties of crystals grown at different temperatures, and the effect of slow or fast cooling, will be discussed later. (Section 8.4).

6.6 Vacuum pulling runs

A return to the use of sealed evacuated tubes was made to see if the improvements in technique and starting material could lead to successful results in this mode of crystal growth. It is very desirable that controlled material should be grown by this method since it offers the best opportunity for exact control over the composition of the charge, and for exclusion of oxygen, water vapour, etc., A given rate of sublimation and growth should be attainable at lower temperatures in an evacuated tube, and the gas-handling system and associated complications can be dispensed with. Also of great importance is the fact that a vertical furnace arrangement would then be possible; with the additional facility of rotation of the tube during the run. Such an arrangement would overcome the problem of temperature gradients across the sample and associated non-uniform crystal growth found in horizontal furnace methods.

The experimental arrangement was exactly as shown in Figure 6.4 for the Piper and Polich runs, with the tube being sealed under vacuum

(10^{-5} mm.Hg.) instead of open via the constriction. The argon jacket was retained for some sealed tube runs so that argon-filled and evacuated tubes could be used under identical conditions in the same run for comparison.

The flow crystal charge was again loosely packed so as to fill the whole tube; about 15 gms. was required. Back sublimation at 1300°C for 24 hours to consolidate the charge and clean the tip was followed by pulling at speeds of 0.8, 1.5 or 3 mm./hour, and with the maximum temperature of the furnace set as necessary for the particular run in the range 1050° - 1300°C. After each run the furnace was slowly cooled, with a maximum cooling rate of 0.5°C/min., over two days.

Even with a flow crystal charge, the rate of sublimation was again found to be very low, as in the previous vacuum methods. The highest temperature, 1300°C, combined with the lowest pulling speed to give a long run, was necessary to get sublimation of an appreciable amount of material; one especially good boule, 3 cm. long, of which 2 cm. was single crystal, grew under these conditions. [Fig. 6.5(d).] These boules were transparent, but with a brown appearance. Much of the darkening was due to a surface layer which could easily be removed with a chromic acid etch.

At such high temperatures the silica tubing was almost at softening point, and in several runs the tube had swollen to a diameter of 1.5 cm. or more, but was still under vacuum when cold. This would seem to indicate a component present in the tube with a partial pressure greater than 1 atmosphere at 1250°C; the vapour pressures of Cd and S above stoichiometric CdS at this temperature should be no more than 0.2 atmospheres.

Boules of 1 - 1.5 cm. in length could be grown with a centre tempera-

ture of 1250°C, (corresponding to the boule growing at about 1200°C) and a faster pulling speed of 1.5 mm/hour or 3 mm./hour. These had a much darker colour than the boules grown more slowly at a higher temperature, being almost red in transmitted light. The difference in shade can clearly be seen in the photographs. (Fig. 6.5(e)).

Another consequence of the low rate of sublimation is that the back transport of material away from the point at the beginning of a run is also impeded; to allow this to happen completely the druation of this stage of the run was increased when sealed tubes were employed. If insufficient time has been allowed, growth proceeds both from the point and by deposition on the polycrystalline 'mat' left by the charge, resulting in departures from single crystal growth. The polycrystalline portion can be seen along the boule in Fig. 6.5(e).

When lower furnace temperatures were used, no appreciable growth occurred. At temperatures of 1200°C growth on the charge was found as in the first vacuum tube experiments (see 6.2) but at temperatures of 1150°C or below, little change in the charge was evident beyond some sintering, unless a run was continued for at least 10 days.

6.7 Addition of sulphur

To regain stoichiometric conditions and allow sublimation and growth to procede normally, additional sulphur had to be incorporated in the charge. This was done in two ways. In the first, a small quantity of sulphur was added directly to the growth tube along with the charge. The amount needed was small, since very large departures from stoichiometry were not expected, and the maximum quantity of sulphur used was 5 mgm. This amount gave a

sulphur partial pressure of 1 atmosphere under the growing conditions used. Smaller quantities of 1.5 and 0.15 mgm., representing concentrations of 0.01 and 0.001% by weight of the charge, were also used; 0.15 mgm. was the smallest amount it was convenient to measure. To avoid errors in transferring this quantity of sulphur from the balance pan to the tube, a crystal of approximately the right size was weighed and used, rather than powder which might be lost on transfer.

Runs were performed at a temperature of 1150°C, using the range of sulphur concentrations specified. No transport occurred in the tubes with the largest sulphur content (5 mgm.), only sintering. The tubes containing 0.15 mgm. sulphur promoted growth of small yellow crystals (2 x 2 x 1 mm.) on the charge. Using the tubes containing 1.5 mgm., or 500 p.p.m. sulphur, a polycrystalline boule, 2 cm. long and orange-yellow, grew from the point. The residue of the charge was also clear yellow crystalline material.

Incorporating the sulphur during the preparation of the flow crystal charge by using an excess of sulphur in the original powder, as described in 5.4, also promoted growth. In tubes filled with these sulphur-rich flow crystals the charge sintered to a clear yellow polycrystalline mat, and a 0.5 cm. long boule could be grown at a temperature of only 1050°C. Increasing the centre temperature of the furnace to 1200°C, so that the boule grew at 1150°C, produced one some 1.5 cm. long, although again it was very polycrystalline. Also the remains of the charge grew as large individual crystals with well developed faces. The crystals were of the order of 3 x 3 x 3 mm., and clear yellow.

The incorporation of excess sulphur into the charge thus enables

crystals to be grown successfully in sealed evacuated tubes, by restoring the necessary near stoichiometric conditions. The reasons for our inability to grow samples in sealed evacuated tubes using normal outgassed powder or flow crystals as a charge, and the necessity for stoichiometric conditions in the tubes for growth to occur, will be discussed in chapter 8.

Further to the above experiments on growing crystals in a sulphur-rich atmosphere, low resistivity crystals grown by earlier sealed tube techniques were heated at 900°C in a partial pressure of 10 atmospheres of sulphur for several days. The colour of the crystals lightened, and their resistivities increased from $\sim 10^{-1}\,\Omega$cm to $10^{4}\,\Omega$cm or higher, but in the case of the very black, highly conducting samples annealing had to be continued for up to 10 days to observe this change.

CHAPTER 7

HALL EFFECT MEASUREMENTS

7.1 Sample Preparation for Hall measurements

A suitable Hall effect sample would be rectangular, with dimensions 10 x 2 x 1.5 mm, although samples of these dimensions could not always be obtained when the size of crystals grown was small. A correction appropriate to the length to width ratio of the sample had then to be applied to correct for Hall voltage shorting by the current contacts.(58)

Large boules, provided they were annealed and not quenched after growth, could be cut with a piercing or jeweller's hand saw, using a very fine (0.004") blade. The crystal was cemented to a mitre block made from dural angle, to prevent movement and cracking of the sample, and to guide the saw-cut. After roughly sawing to shape, (or cleaving, if obvious crystal boundaries are present), the final shaping of the sample was done by grinding. Coarse and fine corundum powders, grades 400 and 800 were used, followed by ultra-micro polishing alumina. The grinding was done on a plate glass base, using water as a lubricant. So that opposite faces of the sample were as near parallel as possible, final grinding was done with the samples cemented into a recess of the correct thickness in the flat base of a steel disc. For the quenched samples, the initial shaping by sawing had to be omitted, since the crystal cracked continually as the sawing progressed. In this case, all of the shaping was done by grinding, but this of course reduced the number of samples obtained from a boule.

Grinding was followed by a short etch (1 - 2 mins.) in chromic acid at 80°C to prepare the sample for evaporated contacts. After the etch, the

sample was thoroughly washed in distilled water and dried. The dimensions were then measured using a micrometer. During these operations care was taken to avoid handling the crystal surfaces, since any contamination by grease, etc., could prevent the successful application of good indium contacts.

7.2 Contacts.

Indium was used exclusively as the contact material, since this forms a good ohmic contact and is convenient to apply. The detailed procedure for applying the contacts formed the subject of a recent paper, which is appended. Any evaporated indium left on the crystal surface when the contacts had been applied could be removed with a further brief etch. The sample was then ready for mounting in the appropriate cryostat.

The major disadvantage of the contacts obtained was their size. The contact diameter was of the order of 1 mm., except for the current contacts which covered the entire end of the sample. Probe contacts 1 mm. in diameter will give rise to errors in the determination of sample resistivity and Hall constant, since they act as conducting layers on the side of the sample and disturb the current flow. Zook and Dexter obtained indium contacts as small as 0.2 - 0.3 mm. diameter using an ultrasonic soldering technique.[47] They found that areas as small as this still do not approximate to point contacts as effects due to shorting by the contacts were evident in their magneto-resistance studies. Their contacts had the disadvantage that their resistance was high; about twice as large as the sample resistance using samples with resistivities in the range 3 - 50 ohm-cm. The authors concluded that a lower limit to the size and resistance of the contacts was determined by the requirement of low noise.

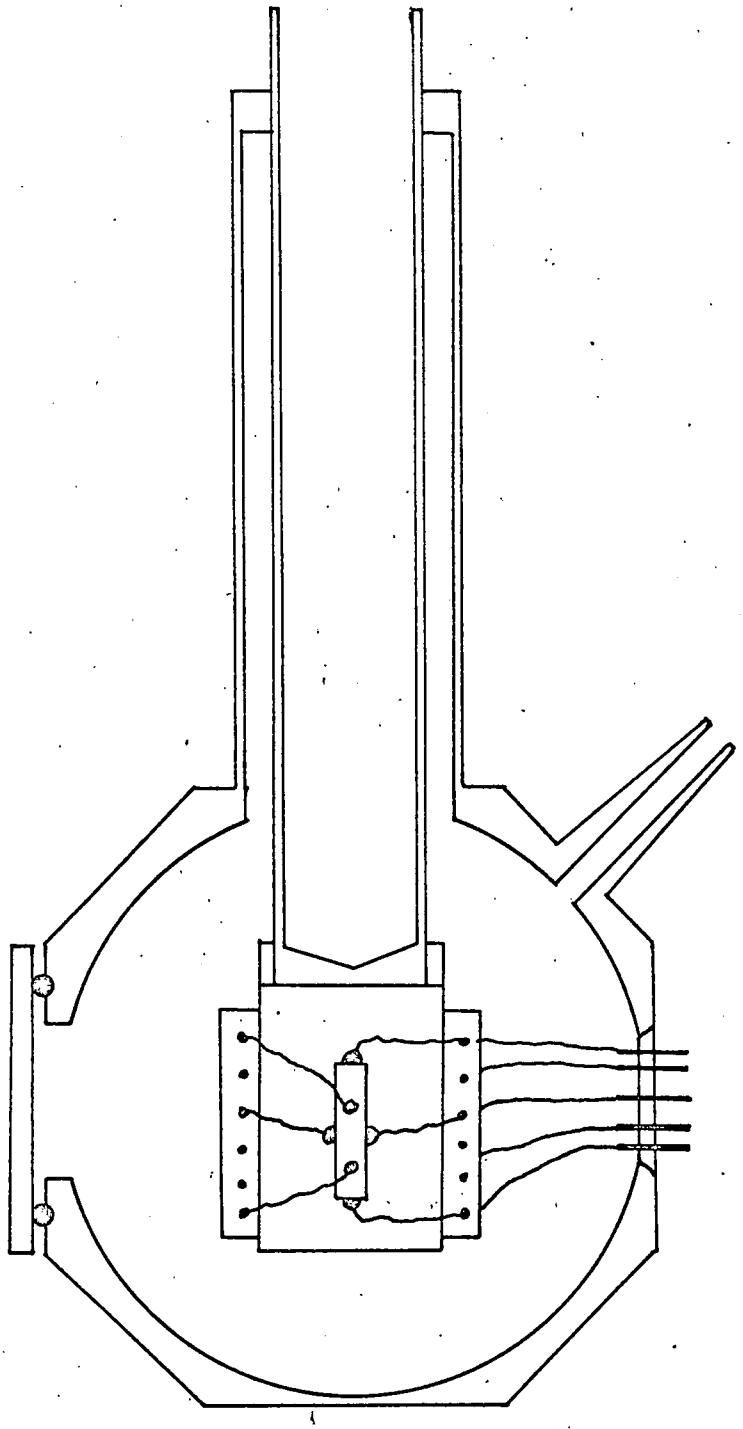

OPTICAL CRYOSTAT

FIGURE 7.1

7.3 Cryostats.

7. 3.1 General

The essential features required of a cryostat for the Hall and other measurements described in this thesis are that the sample can be provided with the necessary electrical leads, and can be held at a known temperature in the range 80 - 300° K, in a reversible magnetic field and perhaps with illumination of a desired wavelength. Two cryostats were constructed; one designed to attain steady temperatures anywhere in the desired range, the other being more portable and with large windows for optical work.

7. 3.2 'Optical' cryostat

The design of this cryostat is shown in Fig. 7.1. The body was turned from a solid copper block, and was provided with a pumping stem, a multiple metal-ceramic seal for electrical leads, and front and side windows. 'O'-ring seals formed vacuum joints at the windows, which could be silica or plate glass as required. Metal blanks were used when measurements of dark current, etc., were made, but the multiple seal had also to be covered as this was translucent.

Two nickel-silver tubes formed a vacuum jacket around a liquid nitrogen reservoir. The copper block on which the sample was mounted formed the base of this reservoir. The block was of large dimensions to provide a large thermal capacity and keep the sample under uniform temperature conditions. A thin sheet of mica on the face of the copper provided good electrical insulation while maintaining thermal contact.

The electrical leads were brought in through the metal-ceramic seal and were terminated in pyrophilite blocks mounted on the sides of the sample block.

Black wax was used to form a vacuum tight joint between the leads and the hollow pins of the seal; soldered joints were found to give rise to thermo-electric e.m.f.'s which interfered with the measurements. A copper-constantan thermocouple was led through the seal in a similar manner. The crystal was mounted on the face of the copper block using a very small quantity of an adhesive such as Durofix which was soluble for later removal of the sample without damage. The flying leads from the crystal contacts (see section 7.2) were soldered to the appropriate leads on the pyrophilite blocks, and the thermocouple was embedded in one of the indium contacts, to measure the sample temperature.

When the cryostat was evacuated to 10^{-2} to 10^{-3} mm. Hg. using a conventional backing pump, the sample cooled to 90°K when the reservoir was filled with liquid nitrogen. Measurements between this lower limit and room temperature could be made while the crystal warmed up after the coolant had evaporated, although at the lower temperatures the rate of rise of temperature was rather fast, being of the order of 10°C per minute. As an alternative, slush baths or freezing mixtures could be used to hold intermediate temperatures, but their use was very inconvenient if many fixed temperatures were required.

The use of the cryostat as described had many important features.

(i) The crystal, complete with flying leads, was easily mounted and removed without heating the sample.

(ii) The crystal was in good thermal contact with the copper block and coolant, whilst the vacuum jacket and nickel-silver tubes provided insulation from the surroundings.

(iii) Temperatures in the range 90 - 300°K could be attained and measured.

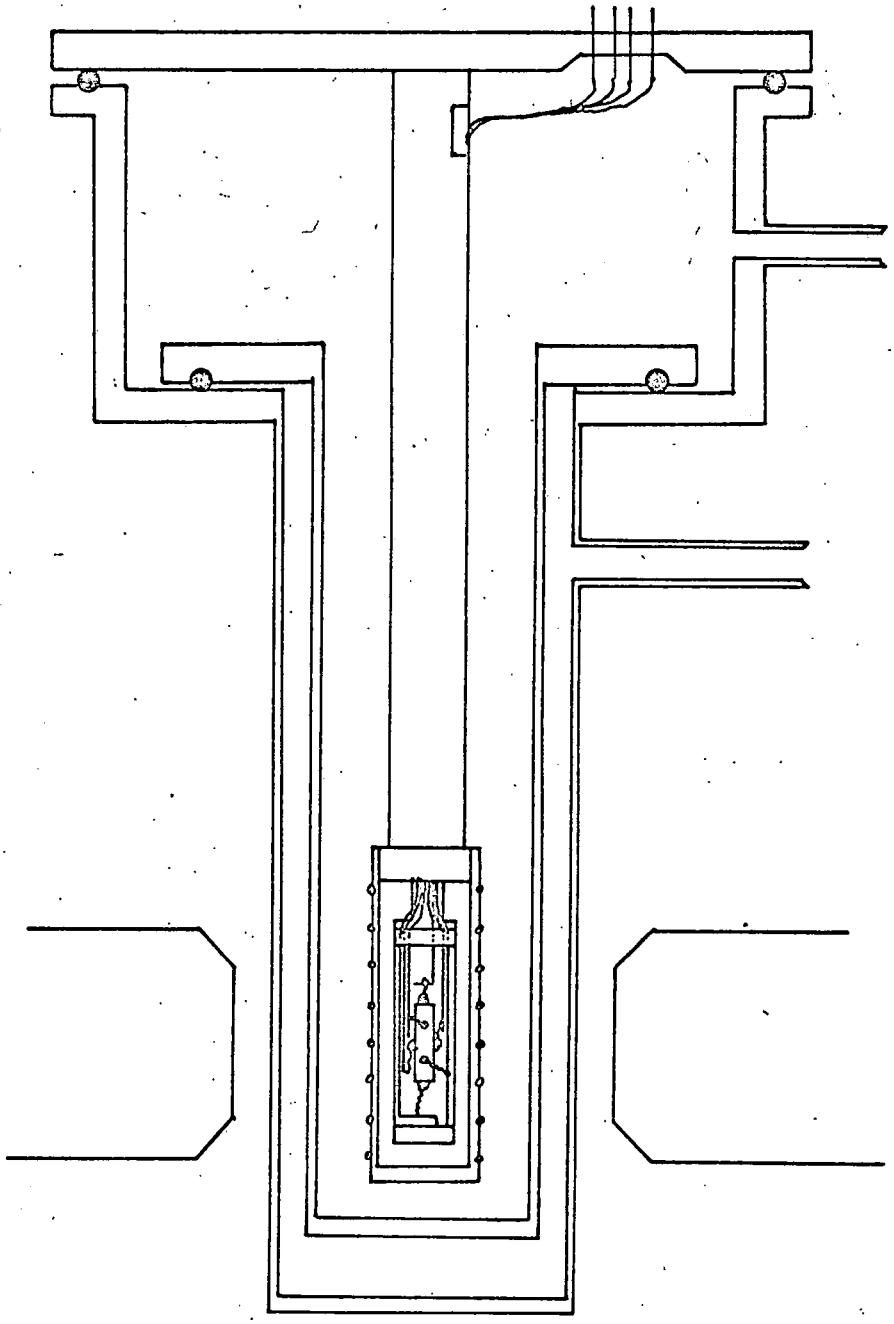

HALL CRYOSTAT.

FIGURE 7.2

(The use of a small heater in the reservoir enabled this range to be extended upwards to 400°K).

(iv) Heat transfer down the leads to the sample was minimised by terminating these leads on the side of the copper block.

(v) The vacuum jacket prevented condensation of water or carbon dioxide on the sample when cold; the crystal was also left under vacuum once measurements had begun so that effects of oxidation or surface absorption of gases were minimised.

(vi) The windows allowed illumination of the sample with infra-red, visible or ultra-violet light, so that resistivity, photoconductivity and other measurements could be performed without the need for removing and remounting the sample.

The difficulty in controlling the lower intermediate temperatures was one disadvantage found with this cryostat. In addition, the thickness of the cryostat body meant using a large magnet pole gap for Hall effect measurements, resulting in a reduction in the magnetic field available. This in turn gave a smaller Hall voltage, decreasing the accuracy of the measurements.

7. 3.3 Hall effect cryostat

This cryostat was designed to allow the samples to be held at any temperature in the range 80 - 375°K, for a period long enough for complete electrical measurements to be made, with less than 2°K temperature drift. The construction of such cryostats has been described many times in the literature, and only brief reference to the details is necessary. (Fig. 7.2) The sample was again mounted on mica on the face of a copper block. The copper was joined to the nickel silver support tube by a small neck, to reduce heat flow.

FIGURE 7.3

The fine-gauge electrical leads were led through the top plate via a metal-ceramic multi-way seal, and passed down the inside of the support tube to the sample block. The leads terminated at the neck of the copper block, where they were connected permanently to miniature 'bus-bars' of 22 s.w.g. tinned copper wire. These were held between pyrophilite blocks and arranged to be adjacent to the appropriate contact on the sample so that the flying leads from the contacts could be soldered in place with a minimum of disturbance. A copper-constantan thermocouple was led to the sample alongside the current leads. As before, soldered contacts at the multi-way seals were avoided, vacuum wax being preferred. Figure 7.3 is a photograph of the sample holder with a sample connected.

When the sample had been mounted, a copper can was fitted around the copper block, sample, and leads. The high thermal conductivity of the copper block and the can, together with the absence of convection currents, ensured steady and uniform temperature conditions along the sample. The outer face of the copper can had a spiral groove cut in it to carry a 'nichrome' wire heater, insulated with 'Refrasil' sleeving. This heater was supplied from a 20 volt transformer and 'Variac', and enabled the sample to be heated above the ambient room temperature. It could also be used to boost the heating rate of the cryostat from low temperatures. The heater leads were led from the cryostat through a separate metal-ceramic seal.

The sample holder and heater were located inside a further tube of nickel silver which completed the nitrogen gas jacket in which the sample was kept. Outside this again was the brass tube forming the outer wall of the cryostat; this was contained in a dewar of liquid nitrogen mounted between the poles of

the electro-magnet. Filling the interspace between the outer wall and the inner gas jacket with nitrogen gas allowed heat transfer between the sample and the liquid nitrogen bath, and the sample temperature slowly fell. When the minimum temperature had been reached, the outer gas jacket was evacuated, reducing the thermal contact. The sample temperature rose slowly due to thermal leakage from the room temperature parts,or more rapidly with the heater in use. The rate of temperature change both in cooling and heating was such that readings of the temperature, current and voltage probe readings, (for resistivity) and four readings of the Hall voltage, for either direction of current and field, could all be taken with no more than $1^{o}C$ change in sample temperature.

As with the optical cryostat, the dimensions of the cryostat necessitated the use of a wide pole gap in the electromagnet. In this case a gap of 2.75 inches was used, giving a maximum field of only 2.05 kilogauss. A further disadvantage was the inability to perform measurements under illumination. This would have been especially useful in the case of high resistance, photoconducting samples, since conventional Hall measurements on such samples are very difficult because of their high impedance.

7.4 Electrical measurements

The current through the Hall samples was supplied from D.C. storage batteries, via variable series resistors to give coarse and fine current control. The current was set approximately to the desired value using a milli-ammeter, and measured accurately potentiometrically using a 1 ohm standard resistance. Currents of between 1 and 5 milliamps were generally used, since higher currents gave appreciable joule heating in the samples. The sample current was reversed with a knife-blade type of reversing switch,

since this was found to give the most reproducible forward and reverse currents.

A Pye portable potentiometer type 7569P, capable of measuring to 0.01 millivolts, and an external galvanometer with a universal shunt formed the basis of the measuring equipment. The input to the potentiometer could be selected using a Cambridge Instruments 2-pole 6-way switch, the switch terminals being enclosed to eliminate convection currents. Connections between the switch inputs and the multi-core screened leads to the sample holder were made with conventional screw-terminal barrier strip to avoid soldered connections. The six inputs were arranged in the desired sequence of measurements and were connected as follows:-

(i) Thermocouple

(ii) Sample Current (Measured across standard resistance)

(iii) Voltage Probe Reading (positive)

(iv) Voltage Probe Reading (negative)

(v) Hall Probe Reading (positive)

(vi) Hall Probe Reading (negative)

The pairs of terminals (iii) and (iv) and also (v) and (vi) were connected to allow readings of either polarity to be taken, so that measurements could be made for both directions of sample current and magnetic field. The results were averaged to eliminate possible errors from thermoelectric or thermomagnetic effects. The readings of sample temperature were made with a copper-constantan thermocouple, the second junction of which was immersed in an ice-bath. An electric stirrer kept the reference junction at a temperature of $0^{\circ}C \pm 0.2^{\circ}C$.

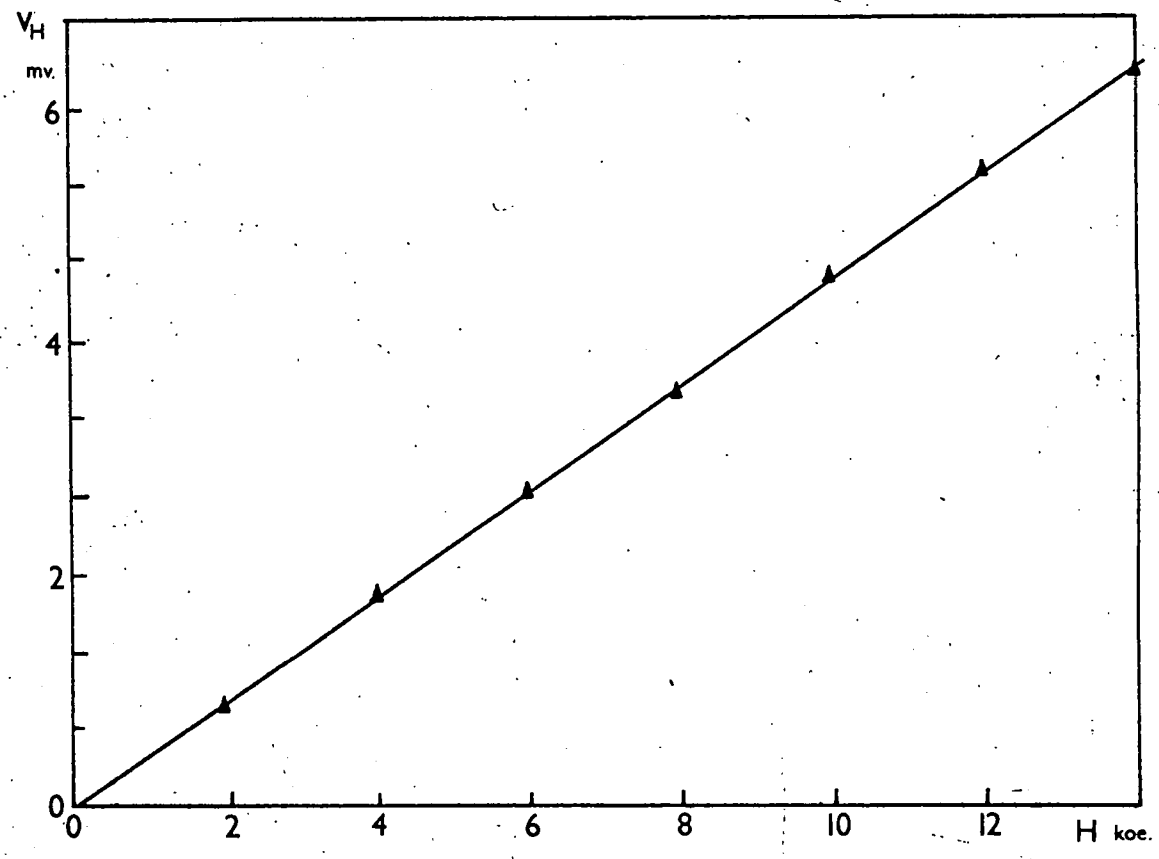

HALL VOLTAGE vs. MAGNETIC FIELD.

FIGURE 7.4

Hall voltage measurements were normally made for only one value of magnetic field, but a measurement of Hall voltage versus magnetic field over the range 0 to 14 kilogausss was made to confirm the linearity of the relation. The results are shwon in Figure 7.4.

7.5. Five probe measurements

When making measurements on samples of higher resistivity, $\sim 10^2$ ohm-cm, any mis-alignment of the Hall probes led to a standing voltage between the contacts which could be much greater than the Hall voltage to be measured. To eliminate this, five-probe measurements were used. One Hall probe was located on one side of the sample as before, but the two voltage probes were spaced on either side of centre on the opposite face. The voltage between these two probes was first measured potentiometrically to determine the sample resistivity in the normal manner. Then the probes were connected to either end of a wire-wound potentiometer, the moving contact of which acted as the second Hall probe. The position of this contact was varied until zero Hall voltage reading was obtained in zero magnetic field. The Hall voltage was then measured for each direction of magnetic field and sample current as before.

7.6 Limitations of the measurements

The resistance connected between the voltage probes in the five-probe measurement must be at least two orders of magnitude higher than the sample resistance between these two contacts before the current flowing through this shunt can be ignored. It must therefore be $\sim 10^4$ ohms or higher, and since approximately half of this resistance appears in series with the galvanometer used to find the null point, and hence the Hall voltage, the sensitivity of the equipment is reduced. Using a shunt of 10^4 ohms, the

Hall voltage could only be measured to 0.05 mv., The potentiometer and galvanometer were replaced with a Philips' microvoltmeter with an input impedance of 10^6 ohms, and this improved the accuracy of Hall voltage measurements, but the effects of leakage currents and the long time constants involved limited Hall measurements to samples with resistivities of 10^4 ohm-cm. or less, although resistivity measurements were possible up to 10^7 ohm-cm. Since homogeneous samples of cadmium sulphide prepared during this research had in general resistivities well below 10^4 ohm-cm. or well above 10^8 ohm-cm., the equipment described was adequate for measurements on the low resistance samples only. Even for these samples with large donor concentrations, when preliminary measurements at liquid helium temperatures were made freezing out of the donors increased the resistivity to 10^8 ohm-cm. However refinement of the apparatus to deal with high resistivity samples is a difficult problem, and was not attempted. An easier solution is to examine specimens under illumination when the resistance is lowered. Initial PhotoHall measurements indicate a mobility of $\sim$225 $cm.^2/v.sec.$, and a carrier density of $\sim 10^{14}/cm.^3$, for the normally insulating samples when illuminated with 800foot-candles from a tungsten lamp.

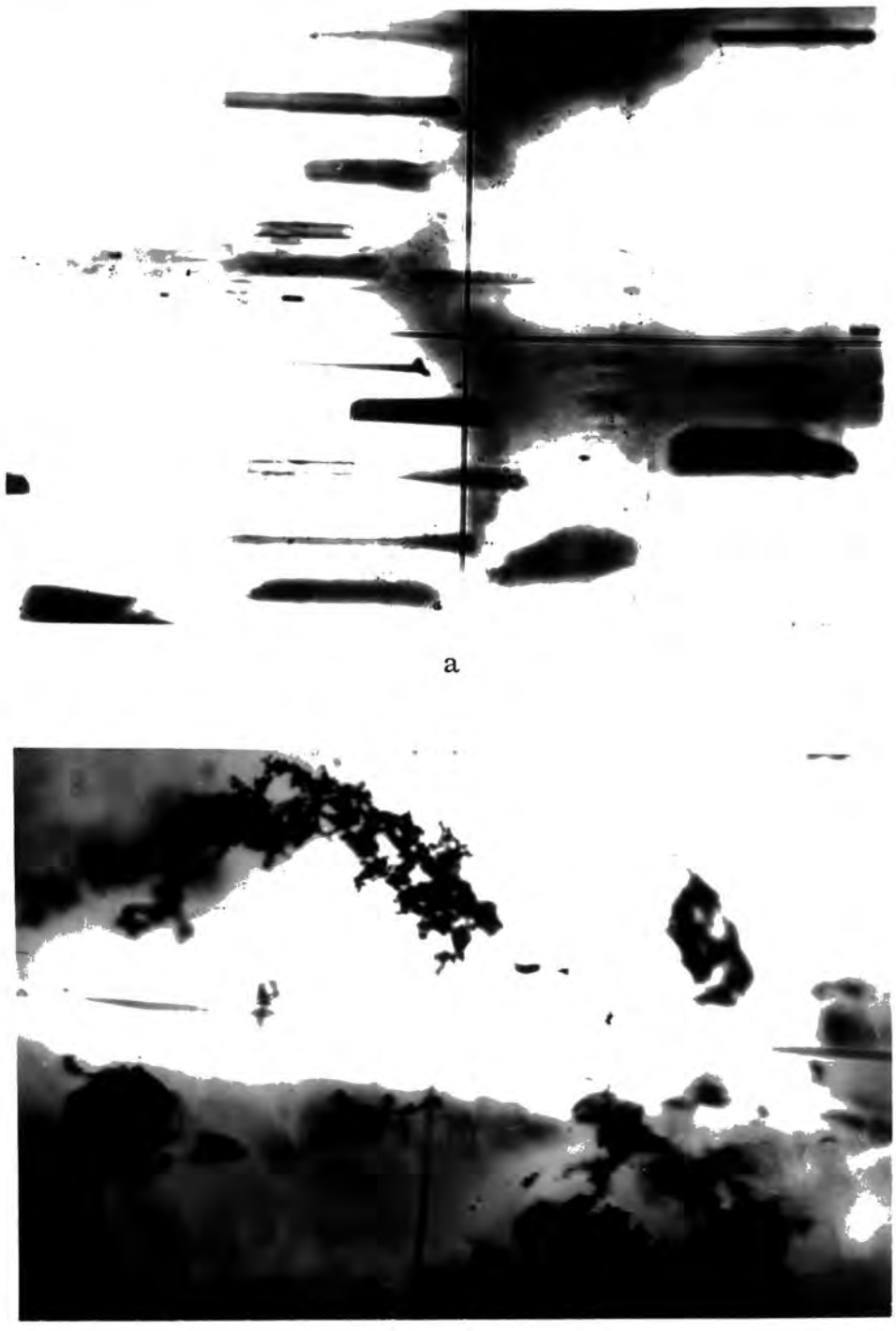

a

b

MICROSCOPIC EXAMINATION OF DEFECTS IN SAMPLES

FIGURE 8.1

CHAPTER 8

PROPERTIES OF CRYSTALS AS GROWN

8.1 Crystals grown in evacuated, stationary tubes

Using a powder charge in a sealed evacuated tube, as described in section 6.2, small dark crystals grew on the charge. These samples were n-type, with resistivities of $\sim 10^{-1}$ ohm-cm. Hall effect measurements showed the carrier density to be about 10^{17} cm.$^{-3}$ with a Hall mobility of 270 cm^2/v.sec. at room temperature, rising to 750 cm^2/v.sec. at 100°K with little change in the carrier concentration.

Microscopic examination of these dark samples was possible by transmitted light, using a natural crystallographic face as the top surface of the specimen. The dominant feature was the presence in the bulk of many rod-shaped defects, thoughtto be voids, all mutually parallel. (Figure 8.1(a)). In a crystal of known c-axis these rods were all parallel to that axis. Variations in the length of these defects were large; they ranged from greater than 1 mm. to 0.01 mm. or less. Diameters were usually less than 0.01 mm., the shorter voids being proportionately smaller in cross-section.

Other defects in the bulk run perpendicular to these rods, but are difficult to distinguish. (Fig. 8.1(b)). They appear to be small, discrete irregular deposits, lying in a line or plane perpendicular to the c-axis. The size of the individual particles is less than 1 micron. The lines may well be dislocations decorated with some second phase precipitate.

Due to the alignment of these defects, light travelling through the crystal in some directions will see a much smaller scattering cross-section than will light travelling perpendicular to this axis. This anisotropic

scattering will be especially marked if defects present are of comparable size to the wavelength of the light.

8.2 Crystals grown in long, argon-filled tubes

These crystals were grown at 1100°C by sublimation from a powder charge at 1200°C, in a tube connected via a constriction to an argon reservoir at room temperature. (Section 6.3). The crystals were small, ~ 2 x 3 x 8 mm., and clear yellow in colour. Hall effect measurements at room temperature showed that $\rho = 1.13 \times 10^{-1}$ ohm.cm., with $\mu = 260$ cm^2/v.sec. and $n = 2.1 \times 10^{17}$ cm.$^{-3}$.

We can note several important points here. Growth had taken place using the same starting material and temperature gradients that had failed to give transport in sealed evacuated tube runs. It must therefore have been possible for any components (probably Cd) present with a high vapour pressure to escape and allow sublimation. The low resistivity of the material indicates the presence of many defects which are acting as donors, since purestoichiometric CdS with a band gap of 2.4 ev. would be an insulator at room temperature in the dark.

The effects of heat-treatment under two different partial pressure conditions were investigated. In the first, the crystal was at the closed end of a long tube connected to an argon reservoir at room temperature. It was thus under the same conditions as it had been during the growth run, (but with of course no powder charge present). This type of heat treatment served as a reference for comparison with the effects of alternative heat treatment. A crystal maintained under these conditions at 900°C for 24 hours

showed no change in appearance beyond a pitting of the surface due to vapourisation, and the resistivity of the sample was unaffected.

If, however the crystals were heated in a short, sealed, argon-filled tube, so that the crystals were at the coolest part of the tube, marked changes occurred. Heating at 900°C for 12 hours resulted in the crystals having a very dark, almost black appearance (deep red in transmitted light). Microscopic examination showed precipitates along lines in the crystals. The deposition appears to lie along dislocation lines, although the small size of the deposits coupled with the darkening of the crystal makes examination difficult. The resistivity of the crystals had also risen sharply, so that the dark resistance was $\sim 10^6$ ohm-cm., falling in daylight to 10^3 ohm-cm.

Both the observed electrical properties and the effects of heat treatment indicate the presence of an excess of cadmium in the crystals as grown. Crystals grown in an excess cadmium partial pressure of 3.69 atmospheres contain donor levels and give carrier concentrations of 10^{17} cm.$^{-3}$ with $\rho \sim 10^{-1}$ ohm-cm.[32] The excess of cadmium is probably present in the samples as sulphur vacancies[103]. The difference in electrical and optical properties produced by the different heat treatments can be understood by reference to the vapour pressure curves for CdS, Cd and S (Fig. 4.1).

The overall vapour pressure of any component in the system, will, when equilibrium has been reached, be the lowest possible in the system. In the heat treatment where the tube is extended to room temperature, material in the vapour above the crystal will be transported by diffusion and deposited in the cooler regions of the tube, since the vapour pressure of each component (Cd and S) is lower over the solid at room temperature than above the heated

CdS. Material will evaporate from the crystal to replenish the vapour, and a steady state situation will be reached, but the crystals and vapour are not in equilibrium.

Using the short sealed tube, the lowest temperature is at the crystal, and sublimation will establish equilibrium between the crystal and the vapour in the tube. Since no (net) diffusion of material from the crystal is taking place, the partial pressures above the crystal will be different from those in the previous case. The large excess of cadmium incorporated into the CdS during the crystal growth will not now be in equilibrium with the vapour, and will deposit out in the crystals as a separate phase. Since the concentration of excess cadmium (or sulphur vacancies) in the crystal has been reduced the number of donors has been reduced and the resistivity increased. The precipitates of Cd formed in the crystals will also give rise to the dark appearance by scattering light passing through the sample.

8.3 Crystals grown by pulling in long argon-filled tubes

The adoption of the pulling method (6.4) with these long argon-filled tubes led to the growth of large (> 1 c.c.) single crystals under similar conditions to those just described. With a furnace centre temperature of 1200°C most of the boule would grow at a temperature of ~ 1150°C. The growth temperature was varied in order to study the crystal properties as a function of growth temperature. The samples produced in these runs were a clear yellow in colour, and showed very little structure in the bulk on microscopic examination, although a few small, rod-shaped voids could be seen. No precipitates could be detected.

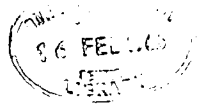

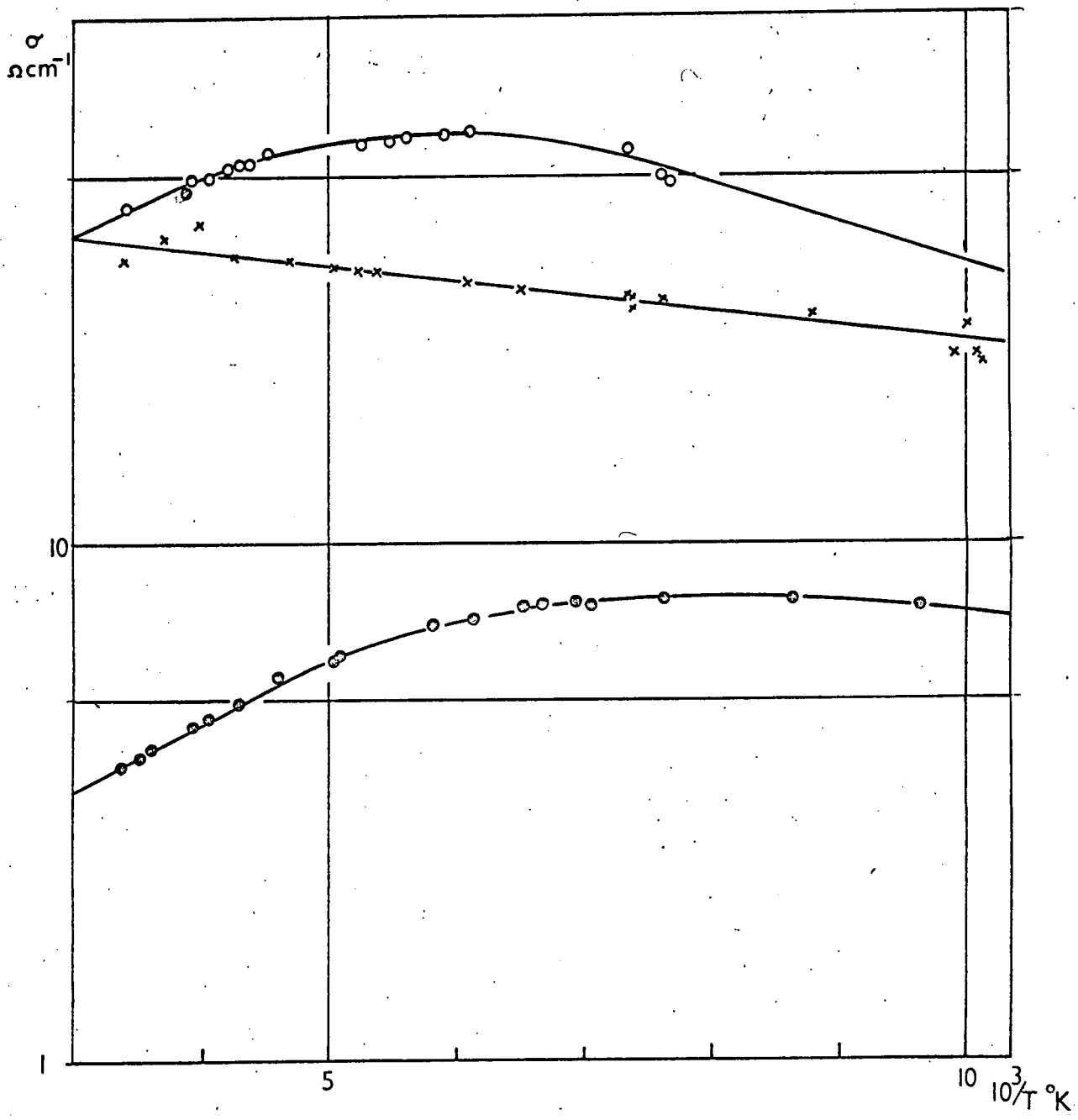

ln σ vs. T^{-1}

FIGURE 8.2

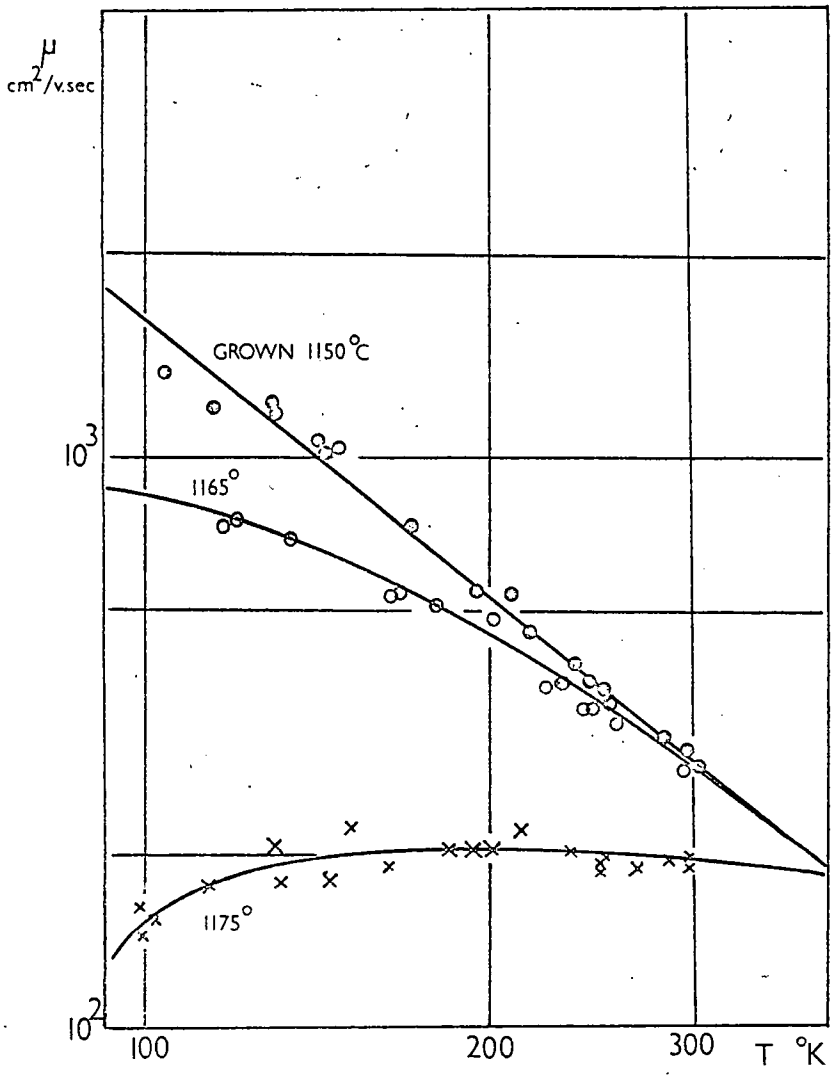

ln μ vs. ln T

FIGURE 8.3

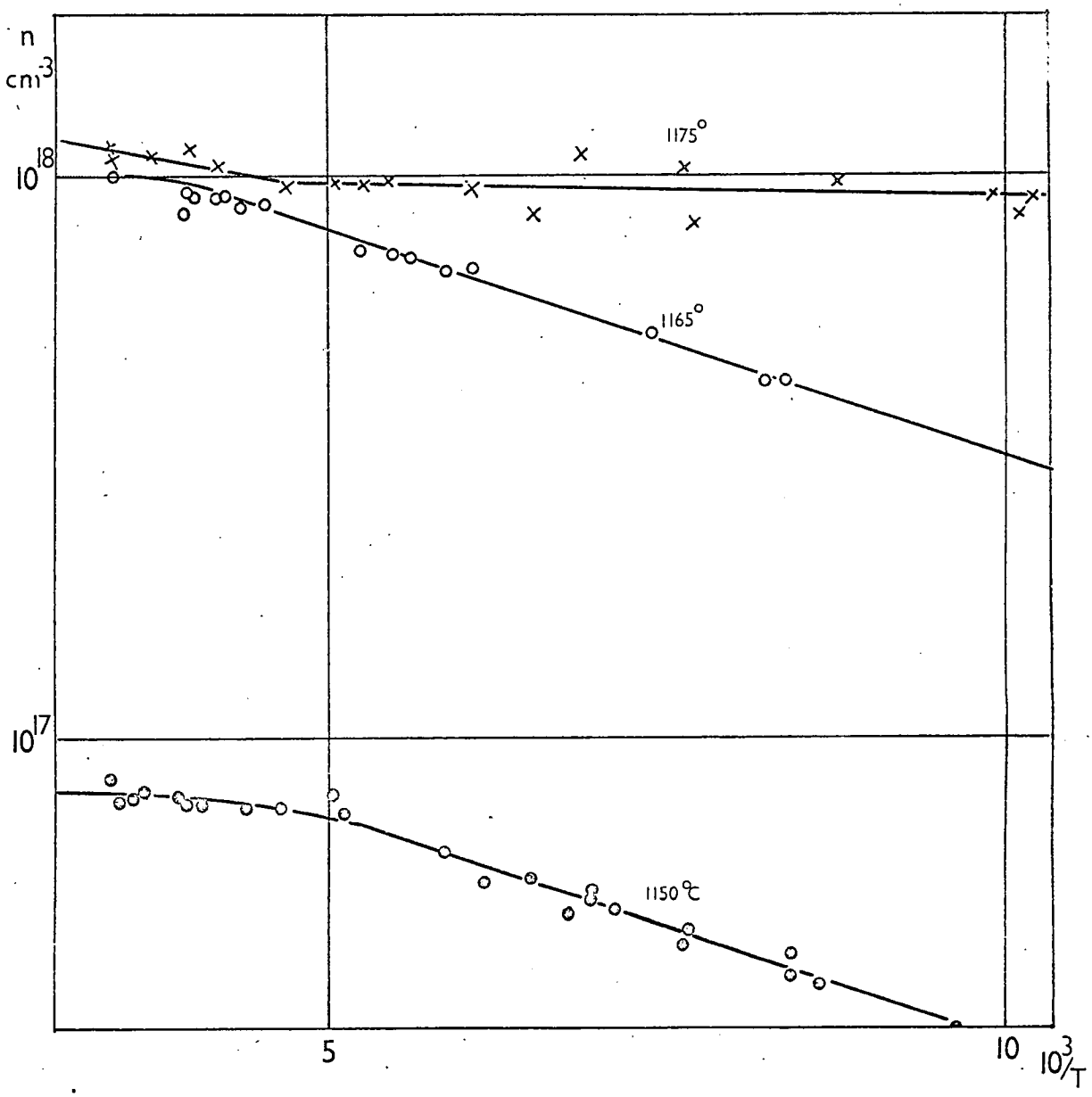

ln n vs. T^{-1}

FIGURE 8 . 4

These larger crystals enabled Hall samples of 3 x 2 x 10 mm. to be ground from the boules. Three samples, cut from boules grown at 1150°C, 1165°C and 1175°C, were measured. The small temperature range studied was limited at the upper end by the working limit of the silica, and at the lower by the difficulty in growing large samples at low temperatures. Curves illustrating the variation of the conductivity, σ, Hall mobility μ_H, and carrier density n with temperature between 100°K and 300°K are shown in figures 8,2, 8.3 and 8.4.

The plot of ln μ_H versus ln T for the crystal grown at the lowest temperature (curve 'a') is a good straight line of slope -1.6, which is very close to the expected value of -1.5 for electron scattering by acoustic mode phonons only. As the growth temperature is increased, departures from curve 'a' become more marked, the mobility becoming smaller than the expected value. This is due to the onset of ionised impurity scattering with the temperature variation $\mu_H \propto T^{+3/2}$. The magnitude of this scattering and hence the temperature at which it causes departures from the lattice scattering value of mobility, is determined by the density of the impurity centres present.

The lower mobility due to an increase in the number of scattering centres is to be expected in crystals grown at a higher temperature. The number of lattice defects in equilibrium in the crystal increases as the temperature rises. The number of such defects at room temperature will be less than that at the growth temperature since some will anneal out on cooling, especially as this is done slowly to minimise strain in the crystals.

However a proportion of the defects will be 'quenched in' as the crystal cools, due to a reduction in the mobility of the defects through the lattice.

The measured carrier densities are shown in Figure 8.4, and these can be taken to indicate the donor density in the crystal since the curves saturate near room temperature. The crystal grown at the lowest temperature (1150°C) has a donor density of 10^{17} cm.$^{-3}$, whilst in those grown at a higher temperature the density is 10^{18} cm.$^{-3}$. Between 300° and 100°K the carrier density for the crystal grown at the highest temperature shows little change, indicating either that the carriers are due to a donor level lying very close to the conduction band, or more probably that the defect density is so high as to give rise to impurity band conduction.(31) The other curves each show a linear region of similar slope at low temperatures which allows a value of the energy depth E_D of the donor level to be calculated. The slope is measured at ~ 100°K since the carrier densities at higher temperatures are too high for an assumption of non-degeneracy to be valid.

The variation of carrier density with temperature in an extrinsic semiconductor over the range where the donors are partially ionised gives $\ln(n/T^{3/2}) \propto E_d/kT$ for a partially compensated semiconductor, or

$$\ln\left(\frac{n}{T^{3/2}}\right) \propto \frac{Ed}{2kt} \quad \text{for } N_D >> N_A;$$

where N_D and N_A are the concentrations of donors and acceptors. (See section 1.3.4.).

Zook and Dexter(47) have shown that for single crystal CdS prepared under similar conditions to ours and with similar electrical properties there is considerable compensation present; the first expression should

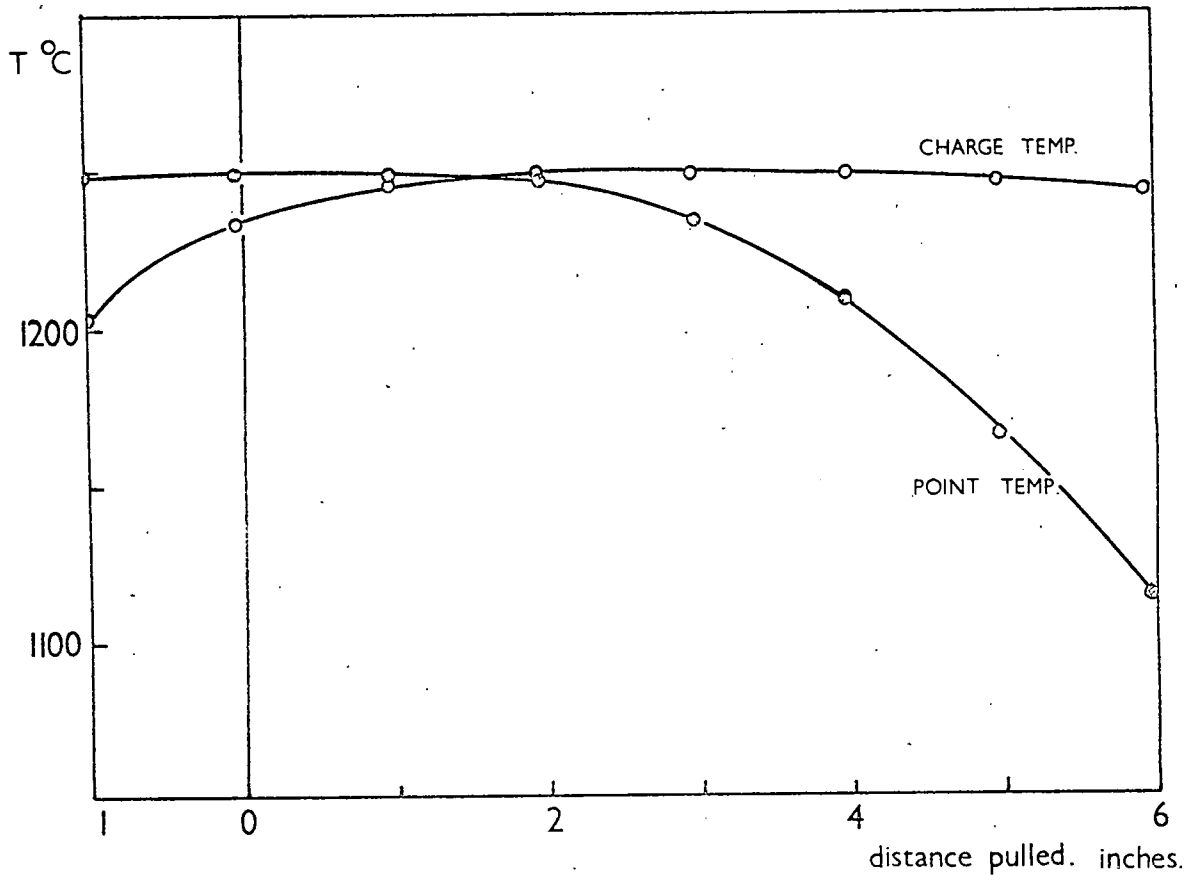
T °C
CHARGE TEMP.
1200
POINT TEMP.
1100
1
0
2
4
6
distance pulled. inches.

FIGURE 8.5

therefore be the more correct. This gives a value for the donor level as 0.014 $\pm$0.004 eV for both samples. The variation of carrier density n with temperature is similar to that reported for ultra-high purity Eagle-picher CdS single crystal by Itakura and Toyoda[104]. They too calculated a donor level at 0.014 ev. below the conduction band. These authors also reported a constant Hall mobility (240cm.^{2}/v.sec.) from room temperature to 200°K, followed by an increase $\propto T^{-3/2}$ to 50°K. We found no evidence of this constant mobility region in our measurements.

8.4 Piper and Polich crystals

8.4.1 Growth conditions (See 6.5)

These crystals were grown in an argon atmosphere, in a short silica tube open via a constriction to an outer argon jacket. Pulling the tube through the furnace so that the point becomes colder than the charge allows nucleation of the boule at a temperature a little below that of the centre of the furnace. Most of the boule grows some 50° lower than this centre temperature, as the pulling proceeds. Figure 8.5 shows curves of the temperature distribution during a run both at the charge and at the point of the tube, plotted against distance pulled. It will be seen that the first part of the boule to grow forms at a higher temperature than the majority of it; any excess of defects incorporated at this stage should anneal out as the tip cools.

8.4.2 Mode of growth

Visual and X-ray examination of boules grown by this method shows that the c-axis of the crystal is not parallel to the pulling direction, although in general it lies within 25° of it. In addition, the growth face is not

perpendicular to the tube, but at an angle to it, as can be seen from Fig. 6.5(d). This non-uniform growth is due to the horizontal furnace system used, where one side of the silica growth tube is in direct contact with the mullite outer. This gives rise to a vertical temperature gradient across the tube and as a result deposition is more rapid on the cooler side, causing the angled growth face. A consequence of this is that any irregularities in the wall of the silica tube nucleate new crystallites which can grow right across the boule, rather than remain localised at the surface. Fig. 6.5(d) shows an area half-way along the boule where a defect on the 'hot' side of the crystal has been localised and has grown out, whereas a similar fault on the cooler side towards the end of the boule has been transmitted through the crystal with the consequent departure from single crystal growth.

These effects are minimised if two parallel growth tubes are pulled together; the point of contact with the mullite outer is no longer also coincident with the point of contact of the gas jacket with the alumina furnace tube, and the transverse temperature gradients across the sample are reduced. The results are seen in Fig. 6.5 (f) and (g), where the growth faces of the two boules, which were pulled together, are more nearly perpendicular to the length of the boule. Mounting a single growth tube on silica runners also reduced the transverse temperature gradients across the sample, but complicated the apparatus.

8.4.3 Effects due to Variations in the Growth Temperature and Pulling Rate

Using the highest furnace temperature (1250°C) and the slowest pulling rate (0.8 mm./hour) large boules of CdS 3.5 cm. long and 1 cm. diameter

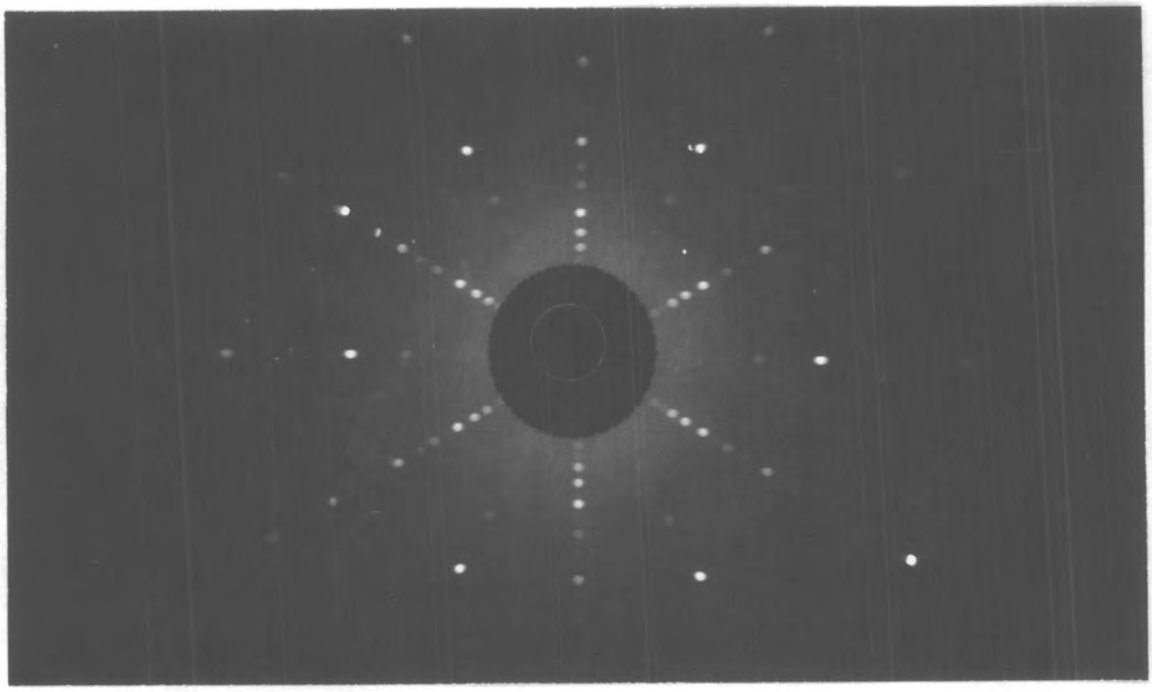

a

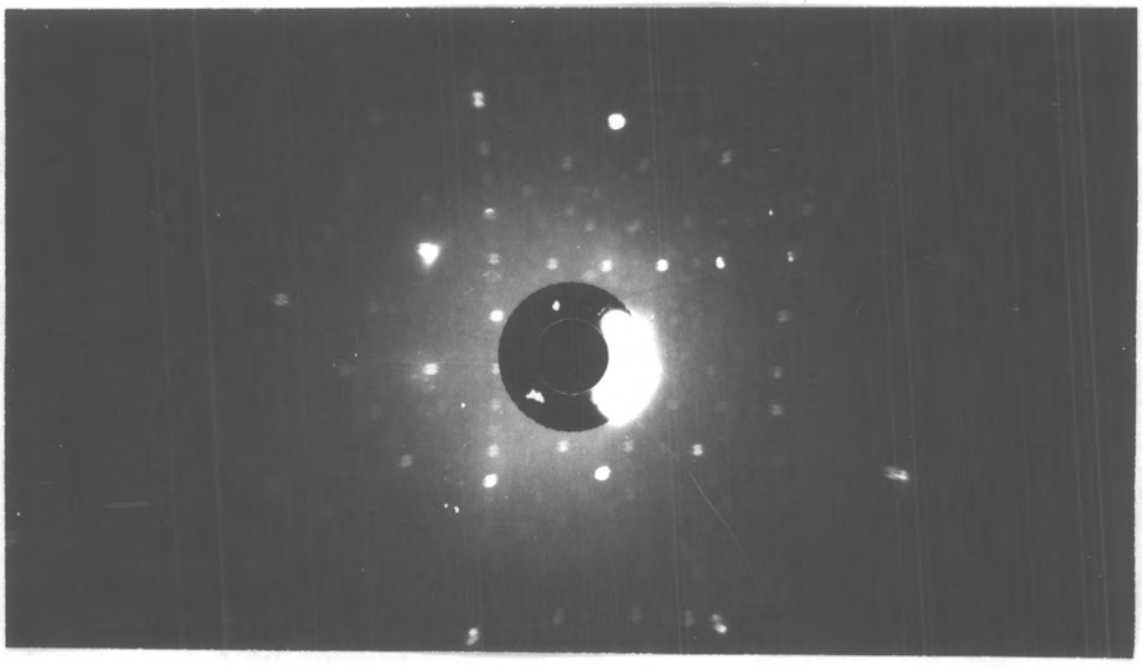

b

FIGURE 8.6

could be grown consistently. These boules were not one single crystal, breaks occurred along the length. However single crystal regions 1 cm. diameter and not less than 1 cm. long could generally be obtained. Figs. 6.5 (e), (f) and (g) show samples grown under these conditions. X-ray back reflection photographs showed little mosaic or c-axis wander in most samples (Fig. 8.6a), although such effects were more noticeable near the edges of the boule (Fig. 8.6b). Optically the crystals were a clear yellow but with a darkened appearance, much of which was associated with a surface layer easily removeable in chromic acid. Hall samples could be obtained from the boules by cutting and grinding, and four probe resistivity measurements showed a uniform high dark resistivity of $> 10^8$ ohm-cm. (the limit of measurement of the equipment) while illumination at room temperature of 800 foot-candles from a 50w.tungsten lamp lowered the resistivity to 2.4×10^2 ohm-cm., with $\mu_H = 224$ cm.^{2}/v.sec. and $n \sim 10^{14}$ cm.$^{-3}$

Using the same temperature distribution, increased pulling rates of 1.5 and 3 mm/hr. reduced the amount of material transported to 2 cm. and 1 cm. respectively, due to the reduction in the time available for growth. However it also caused an obvious darkening of the boules, through orange-yellow to a dark brown. The resistivity of the as-grown material, although still very high near the surface of the boule, was very non-uniform.

The same orange colouration and non-uniform resistance was found in crystals grown from an intermediate temperature, $\sim 1150^\circ$C, unless the slowest pulling rate was used. The reduction in temperature again decreased the rate of transport and the size of the boule, a total length of 2 cm. being obtained. Hall effect samples cut perpendicularly to the

axis of the boule showed an overall high resistance across the current contacts, > $10^8 \Omega$ in the dark, which fell to 10^4 ohm under strong illumination as above. However the centre portion of the crystal was of low resistance and not photo-sensitive. The uniformity of resistance of the centre of the sample could be judged from measurements of the potential difference, or the resistance, between each of the voltage probes and the Hall probes. Where this region showed reasonable homogeneity a Hall effect measurement could be performed to find the resistivity, mobility and carrier density in the low resistance region. To reduce the impedance of the high resistance ends so that a current of ~ 1 ma. could be passed ($V_H \propto I$), measurements were done under illumination from the 50 watt tungsten lamp. This could only be done at room temperature, with the cryostat available. The carrier density n was $5 \times 10^{15}/cm.^3$, with mobility μ_H = 303 $cm.^2/v.sec.$, which corresponds to a resistivity ρ = 4.1 ohm-cm. Readings were consistent with either direction of current or magnetic field. To check that the high resistance was a bulk property of the sample and not due to poor contacts, the contacts were removed, the crystal etched, and the contacts remade, with the same result as before. Grinding down the end of the sample, however, removed the high resistivity region.

It will be seen from the above that two probe resistivity measurements alone must often be regarded with suspicion. A low resistance reading indicates a low resistance sample provided any coating of metallic cadmium has been etched from the surface, but a high resistance reading could be an indication of the surface properties of the boule only. It would appear

that the boules grown at high temperatures (> 1100°C) are deposited initially with a large excess of donors; partial annealing takes place while the growth is proceeding or during the cooling. The darkening of the crystals is probably associated with the non-stoichiometric excess of cadmium. During cooling some of the excess cadmium is precipitated out throughout the bulk, in a range of different sized aggregates which scatter light to give optical darkening. At the same time the donor concentration is reduced. With the crystals grown very slowly at high temperature this annealing could proceed to completion, which explains their dark colour and high resistance. The use of a faster pulling rate would leave insufficient time for the annealing, and also introduce more defects if the transport was too rapid for equilibrium to be maintained between the growing face and the vapour. At lower temperatures, the reduced mobility of defects in the lattice would prevent their free diffusion from the crystal. In either case a non-uniform sample results.

Since the rate of sublimation of material decreases markedly with temperature, all low temperature runs were made using the slowest pulling rate in order to increase the duration of the run and to ensure equilibrium between the crystal and the vapour. This was essential becuase a rapid rate of transport of material to a crystal growing at a low temperature results in very polycrystalline growth. It was difficult to obtain large crystals for Hall samples in boules grown at these low temperatures (~1050°C). The material was found to be of high resistivity, $\rho > 10^8$ ohm-cm., and photoconducting, $\rho_{ill.} \sim 10^4$ ohm-cm. In contrast to the high temperature samples it was a very clear yellow colour, similar in appearance to crystals

TABLE 8.1

PROPERTIES OF CRYSTALS GROWN BY MODIFIED PIPER & POLICH METHOD

Growth Temperature	Pulling Rate	Resistivity (ohm-cm)	Colour	Comments
1250°C	0.8mm/hr > 1mm/hr	$>10^8$ Non-Uniform 10 in parts	Yellow but darkened Dark Brown	~1cc. single Xtal.regions
1150°C	0.8mm/hr > 1mm/hr	$>10^8$ Non-Uniform (10^7 10)	Yellow Brown	
1050°C	0.8mm/hr > 1mm/hr	$>10^8$ too fast for growth	Clear Pale Yellow -	Xtals 2x3x3mm
1050°C (Quenched)	0.8mm/hr	< 1	Clear Pale Yellow	Xtals 2x3x3mm

grown by a flow method.

The properties of crystals produced in our Piper and Polich type growth runs are summarised in table 8.1. The properties depend both on the growth temperature and on the pulling rate. In general, lowering the temperature or the growth rate leads to a higher resistance and lighter colour. Large high resistance crystals are most readily obtained when grown slowly at high temperature, but their optical perfection is poor due to scattering by cadmium precipitates. Clear yellow high resistance material is formed at low temperature, but large crystals are more difficult to obtain.

8.4.4 Effect of quenching

Instead of being cooled slowly, some samples were quenched after the growth run by cutting off the furnace power. The open construction of the silicon carbide furnace meant that the crystals were subject to a fast rate of cooling, > 30°C/min., The complexity of the apparatus prevented quenching in the normal manner i.e. by removing the crystal from the furnace.

Crystals prepared at the higher temperatures (1250°C) and then quenched appeared yellower or clearer than the equivalent slow cooled samples, but no Hall samples were obtained due to the cracked and brittle nature of the material. Two-probe resistance measurements indicated non-uniformity of resistance in the boules. A Hall sample was however obtained from a quenched sample grown at a low temperature, 1050°C, at the slowest pulling rate. This sample was a clear pale yellow, similar to the equivalent annealed sample, but its resistance was low. Hall measurements showed that

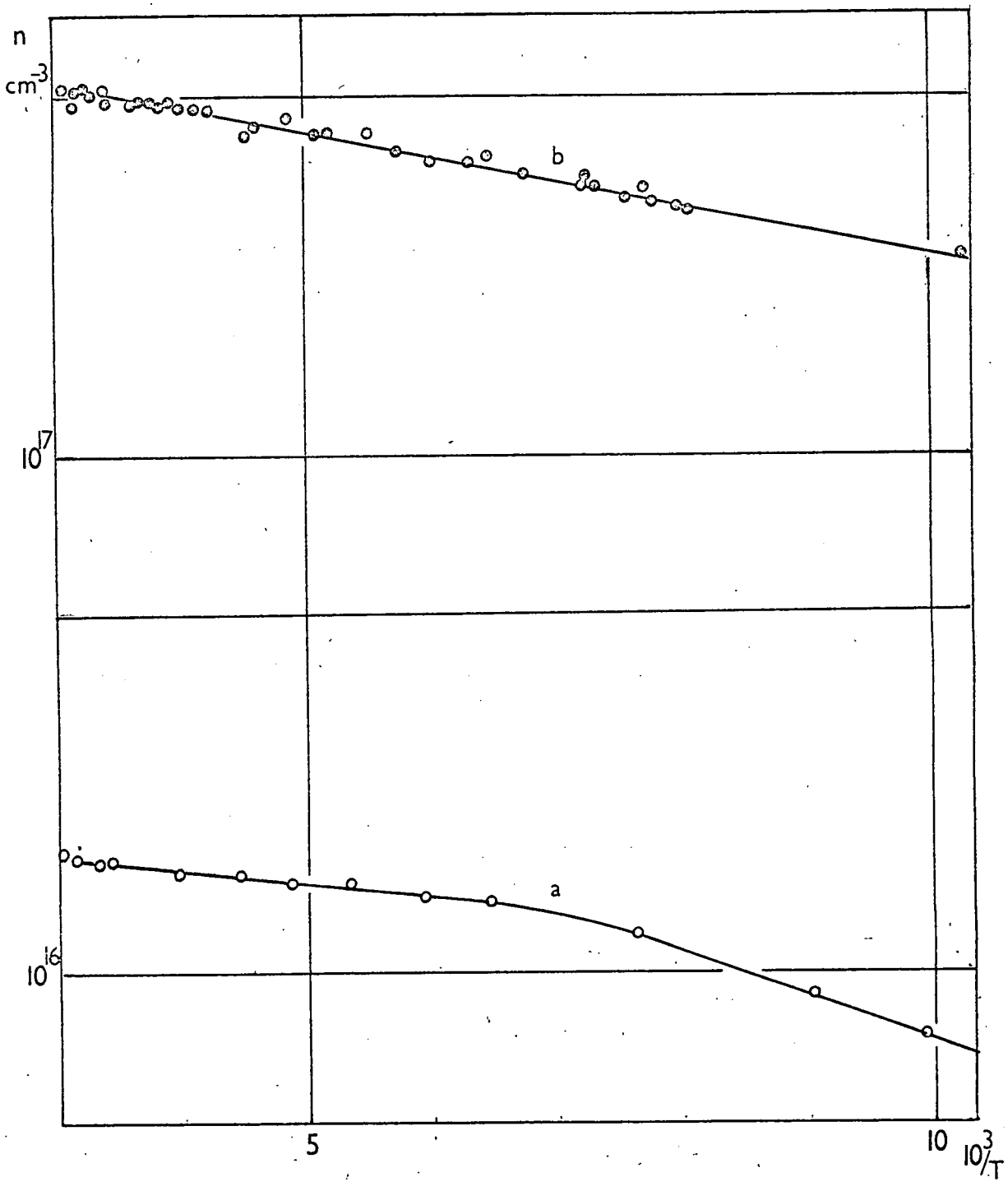

ln n vs. T^{-1}

FIGURE 8.7

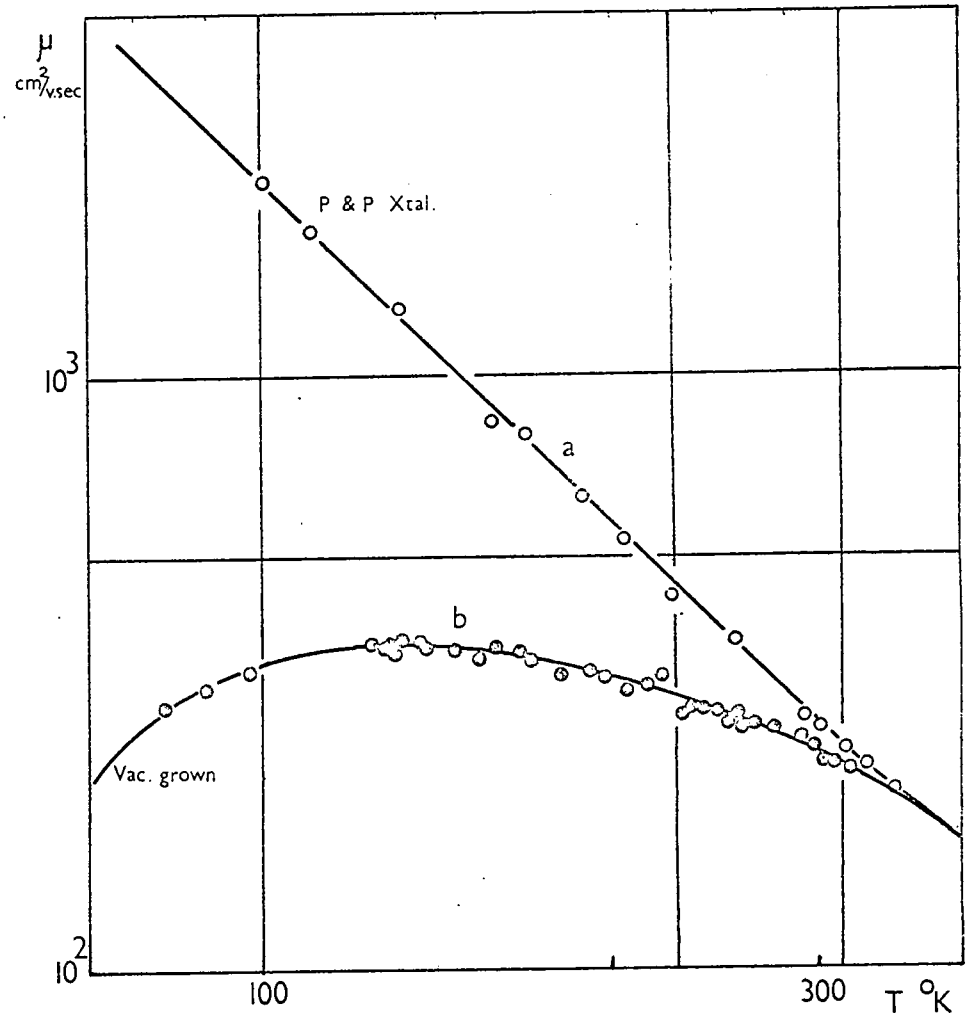

ln μ vs. ln T

FIGURE 8.8

the carrier density n was 2 x $10^{16}/cm^3$, with μ_H = 250 $cm^2/v.sec.$ at room temperature. The variation of these parameters with T in the range 350°-100°K is shown in Fig. 8.7(a) and Fig. 8.8(a). The carrier density saturates near room temperature, but below 150°K the plot of ln.n vs. $^1/T$ shows a slope corresponding to a donor level at 0.016 ev. ± 0.0035 ev. below the conduction band, similar to the level found in the low resistance crystals previously described (Sec. 8.3). A plot of ln μ_H against ln T was linear from 100-350°K, but showed a dependence of $\mu_H \propto T^{-1.82}$, rather than $T^{-1.5}$. The difference between quenched and annealed samples supports the conclusion that an excess of donors is incorporated in the crystals during growth from the charge; quenching freezes in those donors and gives a highly conducting n-type sample, whilst slow cooling allows the donor concentration to be reduced and give high resistivity.

8.4.5 Other experiments

Two further experiments were performed to confirm these ideas. Incorporation of excess sulphur into the charge produced yellow, uniform resistivity (10^4 ohm-cm.) material under the fast pulling rate conditions which had given black, low resistance crystals previously. This proves that the dark colouration and high conductivity were due to excess cadmium.

During the investigation of the effect of the growth temperature on the crystal properties, the method of crystal growth used had automatically entailed a change in the charge temperature when the growth temperature was altered. To exclude the possibility that the rate of dissocation of the charge, and not the crystal temperature, was responsible for the varying properties, the apparatus was modified to allow the furnace to move

relative to the growth tube and control thermocouple. This allowed the charge to be held at a constant temperature while the crystal grew in hotter or colder conditions controlled by the furnace position. For boules growing at a steadily increasing temperature between 1060°C and 1100°C the change from a clear to a dark material was evident along the length of the boule.

The rapid variation of the electrical properties of a sample due to a small change in growth temperature could well account for the wide variations in electrical parameters quoted for CdS by workers using crystals grown under supposedly similar conditions. It emphasises the need for the growth conditions of any crystals studied to be reported in detail.

8.5 Vacuum Pulling Runs

A return to the use of evacuated tubes was made, as described in 6.6, to see if the improvements made in the Piper and Polich runs could be applied to growth in vacuum. The experimental arrangement was as before; the tubes were sealed at less than 10^{-5} mm.Hg after 12 hours on the pumping system. No heat was applied to the tubes during evacuation after filling with the charge although the silica had been previously outgassed at red heat.

Appreciable transport of material leading to the growth of a boule could only be obtained with the use of the maximum temperatures of 1250-1300°C. At lower temperatures the flow crystal charge merely sintered in situ. The crystals grown at the higher temperatures were always very dark, and were deep red in transmitted light. (Fig. 6.5e).

They were invariably n-type and of low resistivity. Hall effect measurements on a sample from such a crystal are illustrated in Figs. 8.7b, and 8.8b, together with the curves for a low resistance crystal grown by the Piper and Polich method for ease of comparison. The rapid departure from lattice scattering to impurity scattering as the temperature is lowered is in accordance with the very high donor concentrations of $5 \times 10^{17}/cm.^3$ The variation of (ln) carrier concentration against reciprocal temperature is linear throughout the range 350-80°K and the slope corresponds to a donor level at 0.009 ± 0.003 ev. Note that this is a different donor depth from that found in crystals grown in argon.

As with the earlier attempts to grow crystals in vacuum, the resulting dark crystals with precipitates in the bulk, and the high donor concentration, are indicative of a non-stoichiometric excess of cadmium in the charge, caused by preferential loss of sulphur during the preparation of the charge. The excess of cadmium also explains the marked reduction in sublimation rate in the sealed tubes compared with open tube methods.

8.6 Evaporation rate of Non-stoichiometric CdS

In a recent paper Somorjai and Jepsen[105] described their work on the temperature dependence of the evaporation rate of cadmium sulphide in vacuum, using large single crystals of Eagle-Picher ultra-high purity grade material. The material was n-type, with a low resistivity of 0.5 - 10 ohm-cm. and mobility between 200 and 280 $cm.^2/v.sec.$ (Note the wide spread in properties of the commercial material).

To obtain reproducible evaporation rates, all single crystals were

annealed at 700°C for three days, after which time the resistivity had risen to 10^3-10^4 ohm-cm. The authors attributed this change to diffusion from the crystal of an excess of cadmium. They further investigated the effect on the evaporation rate of heat-treating the samples in an atmosphere of excess cadmium or sulphur, since crystals exposed to such an atmosphere during some of their experiments showed a change in evaporation rate.(106)

Heat treatment was carried out in a sealed evacuated quartz tube; the crystals were quenched after treatment. Samples heated in a partial pressure of cadmium of 10 atmospheres for several days at 1100°C were darkened, and black spherical precipitates appeared in the bulk. A uniform yellowish-grey colour with no second phase was produced after firing in one atmosphere of cadmium at 800 - 1000°C. However a black surface coating and black precipitates in the bulk were found if these samples were then annealed at 700°C. The surface coating was found to be cadmium by x-ray diffraction.

Crystals fired in an excess sulphur pressure of 20 atmospheres turned orange. This colouration could only be removed by a subsequent firing in excess cadmium.

Evaporation rates were measured by heating the crystal in vacuum with a selected face exposed. (The orientation dependence of the evaporation rate was discussed in a further paper(107)). The weight loss was determined using a quartz spiral microbalance. The untreated Eagle-Picher crystals showed a significantly lower than normal evaporation rate initially, which rose to the normal value in 0.5 to 3 hours. The time required varied from sample to sample. Crystals annealed at 700°C for 72 hours gave reproducible evaporation rates.

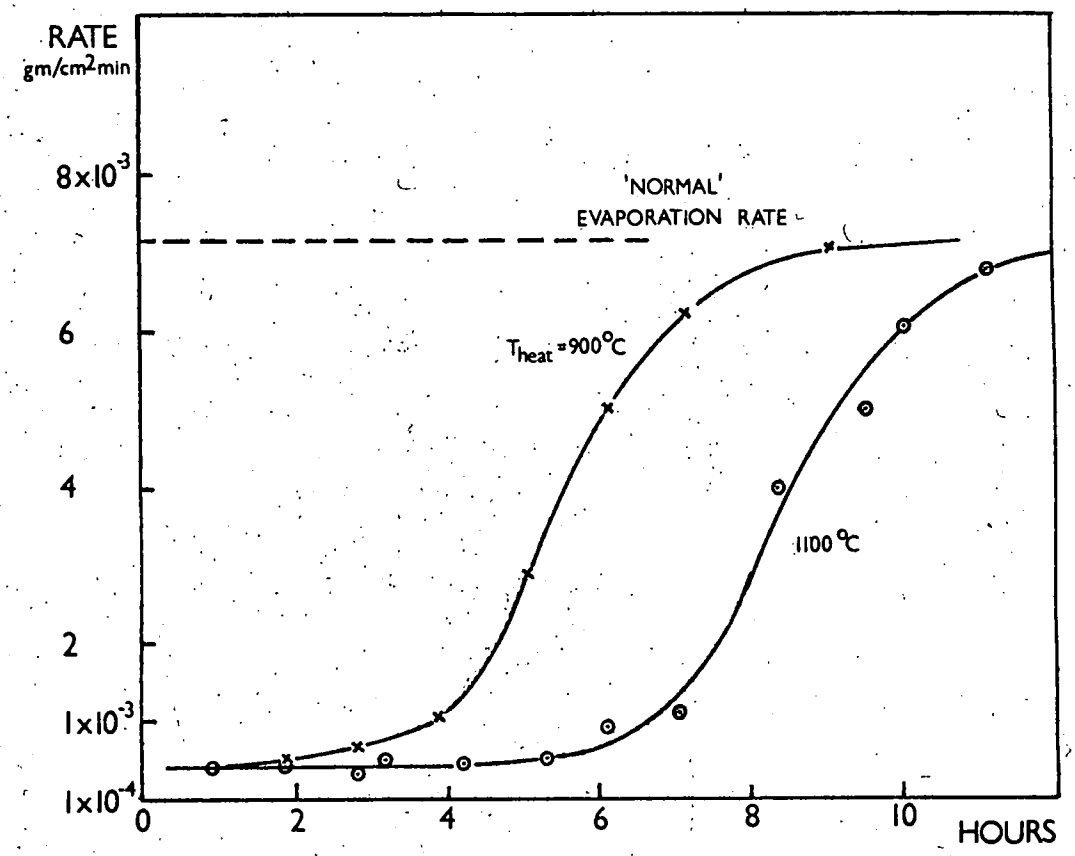

EVAPORATION RATE of Cd-doped CdS. (106)

FIGURE 8.9

For crystals treated in an excess of cadmium, the evaporation rate in vacuum was reduced by almost two orders of magnitude. It could take up to six hours before beginning to return to the normal value depending on the temperature of the sample during the heat treatment. (Fig. 8.9). The return to the normal evaporation rate was accompanied by a disappearance of the black precipitates from the crystal, and a rapid rise in the resistivity of the sample over several orders of magnitude. Heat treatment in sulphur produced a similar transient behaviour, but the effects were not so marked. Table 8.2 shows the room temperature resistivities of the samples before and after heat-treatment and evaporation. Heating in excess cadmium lowered the resistivity, and heating in sulphur raised it. After steady evaporation had been reached all samples showed an intermediate resistivity in the range 10^{3}-10^{7} ohm-cm.

By studying the effect of increasing the concentration of cadmium or sulphur by local deposition at the surface of a crystal by evaporation, Somorjai and Jepsen found that an increase in surface concentration of cadmium or sulphur was not responsible for the lowered evaporation rate. This fact, coupled with the results of experiments where the surface layer of the crystal was removed by grinding, before and after a steady state had been reached, showed that the lowered evaporation rate was controlled by the diffusion of some species from the bulk, associated with a depletion layer of this species near the surface during evaporation. The correlation between the evaporation rate, resistivity, and optical appearance of the sample suggests that the evaporation rate is suppressed by an excess of cadmium over the surface of the crystal, this cadmium being driven off but

being replenished by diffusion from the bulk. The evaporation rate remains low until all internal precipitates have dissolved, then rises to normal as the excess cadmium concentration in the lattice decreases.

The observations of Somorjai and Jepsen on the effects of the presence of excess cadmium or sulphur on the electrical and optical properties are in agreement with our observations, as are the changes in properties reported on annealing. Furthermore, the reduction of the evaporation rate caused by the presence of a non-stoichiometric excess of cadmium accounts for the difficulties experienced in our work in obtaining appreciable sublimation of material in sealed tubes. The evaporation experiments discussed above were carried out in a continuously evacuated chamber, and the evaporation rate returned to normal after any excess of Cd had diffused from the bulk of the crystal and evaporated from the surface. This out diffusion of cadmium will take place more rapidly at higher temperatures, and in the Piper and Polich growth method an excess of cadmium in the charge will escape during the back sublimation period before the growth begins. However in growth runs using a sealed evacuated tube, cadmium will only evaporate from the charge until equilibrium is reached between the cadmium concentration in the solid and in the vapour. The excess of cadmium cannot escape from the system, and the evaporation rate will be permanently reduced, being up to two orders of magnitude lower than in open tube runs. The ability to grow crystals in sealed tubes only at elevated temperatures is therefore explained - the lowered evaporation rate has to be countered by an increase in the charge temperature which increases the rate again, so that appreciable transport occurs in a reasonable time. Using our flow

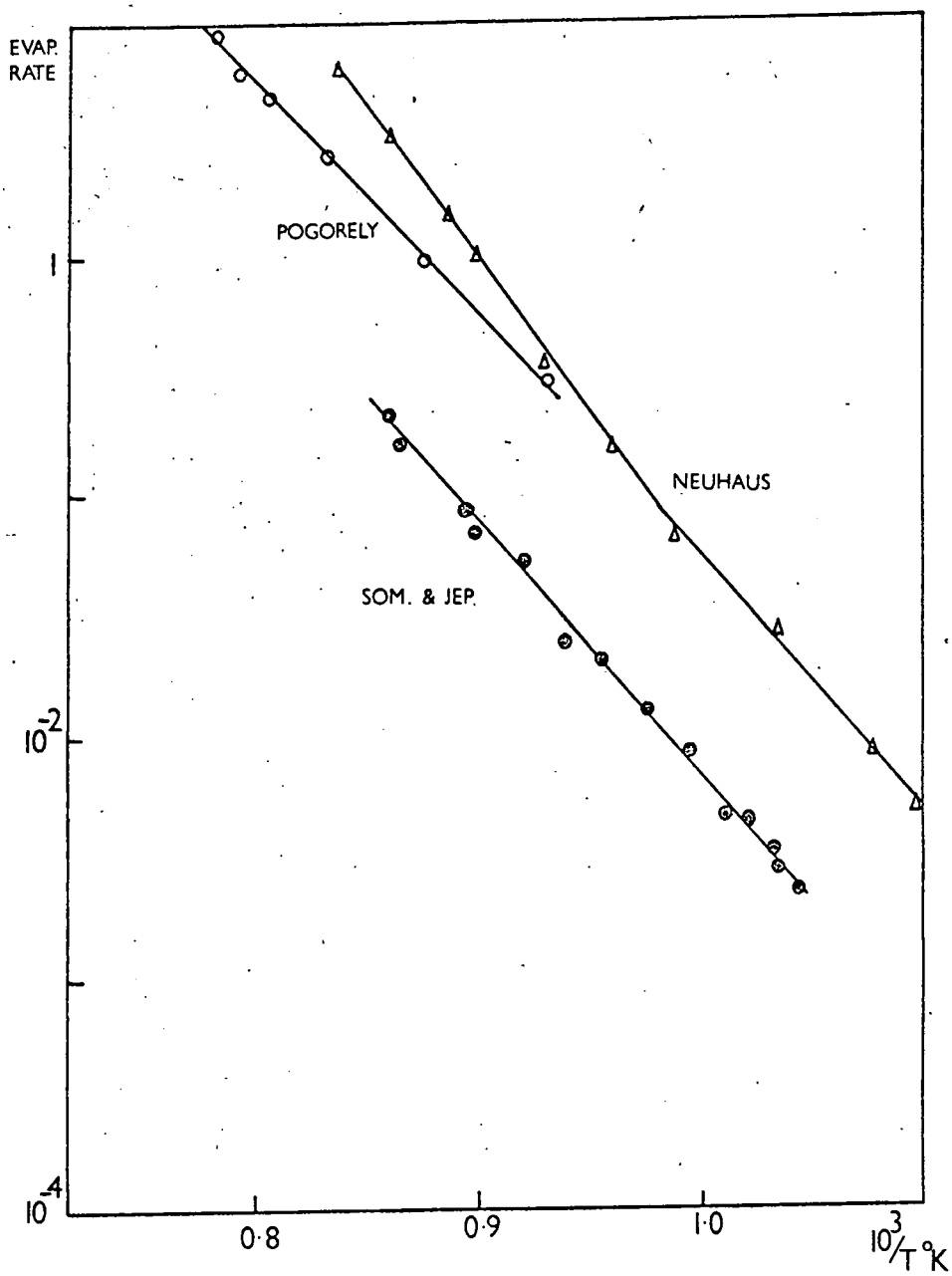

EVAPORATION RATE vs. T^{-1}

FIGURE 8.10

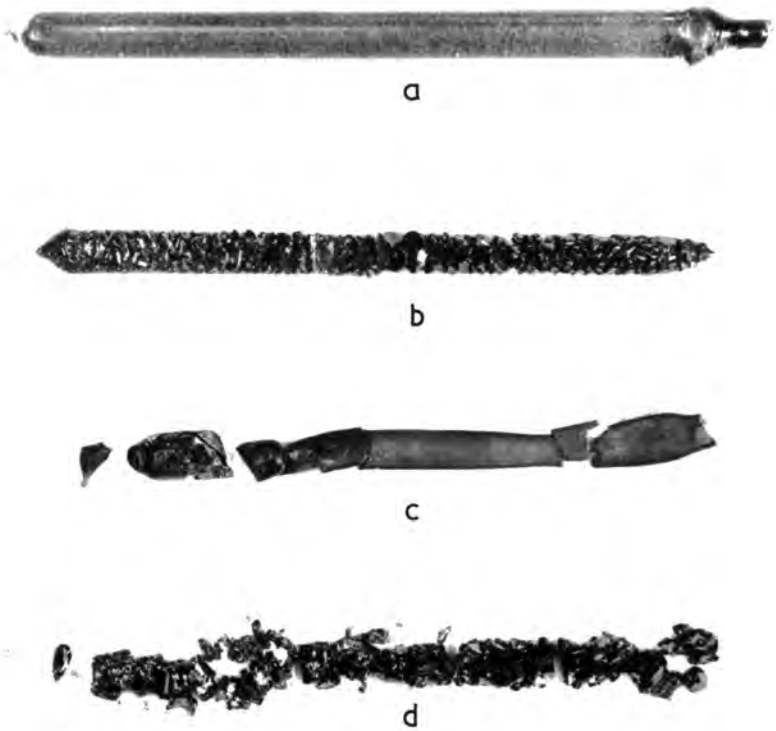

FIGURE 8.11.

crystal charge material, crystal growth by the Piper and Polich method can be performed at temperatures as low as 1050-1000°C; for vacuum runs the minimum is 1250-1200°C. Further data by Somorjai and Jepsen on evaporation rate vs. temperature (Fig. 8.10) indicate that such a temperature rise of 200°C at these temperatures ought to increase the rate of vapourisation by almost two orders of magnitude. We therefore conclude that our flow crystal charge contains a non-stoichiometric excess of cadmium, and the effect of this in sealed tube growth is to suppress evaporation of the CdS as reported by Somorjai and Jepsen. Moreover the open tube crystal growing results are in accordance with the observations of Somorjai and Jepsen.

8.7 Use of Excess Sulphur

Since the reduction in evaporation rate in the sealed tube experiments is due to the inability of any non-stoichiometric excess of cadmium in the charge to escape, deliberate incorporation of the correct amount of free sulphur in the tube should lead to near-stoichiometric conditions and enable crystals to be grown in sealed tubes at temperatures of 1100°C and below. (The reduction in growth temperature is necessary to improve the quality of the crystals). Sulphur was incorporated in two ways, as described in section 6.7; either during the preparation of the flow run crystals, or during the final growth run.

When sulphur is added directly to the sealed growth tube the effect of increasing the amount of sulphur present can be seen from Fig. 8.11, which shows the results without sulphur (a); with 50 p.p.m. sulphur (b); with 500 p.p.m. sulphur (c); and with 1,500 p.p.m. sulphur (d). The

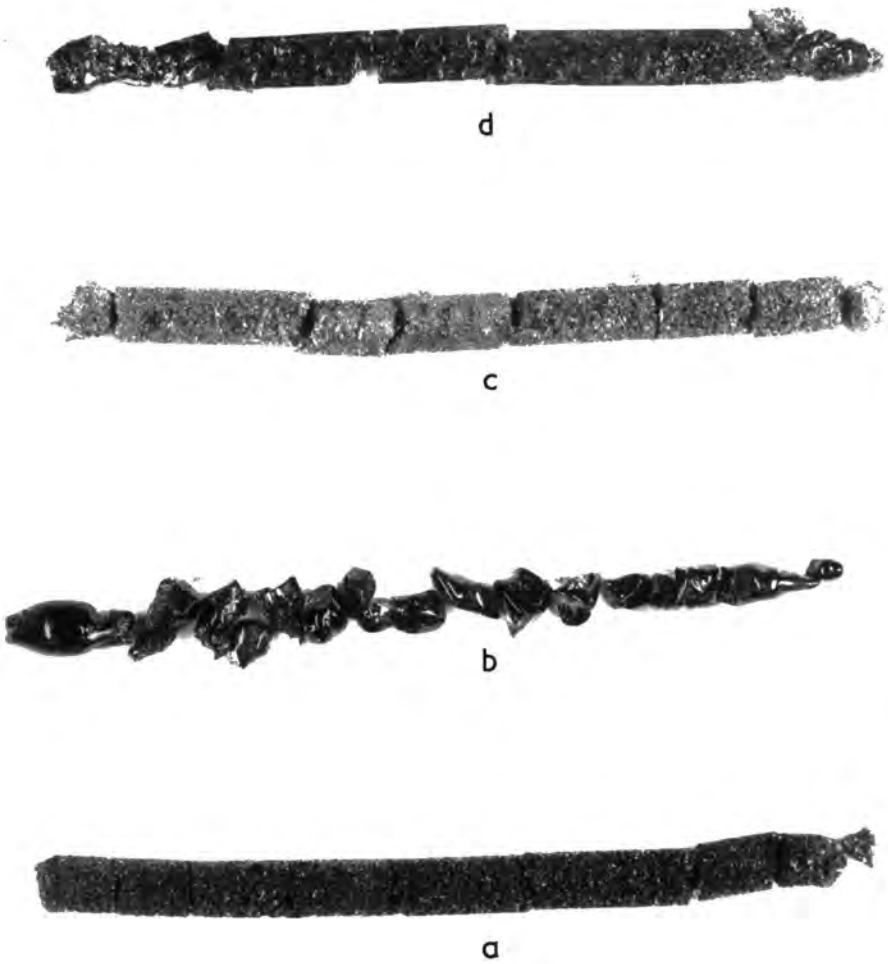

FIGURE 8.12.

latter concentration gives a sulphur pressure of one atmosphere at the growth temperature. These runs were performed using a furnace temperature of 1200°C, so that the point of the tube is at 1150°C. Increasing the sulphur concentration increases the evaporation rate, leading first to growth on the charge, then transport of material to form a boule. Too high a sulphur pressure inhibits growth. The departure from stoichiometry in our starting material must be of the orderof 100-500 p.p.m.

The use of a 'sulphur-rich' flow crystal charge (see section 5.4) leads also to improved transport. The results can be seen in figure 8.12. The products using the normal charge (a and c) and the sulphur-rich charge (b and d) are compared for runs performed at two temperatures, 1200° and 1100°C. At the higher temperature, crystals of a useful size were obtained; their resistivity was 10^4 ohm-cm. This resistivity, although much higher than previously obtained in sealed tube growth, is lower than the value expected for pure stoichiometric CdS, and suggests that growth conditions are very close to but not quite stoichiometric. This is a matter for further experimental investigation.

CHAPTER 9.

SOME PROPERTIES OF CRYSTALS GROWN BY MODIFIED PIPER AND POLICH METHOD

9.1 Introduction

A preliminary survey of some of the optical properties of the large single crystals grown as described in section 6.5 was made in order to obtain an initial comparison with the properties of crystals grown by the more conventional flow methods. Samples up to 1 cc. could usually be taken from single crystal regions as confirmed by back-reflection X-ray examination, although some of the boules grown were found to be polycrystalline. Etching the as-grown crystal surfaces with chromic acid produced etch pits on basal planes corresponding to a dislocation density of 10^5 cm.$^{-2}$ near the centre of the sample, with a higher density at the edges. Difficulty was experienced in producing pits on ground and polished surfaces, and other acid etches were tried. Satisfactory etching has still not been achieved, but etch pits produced, e.g. by hydrochloric acid seem to confirm a dislocation density of 10^5 cm.$^{-2}$.

The electrical properties and the appearance of the single crystal material have already been discussed in section 8.4. In summary: Crystals grown slowly at high temperature are of high resistivity, and photoconducting. They are also dark in appearance. Crystals grown slowly at a lower temperature are also high resistivity, and have a good pale yellow colour; however the crystal size is small. Increasing the rate of growth increases the tendency to produce samples of non-uniform or low resistivity, and increases the dark colouration.

9.2 Transmission and photoconductive spectral response.

The optical transmission of one of the darker specimens was measured in

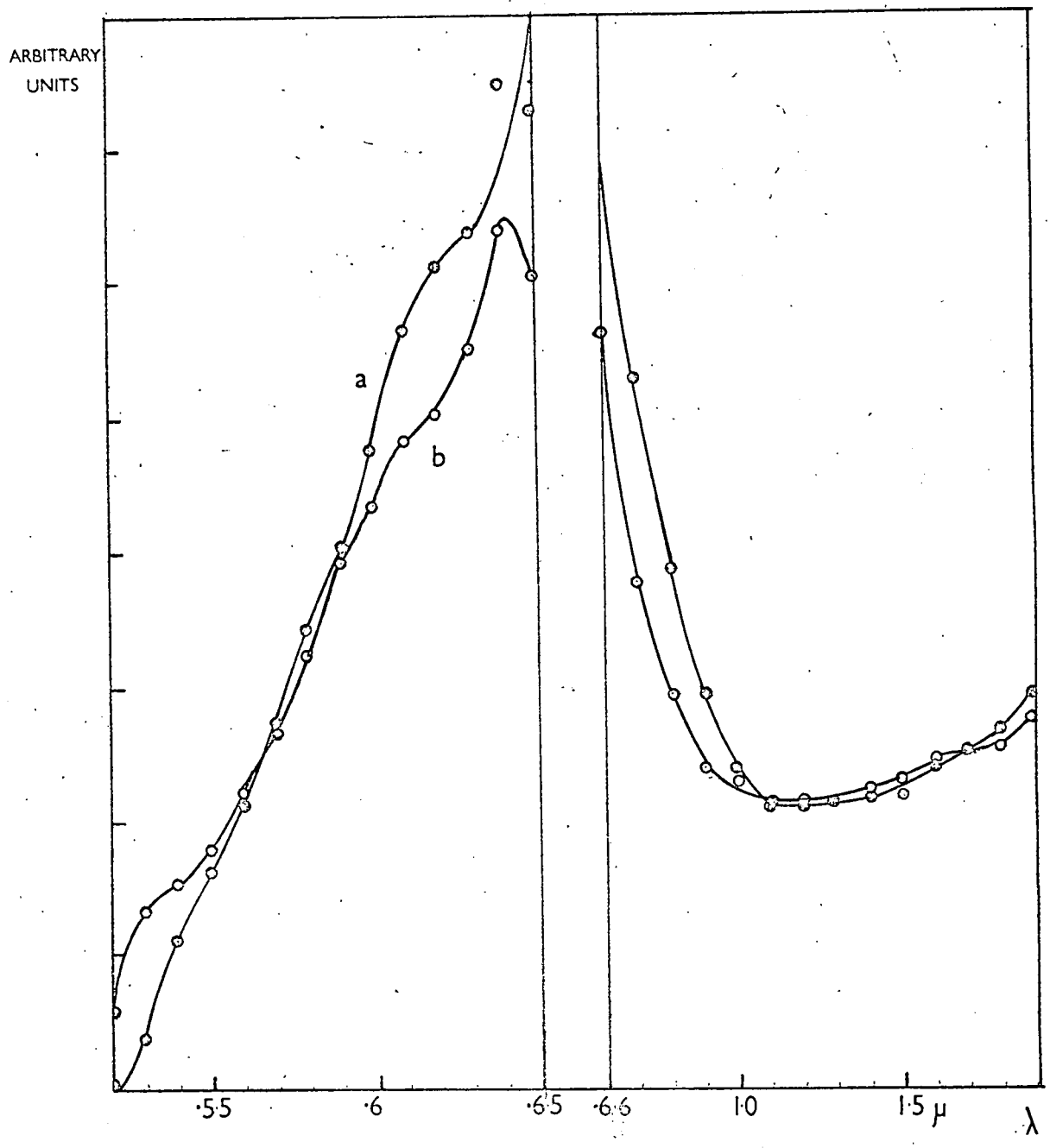

OPTICAL TRANSMISSION

FIGURE 9 . 1

the range 0.5 - 2.0 μ. A slice cut from a boule was mounted in a sample holder between a tungsten lamp and the inlet slits of a Hilger and Watts monochromator, type D 285. The output from the monochromator was detected with a photomultiplier for wavelengths up to 0.65 μ, and with a thermopile and galvanometer amplifier from 0.6 to 2.0 μ. Measurements were taken with the sample in and out of the beam to correct for the spectral distribution of the lamp output, the dispersion of the system, and the response of the detector. The sample holder ensured that the sample was repositioned accurately in the beam, and maintained a constant beam area with the sample in or out.

For comparison, the transmission spectrum of a clear plate of CdS grown in a conventional flow run was also measured. The spectra are shown in Fig. 9.1. The transmission of the large dark single crystal (curve 'a') has a long tail extending to longer wavelengths from the absorption edge. This crystal has a much lower transmission in the region 5200 Å - 5500 Å than the flow crystal. Both crystals show a marked, very broad absorption in the region 0.6 - 2.0 μ, centred on 0.9 μ. This band appears similar to that reported by Halperin and Garlick[108] in measurements on dark crystals grown in sealed tubes in vacuum. Since both detectors have a poor response in the region 0.6 to 0.65μ the possibility that any structure exists in that range could not be resolved.

The equal energy photoconductive response was measured in the region 4000 - 7000 Å. A tungsten lamp source and the Hilger and Watts monochromator provided the incident light of known wavelength, and the spectral energy distribution of the output from the monochromator was measured using the thermopile. The resulting photoconductive response curve is shown in Fig.9.2.

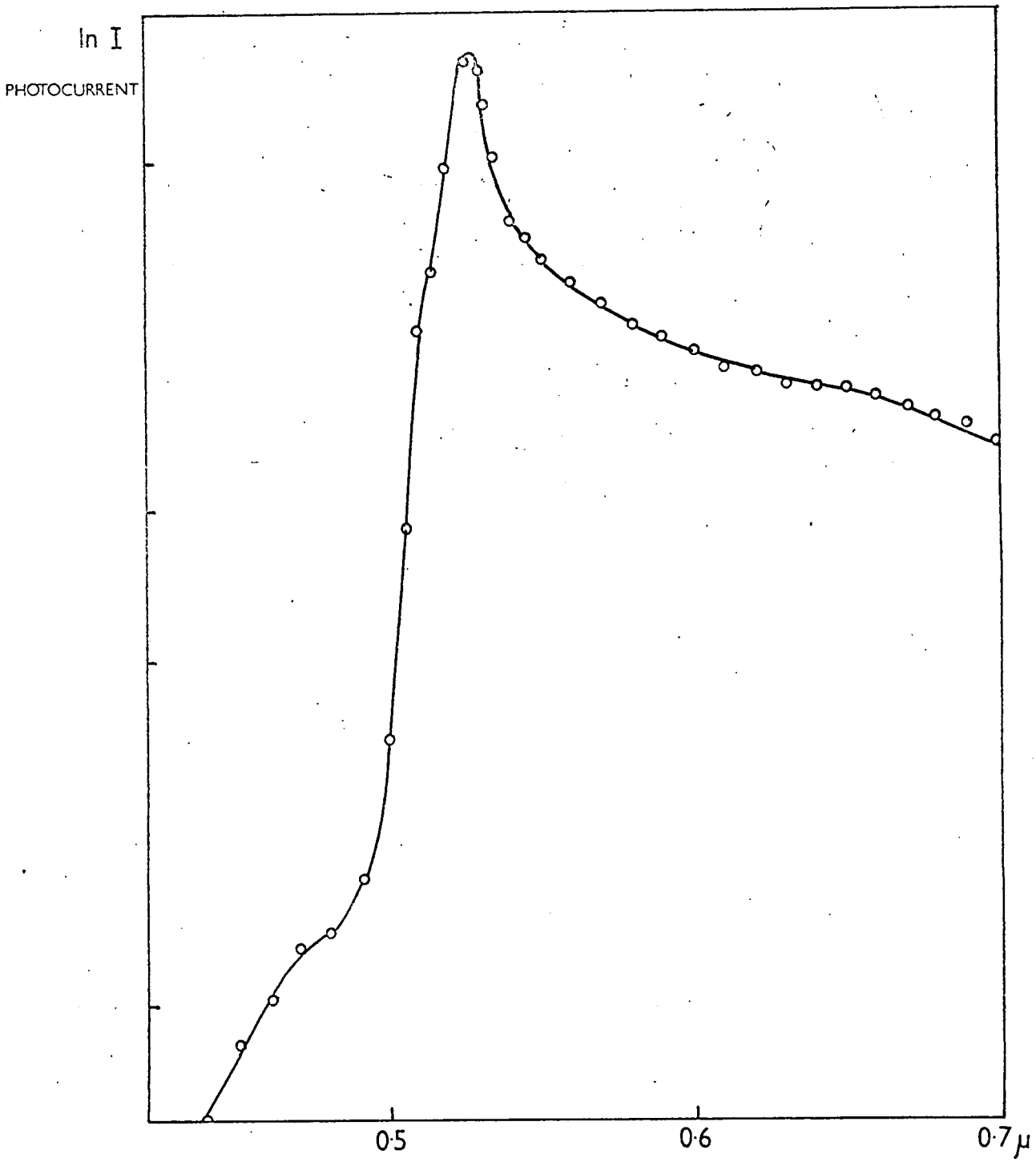

PHOTOCONDUCTIVE SPECTRAL RESPONSE

FIGURE 9 . 2

The maximum occurs at 5250 Å, with shoulders on the short wavelength side at 5100 and 4700 Å. The latter two features are not usually observed in crystals grown by a flow method.

Illumination of the sample with white light with an intensity 50 foot-candles gave a photoconductive gain of $>10^4$.

9.3 Luminescence

Crystals were examined for visible luminesence at 77°K under u.v. ($\lambda = 3650$ Å) stimulation from a high pressure mercury lamp. The luminescence observed was predominantly orange, but some samples showed green 'edge' emission while others showed little at all. Any correlation which may exist between the observed luminescence and other properties, e.g. electrical resistivity, has not yet been pursued. However in Hall samples cut from boules found to be of non-uniform resistivity, the high resistance regions usually emitted an orange luminescence, whereas the lower resistivity regions exhibited a predominantly green emission. The spectral distribution of the luminescence at 77°K under u.v. stimulation was measured for two high resistance samples which had been grown slowly at 1150°C. The measurements were performed on an Optica recording spectrometer type CF4 DRN1. Small signals only could be obtained which showed that the luminescence comprises a single broad band of low intensity, centred on 5200 Å. No phonon structure similar to that usually observed in edge emission could be resolved.

Measurements were also made of the infra-red emission bands from crystals excited in the visible. The emitted radiation was chopped at 800 c/s, and measured using a double prism (rock-salt) monochromator, with a PbS detector and 800 c/s tuned amplifier. Flow crystals generally show the characteristic

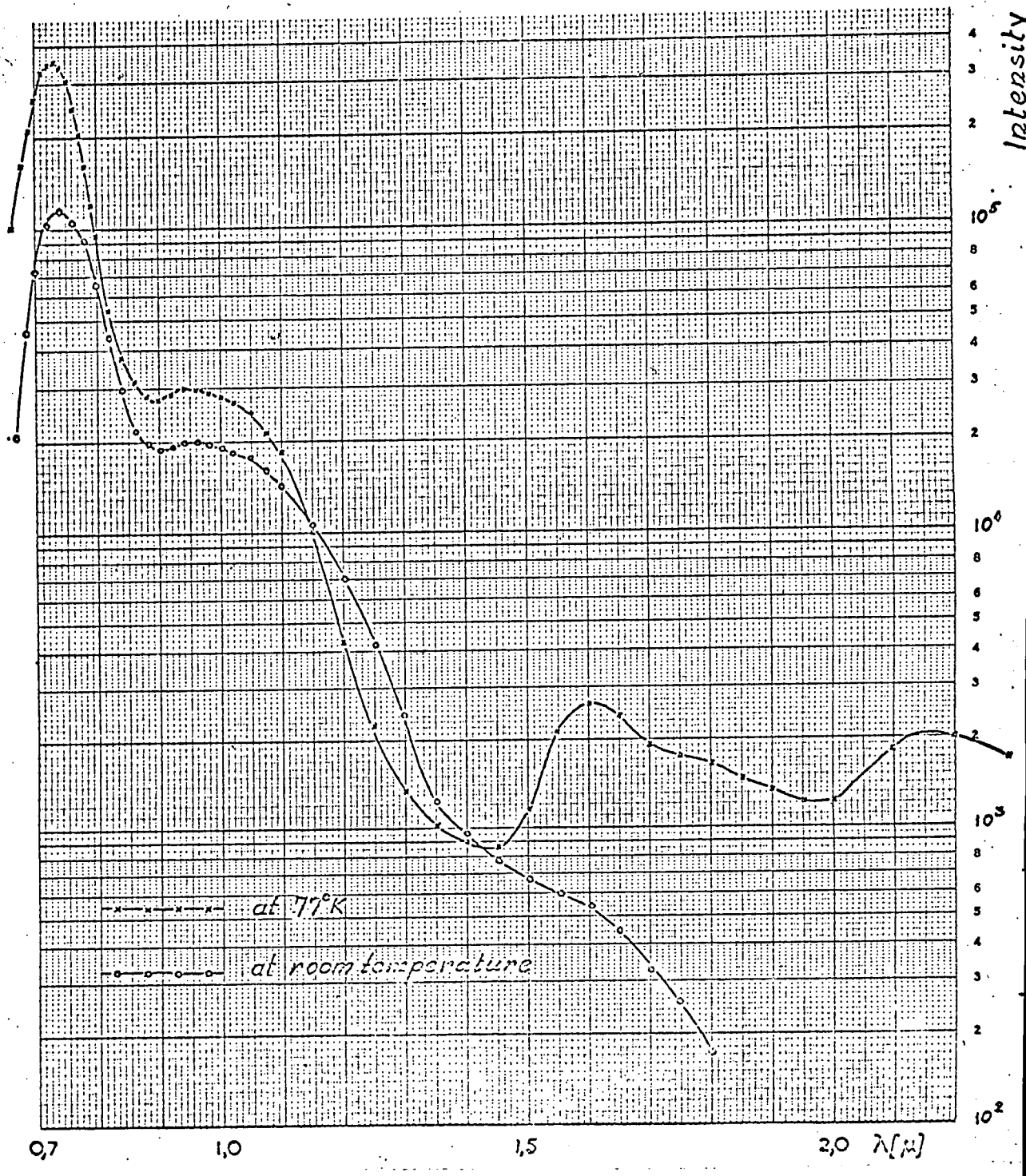
Intensity
4
3
2
10^5
8
6
5
4
3
2
10^4
8
6
5
4
3
2
10^3
8
6
5
4
3
2
10^2
at 77°K
at room temperature
0,7
1,0
1,5
2,0
λ[μ]

FIGURE 9.3

'blue' and 'green' bands at 0.8 and 1.03 μ, together with two further bands at 1.6 and 1.8 μ. The emission can be enhanced by incorporating Cu in the samples.

The measurements on the large crystals showed that the 'blue' and 'green' bands were present, but their maxima were displaced to 0.73 and 0.95 μ.(Fig. 9.3) Longer wavelength bands centred on 1.6μ and 2.15μ were present at 77°K, but their intensity was very low compared with the blue and green bands; they could not be detected at room temperature. The band at 1.8μ was only just detectable at 77°K as a shoulder on the 1.6μ band.

9.4 Thermally Stimulated Current Measurements

Since measurements of the photoconductive gain and spectral response had shown a long response time for the photocurrent, a preliminary investigation of the trapping spectrum of the large crystals was made using the method of thermally stimulated current measurement. Peaks were found which when analysed indicated traps at depths of 0.41, 0.83, and 0.63 ev.below the conduction band. Traps occurring at these three energy depths have been found in crystals grown by many methods. The defects associated with these levels have been tentatively identified by Nicholas (see section 2.2). In addition two peaks occurred at low temperature, just above 77°K, but these could not be separated and resolved. The traps at 0.83 and 0.63 ev. were interdependent in that the density of one of the two levels could be made to increase by suitable heat-treatment at the expense of the other. Further discussion of the measurement of trap depths by T.S.C. methods and the identification of the levels can be found in the references.(37, 109)

CHAPTER 10.

CONCLUSIONS

10.1. The experiments performed during this research programme have shown that the production of large single crystals of cadmium sulphide in small-scale apparatus is feasible, using controlled nucleation of the boule. The method is to be preferred for laboratory use since it offers the prospect of a much closer control over the properties of the material compared with methods using multi-crystal growth on to a seed plate in large bore apparatus. In these latter methods the scaling up of sizes and quantities of starting material needed could be prohibitive when series of runs under different growth conditions are to be investigated.

10.2 Starting Material.

Starting material for single crystal growth can be prepared from commercially available high purity powders using a modified flow crystal growth technique. This allows drying, outgassing, and an increase in density of the charge. Purification from impurities both more volatile and less volatile than CdS is achieved; the principal impurities remaining are zinc, (which is prevalent in some commercial powders and which is difficult to remove) and silicon, which is due to contamination from the silica-ware and increases in concentration at each stage. Other impurities are not present in greater concentrations than about 20 p.p.m., but the presence of oxygen or departures from stoichiometry cannot be determined. Further purification could be achieved by performing further flow runs, but as yet the properties of the single crystals produced are dominated by variations in the growth conditions and departures from stoichiometry. The deficiency of sulphur is the most

serious disadvantage in our starting material. It has partly been overcome by preparing the charge in conditions where sulphur is present in excess, but methods of forming high-purity CdS at room temperature by precipitation from solution are obviously of interest. However it is often necessary to give a heat-treatment to material prepared in this way to remove solvent contaminants, and departures from stoichiometry can again be introduced.

10.3 Modified Piper and Polich method.

The Piper and Polich method can be used to obtain large samples of high resistivity, by growing at 1200°C or higher at a very slow rate, followed by slow cooling. These crystals have poor optical properties, due to the scattering of transmitted light by small cadmium precipitates, and this can be a serious disadvantage in some applications. Clear yellow material can be prepared at ~1050°C; it is highly photoconductive, with a low dark conductivity, but the crystals produced are small (3 x 3 x 10 mm).

10.4 Future Work.

For future progress attention should be concentrated on the use of sealed evacuated tubes rather than the open ones of the Piper and Polich method. Sealed tube work means that the exclusion of oxygen and water vapour should be easier. The furnace arrangement can be simplified since no gas jacket and associated equipment is needed, and the pulling can be done vertically rather than horizontally. This would eliminate the effects of the transverse temperature gradients present in the horizontal system. The charge material would be a (polycrystalline) boule grown either by the Piper and Polich method or in a stationary open tube run, so that the density of the material was that of crystalline CdS. Use of such a charge would also ensure that the material

would sublime at the normal evaporation rate. Alternatively flow crystals or outgassed powder could be used provided care was taken to maintain stoichiometry. In this case back sublimation at the beginning of the run would be used to concentrate the charge. The procedure in such a run would be as follows. Furnace control and pulling arrangements would be similar to that used in horizontal runs, but adapted for vertical operation. The growth tube would be pulled through the maximum temperature region of the furnace at a fast pulling rate, ~5mm./hour, or faster. This would permit nucleation at the tip of the tube as before, but in addition the desired temperatures for the charge and the boule would be attained quickly, before much growth had occurred. Thereafter the tube would be moved slowly through the furnace at the same speed as the rate of growth of the boule (in the order of 1 mm/hour, but determined experimentally) so that the temperature of the growth face remained constant as the run proceeds. The use of a crystalline charge would ensure equal rates of removal of material from the charge and deposition of material on the growth surface, so that the temperature gradient between boule and charge would remain constant. After growth, the furnace should be cooled slowly to minimise thermal strain. Typical temperatures for the charge and the growth surface would be 1100°C and 1050°C. Work is being continued along these lines.

REFERENCES

1. B. Szigeti, Trans. Faraday Soc., 45, 155, 1949.
2. F. Bloch, Z. Phys., 52, 555, 1928.
3. R. deL. Kronig and W.G. Penney, Proc. Roy. Soc., A130, 499, 1931.
4. e.g. R.A. Smith, 'Semiconductors' Cambridge Univ. Press, 1961.
5. J. Bardeen and W. Shockley, Phys. Rev., 80, 72, 1950.
6. W. Shockley, 'Electrons and Holes in Semiconductors,' Van Nostrand, New York, 1950.
7. F.J. Morin and J.P. Maita, Phys. Rev., 94, 1525, 1954.
8. A.R. Hutson, J. Appl. Phys., 32, 2287, 1961.
9. E.M. Conwell and V.F. Weisskopf, Phys. Rev., 77, 388, 1950.
10. F.J. Blatt, Phys. Rev., 105, 1203, 1957; and J. Phys. Chem. Sol., 262, 1957.
11. N. Sclar, Phys. Rev., 104, 1548, 1956.
12. E.M. Conwell, Proc. I.R.E., 40, 1327, 1952.
13. G.L. Pearson and J. Bardeen, Phys. Rev., 75, 865, 1949.
14. C. Erginsoy, Phys. Rev., 79, 1013, 1950.
15. N. Sclar, Phys. Rev., 104, 1559, 1956.
16. D.H. Dexter and F. Seitz, Phys. Rev., 86, 964, 1952.
17. W.T. Read, Phil. Mag., 46, 111, 1955.
18. C. Hilsum and A.C. Rose-Innes, 'Semiconducting III-V Compounds', Pergamon Press, 1961.
19. W.W. Tyler and H.H. Woodbury, Phys. Rev., 102, 647, 1956.
20. W.W. Tyler and R. Newman, Phys. Rev., 98, 961, 1955.
21. H.H. Woodbury and W.W. Tyler, Phys. Rev., 100, 659, 1955.
22. R.O. Carlson, Phys. Rev., 104, 937, 1956.

23. R.H. Bube and H.E. MacDonald, Phys. Rev., 121, 473, 1961.

24. H. Brooks and C. Herring, quoted by Deby and Conwell, Phys. Rev., 93, 693, 1954.

25. V.A. Johnson and K. Lark-Horovitz, Phys. Rev., 82, 977, 1951.

26. M. Onuki and N. Hase, J. Phys. Soc. Japan, 20, 71, 1965.

27. Ormont, 'Structures of Inorganic Matter'.

28. C.A. Escoffery, J. Appl. Phys., 35, 2273, 1964.

29. D. Curie, 'Luminescence in Crystals,' Methuen, 1963.

30. H.S. Sommers, Jr., R.E. Berry and I. Sochard, Phys. Rev., 101, 987, 1956.

31. F.A. Kröger, H.J. Vink and J. Volger, Philips Res. Rep. 10, 39, 1955.

32. F.A. Kröger, H.J. Vink and van den Boomgard, Z. Phys. Chem. Bd., 203, 1, 1954.

33. D.A. Jenny and R.H. Bube, Phys. Rev., 96, 1190, 1954.

34. J. Woods and J.A. Champion, J. Elect. and Control, 7, 243, 1959.

35. R.H. Bube, J. Appl. Phys., 32, 1707, 1961.

36. R.H. Bube and S.M. Thomsen, J. Chem. Phys., 23, 15 and 18, 1955.

37. K.H. Nicholas, Ph.D. Thesis, Durham, 1963.

38. M. Balkanski and des Cloiseaux, J. Phys. Rad., 21, 825, 1960; and 22, 41, 1960.

39. D.G. Thomas and J.J. Hopfield, Phys. Rev., 116, 573, 1959.

40. D.G. Thomas and J.J. Hopfield, Phys. Rev., 112, 35, 1961.

41. J.L. Birman, Phys. Rev. Letters, 2, 157, 1959.

42. D. Dutton, Phys. Rev., 112, 785, 1958.

43. Y.S. Park and D.C. Reynolds, Phys. Rev., 132, 2450, 1963.

44. W.W. Piper and R.E. Halstead, 'Proc. International Conf. on Semiconductor Physics,' Prague 1960; Academic Press, N.Y., 1961.

45. R.N. Dexter, J. Phys. Chem. Sol., 8, 39 and 216, 1959.

46. K. Sawamoto, J. Phys. Soc. Japan, 19, 318, 1964.

47. J.D. Zook and R.N. Dexter, Phys. Rev., 129, 1980, 1963.

48. J. Mort and W.E. Spear, Phys. Rev. Letters, 8, 314, 1962.

49. R.J. Collins, J. Appl. Phys., 30, 1135, 1959.

50. B.A. Kulp and R.H. Kelley, J. Appl. Phys., 32, 1290, 1961.

51. D. Dutton, J. Phys. Chem. Sol., 6, 101, 1958.

52. G.A. Marlor, Ph.D. Thesis, Durham, 1964.

53. P.F. Browne, J. Elect., 2, 1 and 154, 1956.

54. F.J. Bryant and A.F.J. Cox, B. J. Appl. Phys., 16, 463, 1965.

55. H. Gobrecht and A. Bartschat, Z. Physik, 153, 529, 1959.

56. H.D. Nine, Phys. Rev. Letters, 4, 359, 1960.

57. H.D. Nine and R. Truell, Phys. Rev., 123, 799, 1961.

58. I. Isenberg, B.R. Russell and R.F. Greene, Rev. Sci. Instrum., 19, 685, 1948.

59. A.R. Hutson, Phys. Rev. Letters, 4, 505, 1960.

60. A.R. Hutson and D.L. White, J. Appl. Phys., 33, 40, 1962.

61. A.R. Hutson, J.H. McFee and D.L. White, Phys. Rev. Letters, 7, 237, 1961.

62. T.A. Midford, J. Appl. Phys., 35, 3423, 1964.

63. E.C. Adler and G.W. Farnell, Proc. I.E.E.E. 53, 483, 1965.

64. J.H. McFee, J. Appl. Phys., 34, 1548, 1963.

65. W.C. Wang, Proc. I.E.E.E., 53, 330, 1965.

66. W.C. Wang, Appl. Phys. Letters, 6, 81, 1965.

67. B. Tell, Phys. Rev., 136, A772, 1964.

68. A.R. Moore and R.W. Smith, Phys. Rev., 138, A1250, 1965.

69. B. Kandilarov and R. Andreytchin, phys. stat. sol., 8, 897, 1965.

70. M.G. Miksic, E.S. Schlig and R.R. Haering, Sol. State Elect., 7, 39, 1964.

71. R.S. Muller and J. Conragan, Appl. Phys. Letters, 6, 83, 1965.

72. B. Gudden and R. Pohl, Zeits. f. Physik, 5, 176, 1921.

73. R. Frerichs, Naturwissenschaften, 33, 281, 1946.
Phys. Rev., 72, 594, 1947.

74. Lorenz, Chem. Berichte, 24, 1509, 1891.

75. J.M. Stanley, J. Chem. Phys., 24, 1279, 1956.

76. P.D. Fochs, J. App. Phys., 31, 1733, 1960.

77. M.E. Bishop and S.H. Liebson, J. Appl. Phys., 24, 660, 1953.

78. R.H. Fahrig, Electrochemical Technology, 1, 362, 1963.

79. S. Ibuki, J. Phys. Soc. Jap., 14, 1181, 1959.

80. J. Berkowitz and J.R. Marquart, J. Chem. Phys., 39, 275 and 283, 1963.

81. L.C. Greene, D.C. Reynolds, S.J. Czyzack and W.M. Baker, J. Chem. Phys., 29, 1375, 1958.

82. A. Vecht, B.W. Ely and A. Apling, J. Electrochem. Soc., 111, 666, 1964.

83. P.A. Jackson, Paper presented at International Conference on Luminenscence, Hull, 1964.

84. Inorganic Syntheses Vol. 1., 111.

85. R.H. Bube and L.A. Barton, R.C.A. Review 20, 564, 1959.

86. J. Woods, J. Elect. and Control, 5, 417, 1958.

87. S. Kitamura, J. Phys. Soc. Japan, 16, 2430, 1961.

88. H.W. Sturner and C.E. Bleil, Applied Optics, 3, 1015, 1964.

89. E.T. Allen and J.L. Crenshaw, Am. J. Sci., 34, 310, 1912.

90. A. Addamiano, J. Phys. and Colloid Chem., 61, 1253, 1957.

91. W.E. Metcalf and R.H. Fahrig, J. Electrochem. Soc., 105, 719, 1958.

92. Takahashi, Shoji, et. al., Japan. J. Appl. Phys., 2, 666, 1963.

93. D.C. Reynolds and S.J. Czyzack, Phys. Rev., 79, 543, 1950.

94. R.C.A. Labs. "Maximising the Performance of Photoconductors," Report No. 1, ed. R.H. Bube, 1961.

95. D.R. Boyd and Y.T. Sihvonen, J. Appl. Phys., 30, 176, 1959.

96. A.B. Dreeben and R.H. Bube, J. Electrochem. Soc., 110, 456, 1963.

97. Konezenko and Yctyanov, Ukr. Fiz. Zhur., 5, 606, 1960.

98. W.W. Piper and S.J. Polich, J. Appl. Phys., 32, 1278, 1961.

99. M. Aven and W.W. Piper, Investigation of semiconducting properties of II-VI compounds, Scientific Report No. 1, 1961, General Electric Res. Lab.

100. M. Borisov and V. Vasilev, Comptes rendux de l'Academie bulgare des Sciences, 16, 485, 1963.

101. W.O. Milligan, J. Phys. Chem., 38, 797, 1934.

102. E. Grillot, Compt. Rend., 242, 779, 1956.

103. H.H. Woodbury, Phys. Rev., 134, A492, 1964.

104. M. Itakura and H. Toyoda, J. Phys. Soc. Japan, 18, 150, 1963.

105. G.A. Somorjai and D.W. Jepsen, J. Chem. Phys., 41, 1389, 1964.

106. G.A. Somorjai and D.W. Jepsen, J. Chem. Phys., 41, 1394, 1964.

107. G.A. Somorjai and R.N. Stemple, J. Appl. Phys., 35, 3398, 1964.

108. A. Halperin and G.F.J. Garlick, Proc. Phys. Soc., B, 68, 756, 1955.

109. J. Woods and K.H. Nicholas, Brit. J. Appl. Phys., 15, 1361, 1964.

THESIS APPENDIX.

Reprinted from the *Journal of Scientific Instruments*, VOL. 42, pp. 51–52, JANUARY 1965

A method of applying ohmic contacts to cadmium sulphide crystals for Hall measurements

L. CLARK and J. WOODS
Department of Applied Physics, University of Durham
MS. received 10*th August* 1964, *in revised form* 20*th October* 1964

Abstract. A method is described by which a rectangular bar of cadmium sulphide can be provided with a minimum of six ohmic contacts, which are required, for example, for Hall voltage measurements. The sample is simultaneously equipped with flying leads and can be inserted in any crystal holder. The method is also suitable for the application of thermojunctions.

It is well known that indium forms ohmic contacts on cadmium sulphide crystals (Kröger, Diemer and Klasens 1956). However, the indium must be applied in a carefully controlled manner to obtain good ohmic contacts with a high mechanical strength. In particular it is essential to eliminate oxygen from the ambient atmosphere while preparing the electrodes, otherwise the electrical properties are impaired (Marlor and Woods 1963). The purpose of this note is to describe a method of applying a minimum of six indium contacts simultaneously to a rectangular sample of CdS with dimensions of the order 10 mm × 3 mm × 2 mm. Such an arrangement may be required, for example, to measure the Hall coefficient.

Single crystals of cadmium sulphide with lengths up to 3 cm and diameters of 1 cm are grown by a sublimation method in this department. Hall samples are prepared from the starting crystals by sawing and grinding. The grinding is carried out with carborundum powder to 800-mesh size, and thereafter with alumina (particle size 0·5 μm). Subsequently the sample is etched in a chromic acid to remove grinding damage and to clean the surface. The chromic acid is prepared by dissolving 700 g of chromic oxide in two litres of distilled water, and adding 100 cm^3 of concentrated sulphuric acid to the solution. After cooling, a small quantity of this liquid is diluted three times to obtain the required etchant. Etching is carried out at 70° C for 3 to 5 minutes, after which time the solution is progressively diluted before the crystal is removed. Finally the crystal is washed thoroughly in distilled water and allowed to dry.

The contact areas of the sample are coated with layers of indium approximately 1 μm thick using conventional high vacuum (~10 μtorr) evaporation techniques. Indium is outgassed and evaporated from a molybdenum strip. The crystal is mounted above the heater strip and in contact with a suitable aluminium mask, the holes in which allow areas of 1 mm diameter to be coated with indium. Depending on the geometrical arrangement of electrodes required, it may be necessary to perform several evaporations to achieve the desired configuration. In such an event the crystal is surrounded by an inert atmosphere of argon before the bell-jar is removed and the necessary adjustments made. The function of this operation is to enhance the cooling rate of the crystal and prevent the oxidation of the indium.

After all the layers of indium have been deposited the crystal is placed in the apparatus shown in the diagram where it can be heated by radiation from a molybdenum strip heater. The manipulator box is gas tight, and is flushed with nitrogen while the sample is heated radiatively to about 165°C, just above the melting point of indium. This step ensures that the evaporated indium layers wet the sample. Next, the specimen is cooled, and freshly cut 1 mm slices of 1 mm diameter indium wire are pressed on to the evaporated layers.

The pressure is applied using a jig which contains two small spring-loaded pistons terminated by polished nickel end-pieces 2·5 mm in diameter. The pistons face each other

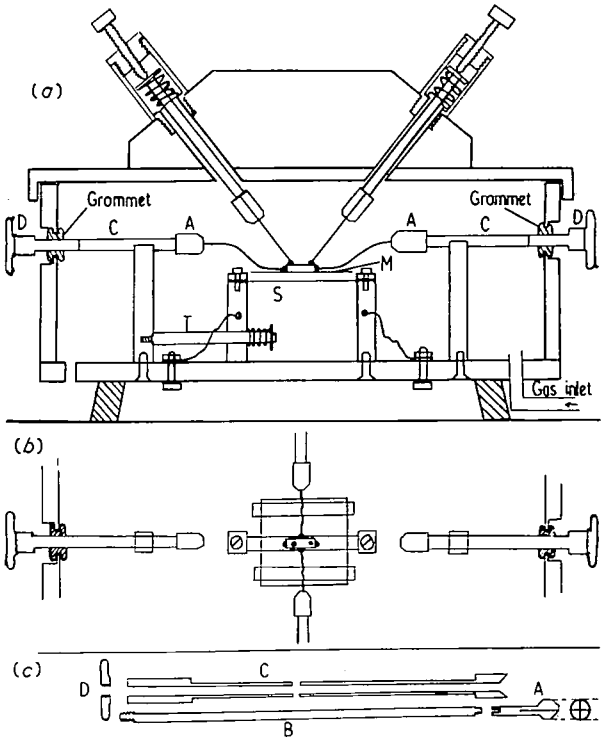

Elevation (*a*) and plan view (*b*) of the Perspex manipulator box. The side of the sample which carries no contacts faces the molybdenum strip heater, and is supported by a sheet of mica M. The heater strip S is held in tension by the spring-loaded arm T. (*c*) illustrates the design of the brass chucks. A is the collet, which is screwed to the collet rod B after B is inserted in the tube C. The threaded nut D screws on to the left-hand end of the rod B and permits the loosening of a wire held in the jaws of the collet A.

and press the pieces of indium wire on to the required evaporated layers, either singly or in pairs. The pressure used is sufficient to compress the indium wire to approximately 80% of its original length. Provided the evaporation procedure has been carried out satisfactorily the indium dots

adhere to the evaporated layers after this treatment. Should a dot not adhere after pressing, the subsequent heating which is required to fabricate the contact will cause the indium wire to fuse into a sphere, when it will either fall off the sample or, at best, provide a noisy, high resistance contact. The failure of a dot to stick after pressing can therefore be taken as an indication that the whole process will be unsuccessful. The failure is due to oxidation or some other contamination of the evaporated layers. In the event of any one dot failing to adhere the process is discontinued, the sample re-etched, and new layers of indium are deposited.

When the pieces of indium have been pressed successfully on to the contact areas, the sample is replaced in the box above the heater. The box is flushed with nitrogen while short lengths of 30 s.w.g. tinned copper wire, held in chucks, as illustrated in the diagram, are adjusted from outside the box so that a wire is adjacent to every indium dot. The sample is once again heated radiatively to about 165°C when the dots melt and fuse to the evaporated layers. The external arms holding the wires are then adjusted so that one wire enters each molten indium dot. After cooling the wires are released from the chucks from outside the box.

In this way a large number of contacts and thermocouple wires can be applied to CdS crystals. The contact areas used were generally 1 mm in diameter, although electrodes $\frac{1}{2}$ mm in diameter have been applied successfully. In our experience it is vital when applying more than two electrodes to melt all contacts simultaneously rather than consecutively, otherwise the operation becomes extremely hazardous, in that the contacts prepared first are likely to deteriorate during the fabrication of the later ones. The deterioration is associated with prolonged heat treatment and the consequent danger of the molten indium covering additional areas of the crystal or even falling from the sample.

The principal features of the method described here are as follows.

1. Whenever the crystal is exposed to heat it is either in vacuum or in an inert atmosphere.
2. The crystal temperature can readily be monitored and controlled at all times.
3. The contacts when finished are equipped with fine gauge flying leads so that the sample can be placed into almost any sample holder without further heating.
4. The success of this method depends on the fact that the heat to melt the indium dots is conducted from within the crystal and not down the contact wire from an external heater, e.g. a soldering iron. We have found that this largely eliminates the tendency for the dots to melt into spheres which drop off the sample. This problem was frequently encountered when external heating techniques were used, even when the pressing operation described earlier appeared to have been performed successfully.
5. Contacts prepared in the manner outlined here can be applied to CdS crystals with resistivities ranging from 10^{-1} to 10^{10} ohm cm. Contact resistances are less than 1% of the bulk resistance over the temperature range 77–420° K.
6. The mechanical strength of the contacts is such that applied stress either breaks a flying lead or removes the wire from the indium.

We would like to acknowledge the assistance given by Messrs. F. Spence and B. Blackburn in the design and construction of the manipulator box. One of us (L.C.) would also like to thank the Department of Scientific and Industrial Research for financial support.

References

KRÖGER, F. A., DIEMER, G., and KLASENS, H. A., 1956 *Phys. Rev.*, **103**, 279.

MARLOR, G. A., and WOODS, J., 1963, *Proc. Phys. Soc.*, **81**, 1013.

UNWIN BROTHERS LIMITED, WOKING AND LONDON

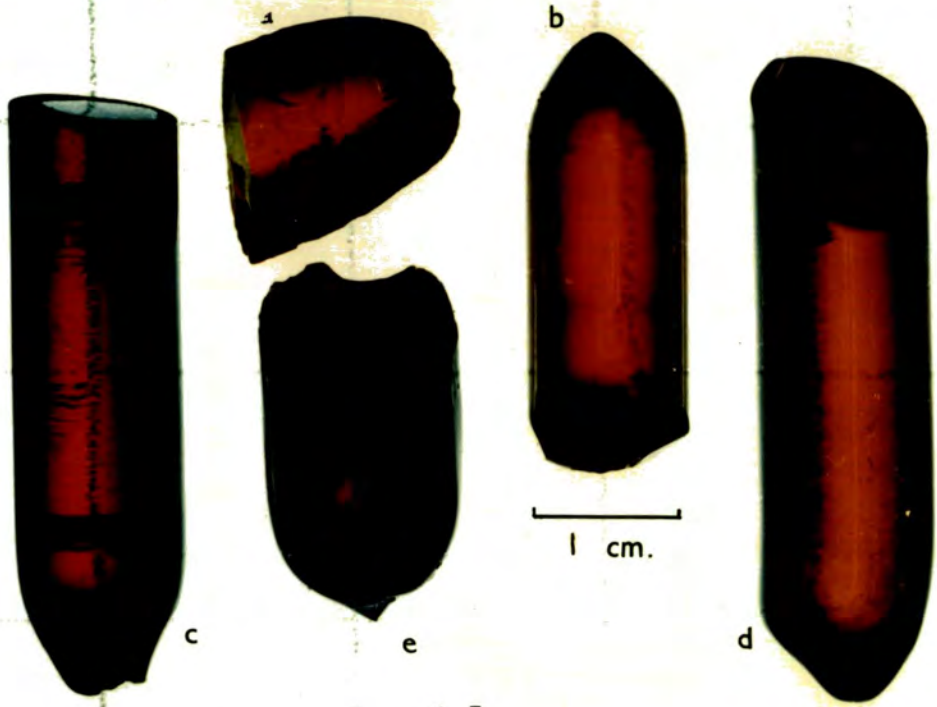

6.5

FIG. 6.5 — Appendix

6.5

FIG. 6.5 (appendix)
(f, g)